

# AN ONLINE CROP COEFFICIENTS DATABASE USING FRACTIONAL VEGETATION COVER AND TREE HEIGHT FOR IRRIGATED FRUIT TREE CROPS

Report to the  
**Water Research Commission**

prepared by

**Zanele Ntshidi<sup>1</sup>, Munashe Mashabatu<sup>2</sup>, Sebinasi Dzikiti<sup>3</sup>,  
Nompumelelo T. Mobe<sup>1</sup>, Munyaradzi Mandava<sup>4</sup>**

*<sup>1</sup>Smart Places Cluster, Council for Scientific and Industrial Research*

*<sup>2</sup>University of the Western Cape, Institute for Environmental and Water Studies*

*<sup>3</sup>Stellenbosch University*

*<sup>4</sup>TEQOA Pty Ltd.*

**WRC Report No. 2963/1/23**  
**ISBN 978-0-6392-0479-6**

**June 2023**



**Obtainable from**

Water Research Commission  
Lynnwood Bridge Office Park  
Bloukrans Building, 2<sup>nd</sup> Floor  
4 Daventry Street  
Lynnwood Manor  
PRETORIA

[orders@wrc.org.za](mailto:orders@wrc.org.za) or download from [www.wrc.org.za](http://www.wrc.org.za)

The publication of this report emanates from a project entitled ***Development of a smart phone crop coefficients database for major irrigated fruit tree crops*** (WRC Project No. K5/2963//4).

Corresponding authors: Zanele Ntshidi, E-mail: [zntshidi@csir.co.za](mailto:zntshidi@csir.co.za) and Sebinasi Dziki, E-mail: [sdziki@sun.ac.za](mailto:sdziki@sun.ac.za)

**DISCLAIMER**

This report has been reviewed by the Water Research Commission (WRC) and approved for publication. Approval does not signify that the contents necessarily reflect the views and policies of the WRC, nor does mention of trade names or commercial products constitute endorsement or recommendation for use.

## EXECUTIVE SUMMARY

### MOTIVATION

South Africa is ranked as one of the driest countries in the world receiving about half of the global average rainfall. Yet the country is a major producer of agricultural crops, most of them for the export markets. More than 95% of horticultural crops produced in the country, for example, are grown under irrigation. So, the availability of adequate water is critical for the sustainability and growth of the horticultural, and other water-intensive sectors. Over the years, the Water Research Commission (WRC) has initiated and funded research on the water use of irrigated crops, often in partnership with industry partners. A detailed update on progress with irrigation research on WRC-funded studies in South Africa was published by Annandale et al. (2011). The outputs from these studies range from complex physically-based models such as the SWB, PUTU, BEWAB, SAPWAT, to simple crop coefficients.

The largest volume of crop water use data collected in recent years has been on fruit tree orchards. But other crops, e.g. biofuel crops like sugarcane (*Saccharum officinarum*), maize (*Zea mays*), and sorghum (*Sorghum bicolor*) have also received attention. This is not only because of the water-intensive nature of the fruit industry. It is also because of significant technological advancements that have allowed detailed quantification of soil-plant-atmosphere interactions under different growing conditions. Two most popular irrigation scheduling approaches in the horticultural sector involve monitoring soil water depletion in the rootzone and the atmospheric conditions. Soil-based irrigation scheduling has been boosted by the commercial availability of many soil moisture sensors that have been developed in recent years. Weather-based

irrigation scheduling, on the other hand, involves estimating the crop water requirements ( $ET_c$ ) using crop coefficients ( $ET_c = K_c \times ET_o$ ), where  $K_c$  is a crop coefficient, and  $ET_o$  denotes the reference evapotranspiration determined from the climatic data. Use of the crop coefficients approach grew rapidly in popularity, not only in South Africa, but globally following the publication of the FAO 56 paper (Allen et al., 1998). This is mostly because of the simplicity and relatively low costs involved with the method, while it is perceived to be fairly accurate if reliable crop coefficients can be found.

In South Africa, the rapid expansion in the network of weather stations across the country further facilitated the extensive use of the crop coefficient-based approach. The major challenge, however, is access to accurate crop coefficient values given that the tabulated values in the FAO 56 paper were derived under temperate sub-humid climatic conditions. This prompted a huge focus towards locally derived crop coefficients and this effort was supported by many entities involved with agricultural water management in the country. The present study was initiated by the WRC with the aim of consolidating and updating existing crop coefficients generated in various studies into a national scale database that can be used to improve water resources management. There was also a need to develop a method to fill in the gaps in crop coefficients given that most crop coefficients were determined over short periods, often a few days to weeks for various reasons. To address these needs, a decision was made to focus only on irrigated fruit tree crops in the current study and to create a strong basis for including other crop types in the database in future studies. The present study was therefore done on the following crops: apple (*Malus domestica*) orchards (different cultivars, tree canopy sizes, and growing regions), nectarines and

peaches (*Prunus persica*) (summer and winter rainfall areas), plums (*Prunus domestica*), pecan nuts (*Carya illinoensis*), macadamia nuts (*Macadamia integrifolia*), mango (*Mangifera indica*), litchi (*Litchi chinensis*), and citrus (different cultivars in different climatic regions).

## **AIMS AND OBJECTIVES**

### **Overall aim**

The main aim of the study was to develop an online database of crop coefficients for irrigated fruit tree crops in South Africa for which water use data have been collected. This database is encapsulated in a Smartphone Application (APP) that can be used anywhere in the country on irrigated fruit tree crops that are included in the database.

### **Specific objectives**

These were to:

- Conduct a detailed knowledge review to document the crop coefficients from water use information derived in various studies and to identify missing crop coefficients;
- Gather historical weather data to calculate the reference evapotranspiration and to develop a simple but accurate method to derive missing crop coefficients using readily available information;
- Estimate the crop coefficients following the FAO's four stage crop coefficient approach, and;
- Develop an interactive crop coefficient database with a user-friendly graphical user interface for a smartphone.

## METHODOLOGY

The study used historical data collected in orchards in the summer and winter rainfall areas of the country. The data used were collected in the period 2008 to 2023. Tree species included apples, peaches, plums, nectarines, pecans, mango, macadamia, litchi, and citrus. Data from more than 25 different orchards were used in the study. The data included tree transpiration rates, measured mostly using the heat ratio method of monitoring sap flow on older trees, and thermal dissipation or Granier probes on younger orchards. Evapotranspiration (ET) was measured using the open path eddy co-variance and surface renewal systems. However, these data tended to be of short duration (a few days to weeks at most). The main reason for this is the high demand on the expensive equipment which was also needed on other projects. This also meant that the single orchard crop coefficient ( $K_c = ET/ET_o$ ) could only be calculated at these short intervals. This explains why data are analysed at different time scales in Chapter 4 of this report. The other data collected included the site microclimate, soil type, soil water content, tree dimensions, and leaf area index (LAI –  $m^2$  of leaf area per  $m^2$  of ground area). The fractional vegetation cover was only measured in a few of the orchards. So, it had to be estimated from the leaf area index.

We adopted the dual crop coefficient approach. According to this method the whole orchard crop coefficient ( $K_c$ ) is calculated as the sum of a basal crop coefficient ( $K_{cb}$ ) and a soil evaporation coefficient ( $K_e$ ).  $K_{cb}$  was calculated as the ratio of the orchard transpiration (T) to the reference crop evapotranspiration ( $ET_o$ ). The reference crop evapotranspiration was calculated using the modified Penman-Monteith equation for a short grass that is healthy, actively growing, uniformly covering the ground, and not short of water. The single crop coefficient ( $K_c$ ) was calculated as the ratio of the actual

evapotranspiration to  $ET_o$  while the soil evaporation coefficient ( $K_e$ ) was derived as the difference between  $K_c$  and  $K_{cb}$  (Allen et al., 1998).

The database is presented in the form of a Smartphone Application (hereafter called the APP). The landing page of the APP has two icons namely the “**Experimental Crop Coefficients**” and the “**Derived Crop Coefficients**”. The experimental crop coefficients are determined from the observed values at a specific location based on the actual measured experimental data. To facilitate their transfer to other locations, the crop coefficients are first converted into crop coefficients for the standard climate using equations proposed in the FAO 56 paper (Allen et al., 1998) – see equations 7 and 8 in Chapter 2. Figure I shows a schematic illustration of the sequence of computations to arrive at the user crop coefficients. According to the FAO 56, standard crop coefficients are defined as values that are determined for a temperate sub-humid climate with long-term average wind speeds around  $2.0 \text{ m s}^{-1}$  measured at 2.0 m height, and minimum relative humidity around 45%. The standard crop coefficients can be used to recalculate the required crop coefficients at a given location provided the user has climatic and tree height data for the orchard of interest. In the APP, long-term climate data is provided for every quaternary catchment in the country from a 50-year daily climate record spanning from 1950 to 1999 developed by the ACRU team (Schulze, 2012). When the user enters the coordinates of their orchard and tree height (which are required inputs), the APP links them to a weather station located at the centroid of the nearest quaternary catchment. The APP then does the conversion from the standard to the actual crop coefficients at the site of interest as illustrated in Figure I.

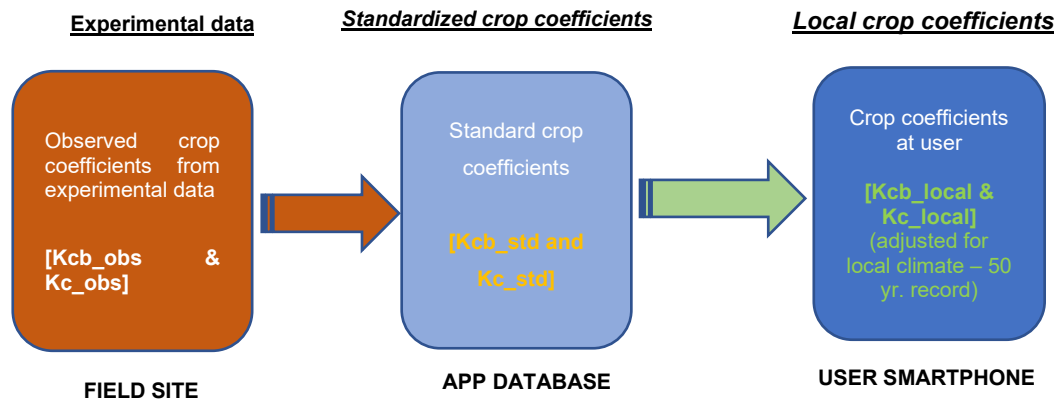


Figure 1. Schematic representation of the determination of the “Experimental Crop Coefficients” in the APP.

This approach maintains the integrity of the actual field observed crop coefficients as the conversions are done using internationally accepted equations. To address the question of transferability of the tabulated crop coefficients, Allen and Pereira (2009) proposed a method to derive crop coefficients from readily available data, effectively extending the FAO 56 methodology. Input data required in this method includes the average vegetation height, fractional vegetation cover, and a stomatal sensitivity factor. They defined a canopy density function ( $K_d$ ) which is dependent on the amount of foliage in each canopy. The stomatal sensitivity factor differentiates the transpiration response of different crop species which may have the same fractional cover and height. While the Allen and Pereira (2009) approach (hereafter called the A&P method) has been successfully validated on most annual crops, its implementation on fruit tree orchards has been unsuccessful so far. Despite these difficulties, the A&P method has a huge potential to address one of the objectives of this study, namely to develop a methodology for estimating missing crop coefficients using readily available data. Secondly, the approach lends itself to automation, so it is possible to include this method in the APP as the “Derived Crop Coefficients” tab. The derived crop coefficients allow the user to input information that is relevant to their specific orchard

and to get reasonably accurate estimates of the crop coefficients. So, in this study we have investigated possible improvements to the A&P approach using data from a range of commercial tree crops grown in South Africa.

## **RESULTS AND DISCUSSION**

Most of our efforts were aimed at finding a general solution to the A&P method for fruit tree crops especially the stomatal sensitivity function which is most difficult to determine for tree crops. In the original A&P method, the stomatal sensitivity factor ( $F_r$ ) is calculated from, among other things, the ratio of the leaf resistance ( $r_l$ ) of the specific crop to a reference standard value of  $100 \text{ s m}^{-1}$  which is the mean resistance of annual crops. Applying the original resistance parameters as recommended by Allen and Pereira (2009) to a selection of tree crops led to errors exceeding 110% for different apple, citrus, and olive cultivars (Dzikiti et al., 2018a; Gush and Taylor, 2014).

Given the physiological differences between tree and herbaceous annual crops, we suspect that use of the constant standard resistance of  $100 \text{ s m}^{-1}$  for all crop types is a major source of uncertainty in the A&P method. In this study, we replaced this value with a crop-specific empirical parameter  $\alpha$  and we recalculated this value for each tree crop. This was feasible because in most instances, all the input data required to calculate this parameter were measured. So, we effectively proposed a new crop-specific reference that is different from the one used by A&P (2009). The calculated values of  $\alpha$  ranged from 19 to  $37 \text{ s m}^{-1}$  for pome and stone fruit. This reached up to  $200 \text{ s m}^{-1}$  for the low transpiring citrus and macadamia species. So, no single standard resistance value seems to be applicable for the range of fruit tree crops included in this study. A value around  $20 \text{ s m}^{-1}$  appeared to work for most species, but

certainly not for citrus and macadamia orchards. Within the APP, indicative values of parameter  $\alpha$  and the mean leaf resistance ( $r_l$ ) for each species exist in a “crops database”. The user is pointed to the appropriate values when they select the crop type. So, they do not have to grapple with onerous calculations to determine these.

Next, validations of the derived crop coefficients were done by comparing them with the observed values. In particular, we sought to answer the question: “*if the user were to use the crop coefficients derived by the APP, how much error would be in their monthly water use estimates?*” We applied different statistics namely the  $R^2$ , mean absolute error (MAE) and root mean square error (RMSE) to quantify how closely the simulated water use values matched the actual measured values. Results show that for most species, simulated water use was close to the measured values except during periods of water deficit. This was not surprising because the derivation of the crop coefficients using the approach proposed here does not consider the effects of water stress either due to water deficit or excess water in the rootzone. Some species showed larger error margins either because of their unique situations (e.g. pecans which were very tall and had different aerodynamic characteristics), or the poor quality of the input data.

## **NEW KNOWLEDGE AND INNOVATION**

There are two main innovations arising from this study. From a scientific perspective, this study is the first one to assess the performance of the Allen and Pereira (2009)-method, basically an extension of the FAO 56 paper, on a range of irrigated fruit tree crops. This was possible because of the detailed data that were collected in numerous orchards in local studies. The main finding is that no unique standard resistance ( $\alpha$ ) exists for most tree crops. Generally, each species has its own standard resistance,

although a value close to  $20 \text{ s m}^{-1}$  may give reasonable estimates for pome and stone fruit. The idea of a new reference resistance for fruit tree crops was published in an international peer reviewed article by Mobe et al. (2020) and there is interest in this approach from the scientific community (Pereira et al., 2020; Pereira et al., 2021a&b).

The second innovation is that this study consolidates the existing crop coefficients derived from the local studies on fruit tree crops into a single database that can facilitate the estimation of the crop coefficients for any location in the country. The experimentally observed crop coefficients are transformed into standard values in the APP. When a user (from anywhere in the country) enters the crop type, coordinates, and average tree height, the standard crop coefficients are converted to values that are appropriate for the user's location using a 50 yr. daily climate dataset for quaternary catchment closest to them. The crop coefficients are readily accessible through the Smartphone APP.

### **CAPACITY BUILDING**

One MSc student graduated summa cum laude from this project. The student's thesis entitled "Determining crop coefficients for irrigated fruit tree crops" was registered with the Institute for Water Studies at the University of the Western Cape.

Further capacity building proved difficult on the project mostly due to staff turnover which saw the project lag behind by up to 9 months. The team is sincerely grateful to the WRC for working out an emergency plan to rescue this project.

Results from this study were presented at the 10<sup>th</sup> International Symposium on the Irrigation of Horticultural Crops held in Stellenbosch from 29 January to 2 February 2023.

## **CONCLUSIONS**

This study has attempted to put together the data on crop water use that has been collected in past projects into a single platform that can be used for irrigation decision making. We analysed data from various fruit tree crops that fall into the broad categories of deciduous fruit, subtropical fruit, and citrus growing in the summer and winter rainfall areas of the country. Tabulated crop coefficients were created using locally measured data and these were standardized into a format that facilitates their transferability from one location to another. While many approaches have been proposed in literature to derive crop coefficients from readily available data, few are amenable to automation than the A&P approach. This study attempted to close an important information gap regarding the applicability of the A&P method on fruit tree orchards using measured data from different fruit types. These data were included in a Smartphone application that is the end product of this project. Target users for the APP include farmers, catchment managers, irrigation boards, and researchers.

## **RECOMMENDATIONS FOR FUTURE RESEARCH**

Further research is required to address the following:

- 1) While the current APP has been validated for selected tree crops, there is need to further test the APP with independent data to ascertain the accuracy of the outputs.
- 2) More crops should be added to the database to cover the wide range of irrigated crops in the country.

- 3) Point no 2 requires further support for primary research to collect data on water use and its environmental drivers.
- 4) Some of the methods proposed here can be built into more sophisticated decision support platforms such as SAPWAT which has the option for the user to enter their own crop coefficients. Lack of accurate crop coefficients is often cited as a major source of uncertainty of SAPWAT despite the science behind the model being sound.

## **ACKNOWLEDGEMENTS**

This project was initiated, funded, and managed by the Water Research Commission. Their support is sincerely appreciated. Additional funding from the CSIR Parliamentary Grant, project no P1DHS01 (PG: Smart Water Saving Technologies) is also gratefully acknowledged. We also thank various researchers who have provided the data used in this project namely Dr Mark Gush (Formerly CSIR, now with the Royal Horticultural Society in the UK) and Dr Nicolette Taylor (University of Pretoria) and the various students who took part in the data collection. We also thank the various farmers who allowed data to be collected on their productive farms.

Lastly, we gratefully acknowledge the guidance and advice from the following members of the project reference group:

Dr G Backeberg	Water Research Commission (retired)
Prof S Mpandeli	Water Research Commission
Dr L Nhamo	Water Research Commission (Chairman)
Dr S Hlophe-Ginindza	Water Research Commission
Miss M Kapari	Water Research Commission
Prof JG Annandale	University of Pretoria
Prof A Singels	South African Sugarcane Research Institute
Prof S Walker	Agricultural Research Council
Dr T Volschenk	Agricultural Research Council

## TABLE OF CONTENTS

EXECUTIVE SUMMARY.....	i
NEW KNOWLEDGE AND INNOVATION.....	viii
RECOMMENDATIONS FOR FUTURE RESEARCH .....	x
ACKNOWLEDGEMENTS .....	xii
LIST OF ABBREVIATIONS AND SYMBOLS .....	xv
LIST OF FIGURES.....	xvii
LIST OF TABLES.....	xxiv
CHAPTER 1: INTRODUCTION.....	1
1.1 RESEARCH BACKGROUND .....	1
1.2 THE PROPOSED SOLUTION .....	3
1.3 AIMS AND OBJECTIVES .....	4
CHAPTER 2: KNOWLEDGE REVIEW.....	5
2.1 INTRODUCTION .....	5
2.2 CROP COEFFICIENTS FOR IRRIGATED CROPS.....	7
2.2.1 Single and dual crop coefficient concepts.....	7
2.2.2 The crop coefficient curve .....	10
2.2.3 Limits of maximum crop coefficients .....	12
2.2.4 Transferability of crop coefficients and adjustment to standard conditions .....	14
2.3 SOURCES AND ACCURACY OF FIELD DATA FOR DERIVING CROP COEFFICIENTS.....	15
2.3.1 Evapotranspiration measurements.....	15
2.3.2 Transpiration measurements.....	24
2.4 CONCLUSIONS.....	34
CHAPTER 3: DERIVATION OF CROP COEFFICIENTS FROM TREE HEIGHT AND VEGETATION COVER .....	35
3.1 INTRODUCTION .....	35
3.2 CALCULATION OF THE BASAL CROP COEFFICIENT ( $K_{cb}$ ).....	37

3.3 SINGLE CROP COEFFICIENT (Kc) .....	45
CHAPTER 4: VALIDATION OF CALCULATED CROP COEFFICIENTS FOR TREE CROPS .....	48
4.1 INTRODUCTION .....	48
4.2 VALIDATION OF CROP COEFFICIENTS AND WATER USE SIMULATIONS .....	49
4.2.1 Deciduous fruit tree orchards .....	49
4.2.2 Evergreen subtropical fruit tree orchards .....	93
4.2.3 Citrus orchards.....	111
4.3 CONCLUSIONS.....	127
CHAPTER 5: DEVELOPMENT OF AN ONLINE CROP COEFFICIENTS DATABASE FOR IRRIGATED TREE CROPS .....	128
5.1 DESCRIPTION OF THE CROP COEFFICIENTS SMARTPHONE APPLICATION .....	128
5.2. EXPERIMENTAL CROP COEFFICIENTS .....	130
5.3 DERIVED CROP COEFFICIENTS .....	132
CHAPTER 6: CONCLUSIONS AND RECOMMENDATIONS .....	135
REFERENCES.....	137
CAPACITY BUILDING .....	148
Staff development .....	148
Community development .....	148
Institutional development .....	148
Students on course for graduation .....	148
KNOWLEDGE DISSEMINATION & TECHNOLOGY TRANSFER .....	148
Scientific articles .....	148
Popular articles .....	148
APPENDIX A.....	149

## LIST OF ABBREVIATIONS AND SYMBOLS

### Roman symbols

A	Branch leaf area	cm <sup>2</sup>
A <sub>st</sub>	Stem cross sectional area	cm <sup>2</sup>
C <sub>p</sub>	Specific heat at constant pressure	J kg <sup>-1</sup> K <sup>-1</sup>
d	Zero plane displacement height	m
E	Soil evaporation	mm d <sup>-1</sup>
e <sub>a</sub>	Actual vapor pressure of the air	kPa
e <sub>sat</sub>	Saturation vapor pressure of the air	kPa
ET	Actual evapotranspiration	mm d <sup>-1</sup>
ET <sub>o</sub>	Reference evapotranspiration	mm d <sup>-1</sup>
G	Soil heat flux	W m <sup>-2</sup>
g <sub>m</sub>	Maximum surface conductance	m s <sup>-1</sup>
g <sub>s</sub>	Surface conductance	m s <sup>-1</sup>
H	Sensible heat flux	W m <sup>-2</sup>
k	Extinction coefficient	-
k <sub>d1</sub>	Parameter for VPD stress factor	kPa <sup>-1</sup>
K <sub>sh</sub>	Radial sheath conductance	W K <sup>-1</sup>
k <sub>st</sub>	Stem thermal conductivity	W m <sup>-1</sup> K <sup>-1</sup>
LAI	Leaf area index	-
Ma	Molar mass of air	g
Mw	Molar mass of water vapor	g
Pa	Atmospheric pressure	kPa
P <sub>in</sub>	Input power	W
q <sub>f</sub>	Heat carried by sap	W
q <sub>r</sub>	Radial heat loss across instrument	W
q <sub>v</sub>	Axial heat conduction along stem	W
r <sub>a</sub>	Aerodynamic resistance	s m <sup>-1</sup>
RH	Average relative humidity	%
RH <sub>max</sub>	Maximum relative humidity	%
RH <sub>min</sub>	Minimum relative humidity	%
R <sub>n</sub>	Net all wave radiation	W m <sup>-2</sup>
R <sub>ns</sub>	Net shortwave radiation	W m <sup>-2</sup>

$R_{nl}$	Net longwave radiation	$W m^{-2}$
$R_s$	Shortwave radiation	$W m^{-2}$
$r_s$	Stomatal resistance	$s m^{-1}$
$R_{so}$	Clear sky shortwave radiation	$W m^{-2}$
SF	Stem sap flow	$g h^{-1}$
SWC	Soil water content	$cm^3 cm^{-3}$
$SWC_{max}$	Soil water content at saturation	$cm^3 cm^{-3}$
$SWC_{min}$	Soil water content at the wilting point	$cm^3 cm^{-3}$
T	Average air temperature	$^{\circ}C$
$T_a$	Gauge temperature downstream of heater	$^{\circ}C$
$T_b$	Gauge temperature upstream of heater	$^{\circ}C$
$T_c$	Area averaged transpiration	$mm d^{-1}$
$T_{max}$	Maximum air temperature	$^{\circ}C$
$T_{min}$	Minimum air temperature	$^{\circ}C$
$u_2$	Wind speed at 2.0 m.	$m s^{-1}$
VPD	Vapor pressure deficit of the air	kPa
$VPD_{open}$	Vapor pressure deficit for stomata to open	kPa
x	Thermocouple gauge spacing	cm
$z_h$	Height of measurement of relative humidity	m
$z_m$	Height of measurement of wind speed	m
$z_{oh}$	Roughness length for heat and humidity	m
$z_{om}$	Roughness length for momentum transfer	m

### **Greek symbols**

$\alpha$	surface albedo	-
$\Delta$	slope of saturation vapor pressure vs temperature curve	$kPa K^{-1}$
$\rho$	density of air	$kg m^{-3}$
$\epsilon_a$	emissivity of the air	-
$\epsilon_s$	emissivity of the surface	-
$\gamma$	psychrometric constant	$kPa K^{-1}$
$\lambda$	latent heat of vaporization	$J kg^{-1}$

## LIST OF FIGURES

Figure 2.1: The four-stage segmented crop coefficient curve (after Allen and Pereira, 2009).....	11
Figure 2.2: Schematic representation of an eddy covariance micrometeorology .....	19
Figure 2.3: An ideal surface renewal analysis ramp model with ramp amplitude for stable ( $a > 0$ ) and unstable ( $a < 0$ ) conditions, ramp period $L_r$ , quiescent period $L_q$ – during which there is no change in air temperature (after Mengistu and Savage, 2010). $\tau = L_r + L_q$ is the total ramp period.....	20
Figure 2.4: Components of the soil water balance in the root zone of plants (after Allen et al., 1998). .....	23
Figure 2.5: Schematic representation of the heat balance sap flow gauge (Dynamax, Houston, TX, USA). (a) Vertical section through the stem heat balance sap flow gauge. (b) Energy balance components of the heat balance sap flow sensor. ....	25
Figure 2.6: Measurement of transpiration in young orchards using Granier probes.	29
Figure 2.7: Schematic diagram of the heat ratio method (HRM) of monitoring sap flow (after Rafael Oliveira).....	32
Figure 3.1: Schematic illustrating the fractional cover ( $f_c$ ) and the effective fractional cover (after Allen and Pereira, 2009).....	38
Figure 3.2: Basal crop coefficients for: (a) low, (b) medium and (c) high canopy cover apple orchards in the Western Cape derived using the original Allen and Pereira parameters for apple orchards (after Mobe et al., 2020).....	40
Figure 3 3: Stem heat balance sap flow sensor measuring transpiration by grass species on the floor of an apple orchard. ....	42

Figure 3.4: Comparison of grass transpiration measured using a stem heat balance sap flow gauge with that measured with an infrared gas analyser (Ntshidi et al., 2021a; published in the Agricultural Water Management journal). .....	44
Figure 4.1: Alpine nectarine orchard at Ou Stasie Farm in Wolseley, Western Cape (after Gush and Taylor, 2014). .....	50
Figure 4.2: Comparison of the observed $K_{cb}$ (open circles) and the 4-stage $K_{cb}$ curve (orange line) for a mature Alpine nectarine orchard in Wolseley, Western Cape. ....	54
Figure 4.3: Comparison of the measured and simulated weekly $K_{cb}$ for a mature Alpine nectarine at Wolseley, Western Cape. ....	55
Figure 4.4: Measured vs simulated daily $K_c$ for a mature Alpine nectarine orchard in Wolseley, Western Cape. ....	55
Figure 4.5: Seasonal changes in the simulated daily crop coefficients for a mature Alpine nectarine orchard at Wolseley in the Western Cape. ....	57
Figure 4.6: Comparison of measured and modelled monthly total transpiration for the Alpine nectarine orchard at Wolseley, Western Cape. ....	58
Figure 4.7: An Alpine nectarine orchard at Rustenburg, in the Northwest Province (after Gush and Taylor, 2014). ....	59
Figure 4.8: Comparison of the measured $K_{cb}$ of the nectarine orchard at Rustenburg against the four stage $K_{cb}$ curve. ....	61
Figure 4.9: Comparison of the measured and derived $K_{cb}$ values for an Alpine nectarine orchard in Rustenburg, Northwest Province. ....	61
Figure 4.10: Comparison of the measured and modelled monthly transpiration by an Alpine nectarine orchard in Rustenburg, Northwest Province. ....	62
Figure 4.11: Four-year-old Juliepretty peach orchard at Denou Farm in Ceres, Western Cape (after Dzikiti and Schachtschneider, 2015). ....	63

Figure 4.12: Comparison of the measured and modelled weekly $K_{cb}$ for a mature peach orchard at Ceres, Western Cape Province. ....	66
Figure 4.13: Comparison of the $K_c$ values from actual measurements (black continuous line) with the simulated values (orange circles).....	67
Figure 4.14: Seasonal changes in the crop coefficients for a peach orchard in Ceres simulated using the modified A&P method.....	68
Figure 4.15: Comparison of the measured vs simulated weekly transpiration for the peach orchard at Ceres.....	68
Figure 4.16: Transvalia peach orchard at Rustenburg in the Northwest. ....	69
Figure 4.17: Weekly $K_{cb}$ values for a peach orchard at Rustenburg, Northwest Province in relation to the four-stage curve. ....	71
Figure 4.18: Comparison of the actual weekly $K_{cb}$ (black line) measured in a mature peach orchard in Rustenburg, Northwest Province with simulated values (orange circles).....	71
Figure 4.19: Crop coefficients for a peach orchard at Rustenburg, Northwest Province. ....	72
Figure 4.20: Comparison of the measured vs modelled monthly transpiration of a peach orchard in Rustenburg, Northwest Province. ....	73
Figure 4.21: An African Delight plum orchard at Sonskyn farm in Robertson, Western Cape (after Dzikiti and Schachtschneider, 2015). ....	74
Figure 4.22: Comparison of the measured and simulated $K_{cb}$ for a mature plum orchard in Robertson, Western Cape Province. ....	77
Figure 4.23: Validation of the calculated $K_c$ values (orange circles) with measured data in a plum orchard at Robertson, Western Cape. ....	77

Figure 4.24: Comparison of the actual measured transpiration by the plum orchard at Robertson with the simulated values.....	78
Figure 4.25: Pecan orchard at Cullinan, Gauteng (after Gush and Taylor, 2014). ...	79
Figure 4.26: Comparison of the measured and simulated $K_{cb}$ curve for a mature pecan orchard at Culinan, Gauteng.....	82
Figure 4.27: Comparison of the measured and simulated $K_c$ for a mature pecan orchard at Culinan, Gauteng. ....	83
Figure 4.28: Measured vs simulated monthly transpiration for a mature pecan orchard in Culinan, Gauteng. ....	83
Figure 4.29: Measured vs simulated monthly evapotranspiration for a mature pecan orchard in Culinan, Gauteng. ....	84
Figure 4.30: Typical layout of an apple orchard in the Western Cape. $T$ is transpiration by the trees, $T_c$ transpiration from the cover crop, $E_{dz}$ – soil evaporation from the dry zone, $E_{wz}$ – soil evaporation from the wetted zone (after Dzikiti et al., 2018a).....	85
Figure 4.31: Illustration of the performance of the improved Allen and Pereira basal crop coefficient calculation method on ‘Golden Delicious’ and ‘Cripps’ Pink apple cultivars in: (a-b) – high canopy cover, (c-d) – medium canopy cover, and (e-f) – low canopy cover orchards (after Mobe et al., 2020).....	88
Figure 4.32: (a) Comparison of the crop coefficients determined with the improved A&P method with measured values for 12 apple orchards. (b) Evapotranspiration predicted using the improved crop coefficients and measured by the eddy covariance system.....	89

Figure 4.33: Comparison of the measured and calculated monthly total transpiration rates of orchards with high (a), medium (b) and low canopy cover (c) (after Mobe et al., 2020).	91
Figure 4.34: Mature mango orchard at Riverside farm in Malelane, Mpumalanga province.	93
Figure 4.35: Crop coefficient curve for a mature mango orchard in Malelane, Mpumalanga Province.	96
Figure 4.36: Observed vs simulated weekly $K_{cb}$ for a mature mango orchard in Malelane, Mpumalanga Province.	97
Figure 4.37: Measured vs simulated $K_c$ values for a mature mango orchard in Malelane, Mpumalanga.	97
Figure 4.38: Seasonal changes in the simulated daily crop coefficients for a mango orchard in Malelane, Mpumalanga Province.	98
Figure 4.39: Comparison of the measured vs simulated monthly total transpiration for a mango orchard in Malelane, Mpumalanga Province.	99
Figure 4.40: Macadamia orchard at White River in Mpumalanga Province (after Gush and Taylor, 2014).	100
Figure 4.41: Comparison of the measured and simulated $K_{cb}$ for a mature macadamia orchard in White River, Mpumalanga Province.	105
Figure 4.42: Comparison of the measured and simulated $K_c$ for a mature macadamia orchard in White River, Mpumalanga Province.	105
Figure 4.43: Comparison of the measured and simulated transpiration for a mature macadamia orchard in White River, Mpumalanga Province.	106
Figure 4.44: Drone image of the litchi orchard at Riverside farm in Malelane, Mpumalanga.	107

Figure 4.45: Comparison of the measured and simulated weekly $K_{cb}$ for a mature litchi orchard in Malelane, Mpumalanga Province. ....	109
Figure 4.46: Seasonal changes in the crop coefficients for a mature litchi orchard at Malelane, Mpumalanga Province. ....	110
Figure 4.47: Comparison of the measured and simulated monthly transpiration for a mature litchi orchard at Malelane, Mpumalanga Province.....	111
Figure 4.48: View of the Rustenburg Navel citrus orchard in Citrusdal, Western Cape (after Gush and Taylor, 2014). ....	112
Figure 4.49: Comparison of the observed and calculated $K_{cb}$ for a Rustenburg navel citrus orchard in Citrusdal, Western Cape.....	114
Figure 4.50: Seasonal variations in the crop coefficients for a mature Rustenburg navel citrus orchard in Citrusdal, Western Cape. ....	115
Figure 4.51: Comparison of the measured and simulated monthly transpiration by a mature Rustenburg Navel. ....	116
Figure 4.52: View of the Midnight Valencia orange orchard in Malelane (after Gush and Taylor, 2014). ....	117
Figure 4.53: Comparison of the observed and calculated $K_{cb}$ for a Midnight Valencia citrus orchard in Malelane, Mpumalanga.....	119
Figure 4.54: Comparison of the observed and calculated weekly $K_c$ for a Midnight Valencia citrus orchard in Malelane, Mpumalanga Province. ....	120
Figure 4.55: Simulated daily crop coefficients for a Midnight Valencia orchard at Malelane.....	121
Figure 4.56: Bahianinha navel citrus orchard at Groblersdal, Mpumalanga (after Gush and Taylor, 2014).....	122

Figure 4.57: Comparison of the measured and simulated $K_{cb}$ for a mature Midnight Valencia orchard in Groblersdal, Mpumalanga Province.....	124
Figure 4.58: Comparison of the measured and simulated $K_c$ for a mature Bahianinha navel citrus orchard in Groblersdal, Mpumalanga Province. ....	125
Figure 4.59: Seasonal changes in the crop coefficients for a mature Bahianinha navel citrus orchard in Groblersdal, Mpumalanga. ....	125
Figure 4.60: Comparison of the measured and simulated monthly total transpiration rates for a mature Midnight Valencia orchard at Groblersdal, Mpumalanga.....	126
Figure 5.1. Landing page for the fruit orchards Crop Coefficients APP.....	129
Figure 5.2. Schematic representation of the Experimental Crop Coefficients calculator APP.....	130
Figure 5.3. Typical outputs from the experimental database for a macadamia orchard. ....	131
Figure 5.4. Derivation of the 4-stage crop coefficient curve using the modified A&P approach. ....	132
Figure 5.5. (a) Input page for the Derived crop coefficients tab; (b) range of tree crops included in the database (data not available for avocado and banana), and (c) soils information required. ....	133
Figure 5.6. (a) Wetted soil fraction information represented by default values for drip, micro sprinkler and flood, (b) user inputs based on the amount of vegetation cover on the orchard floor, and (c) tabular outputs of the crop coefficients. These can also be plotted graphically. ....	134

## LIST OF TABLES

Table 3.1: Typical Readily Evaporable Water (REW), Maximum Total Evaporable Water (TEW) for General Soil Classifications (after Allen et al., 2005).....	47
Table 4.1: Attributes of the mature nectarine orchard at Wolseley in the Western Cape.....	50
Table 4.2: Observed and standardized basal crop coefficients for a mature nectarine orchard at Wolseley, Western Cape (Gush and Taylor, 2014).....	52
Table 4.3: Observed and standardized crop coefficients on a mature nectarine Alpine orchard at Wolseley, Western Cape (Gush and Taylor, 2014).....	53
Table 4.4: Attributes of the mature nectarine orchard at Rustenburg in the Northwest Province (after Gush and Taylor, 2014). ....	59
Table 4.5: Observed and standardized basal crop coefficients for a mature Alpine nectarine orchard in the summer rainfall area in Rustenburg, Northwest Province (Gush and Taylor, 2014). ....	60
Table 4.6: Properties of the Juliepretty peach orchard in Ceres (after Dzikiti and Schachtschneider, 2015).....	64
Table 4.7: Observed and standardized basal crop coefficients for a mature peach orchard in the Western Cape Province (Dzikiti and Schachtschneider, 2015). ....	65
Table 4.8: Observed and standardized crop coefficients for a mature peach orchard in the Western Cape.....	65
Table 4.9: Observed and standardized basal crop coefficients for a peach orchard in the summer rainfall areas (Gush and Taylor, 2014).....	70
Table 4.10: Summary of the characteristics of the plum orchard at Robertson, Western Cape (after Dzikiti and Schachtschneider, 2015). ....	75

Table 4.11: Observed and standardized basal crop coefficients for a plum orchard in Robertson, Western Cape (Dzikiti and Schachtschneider, 2015).....	76
Table 4.12: Observed and standardized crop coefficients for a plum orchard in Robertson, Western Cape (Dzikiti and Schachtschneider, 2015).....	76
Table 4.13: Characteristics of the pecan orchard at Cullinan, Gauteng. ....	80
Table 4.14: Observed and standardized basal crop coefficients for pecan orchards (Gush and Taylor, 2014). ....	81
Table 4.15: Observed and standardized crop coefficients for pecan orchards (Gush and Taylor, 2014). ....	82
Table 4.16: Details of the 12 orchards used in the Koue Bokkeveld (KBV) and Elgin/Grabouw/Vyeboom/Villiersdorp (EGVV) production regions from 2014-2017. High, medium, and low canopy cover denotes >50%, 20-49% and <20% fractional vegetation cover. LAI = Leaf area index (after Mobe et al., 2020).....	86
Table 4.17: Typical soil classification analysis for the orchards of different age groups monitored at KBV and EGVV in 2014/15, 2015/16 and 2016/17 growing seasons. $\theta_{FC}$ = volumetric soil water content at field capacity; $\theta_{WP}$ =volumetric soil water content at the permanent wilting point; REW= readily evaporable water; TEW= total evaporable water, FBGD= Mature ‘Golden Delicious’, FBCP= Mature ‘Cripps Pink’, NBGR= Non-bearing ‘Golden Delicious Reinders®’, NBRG= Non-bearing ‘Rosy Glow’, NBCR= Non-bearing ‘Cripps’ Red’, BGD= Bearing ‘Golden Delicious’, BGR= Bearing ‘Golden Delicious Reinders®’ BCP= Bearing ‘Cripps Pink’.....	87
Table 4.18: Comparison between monthly predicted and measured transpiration for orchards with varying canopy cover. $R^2$ is the coefficient of determination, RMSE is the root of the mean square error, MAE is mean absolute error and N is the number of observations. ....	92

Table 4.19: Characteristics of the mature mango orchard at Riverside farm in Malelane, Mpumalanga Province.....	94
Table 4.20: Observed and standardized basal crop coefficients for mature mango orchards (Dzikiti et al., ongoing).....	95
Table 4.21: Observed and standardized crop coefficients for mature mango orchards (Dzikiti et al., ongoing).....	95
Table 4.22: Details of the macadamia orchard at White River, Mpumalanga.....	100
Table 4.23: Observed and standardized $K_{cb}$ for a mature macadamia orchard in White River, Mpumalanga (after Gush and Taylor, 2014).....	101
Table 4.24: Observed and standardized $K_c$ for a mature macadamia orchard in White River, Mpumalanga (after Gush and Taylor, 2014). ....	102
Table 4.25: Observed and standardized $K_{cb}$ for a mature macadamia orchard in Mpumalanga (Taylor et al., 2021). ....	103
Table 4.26: Observed and standardized $K^c$ for a mature macadamia orchard in Mpumalanga (after Taylor et al., 2021). ....	104
Table 4.27: Characteristics of the litchi orchard at Riverside farm, Mpumalanga...	108
Table 4.28: Characteristics of the Rustenburg navel citrus orchard at Citrusdal (after Gush and Taylor, 2014).....	112
Table 4.29: Observed and standardized basal crop coefficients for Rustenburg navel citrus at Citrusdal, Western Cape.....	113
Table 4.30: Properties of the Midnight Valencia citrus orchard at Malelane.....	117
Table 4.31: Observed and standardized basal crop coefficients for Midnight Valencia navel citrus at Malelane, Mpumalanga .....	118
Table 4.32: Observed and standardized crop coefficients for Bahianinha navel citrus at Malelane, Mpumalanga .....	119

Table 4.33: Bahianinha navel citrus orchard at Groblersdal, Mpumalanga. ....	122
Table 4.34: Observed and standardized basal crop coefficients for Midnight Valencia citrus in Groblersdal, Mpumalanga .....	123
Table 4.35: Observed and standardized crop coefficients for Midnight Valencia citrus Groblersdal, Mpumalanga. ....	123

This page was intentionally left blank

## CHAPTER 1: INTRODUCTION

### 1.1 RESEARCH BACKGROUND

South Africa's average annual rainfall (~495 mm) is lower than the global average (~840 mm) and more than 60% of the country's water resources are used for agriculture (Reinders et al., 2013). The agricultural sector is very sensitive to climatic variability and to extreme events such as droughts whose frequency and severity is expected to increase in future. Therefore, it is essential to invest in building the resilience of farmers, e.g. through increasing the area under irrigation to mitigate against the effects of climate variability and change as outlined in the National Development Plan (2030). However, given the scarce water resources in the country with about 98% of the surface water already allocated (Le Maitre et al., 2019), it is essential that water is used efficiently for the sustainability and growth of the country's agricultural sector. Competition for water between different sectors of the country's economy is also increasing. This is compelling water resources managers to find solutions to alleviate pressure on the water resources.

The second National Water Resources Strategy for South Africa (NWRS 2, 2013) cites irrigated agriculture as one of the most inefficient sectors with respect to water use. The NWRS2, estimates that between 30 and 45% of water allocated for irrigation is wasted either through leakages, poor irrigation scheduling, or other non-beneficial uses. Over the years, the WRC has supported many projects on the water use of irrigated crops in different parts of the country. This was to avail information to develop tools that can assist water managers and growers to optimize irrigation water use efficiency (Annandale et al., 2011). Some of the crops studied include cereals, e.g. maize (Jarman et al., 2014), irrigated pastures, e.g. rye and kikuyu grass

(Fessehazion et al., 2012), sugarcane (Olivier et al., 2009; Jarman et al., 2014), and fruit tree crops, e.g. citrus (Gush and Taylor, 2014), deciduous fruit trees, e.g. apples (Volschenk et al., 2003; Gush and Taylor, 2014; Dzikiti et al., 2018a&b), subtropical fruit trees such as macadamia and pecan nuts (Gush and Taylor, 2014; Taylor et al., 2021), and wine grapes (Lategan et al., 2016), among others. There have also been national scale studies that have estimated the extent of the irrigated land area in the country and the associated water use by the crops using remote sensing methods (e.g. Van Niekerk et al., 2018).

The site-specific studies collected the water use data using internationally recognized methods which include micrometeorological techniques (e.g. the open path eddy covariance system, scintillometers, surface renewal methods, etc.), soil water balance approaches, remote sensing, and various sap flow techniques in the case of tree crops. Moreover, several models have also been developed. Examples of the WRC supported irrigation models include BEWAB, PUTU, SWB, SAPWAT 3&4, and MyCanesim. The uptake and use of these models has been limited due to a range of factors which include complexity of the models, input data requirements, etc. A survey of 332 irrigation schemes in South Africa by Stevens et al. (2005) indicated that objective irrigation scheduling was being applied by only 18% of farmers. The rest relied on intuition, experience, and confidence built over many years of farming. Therefore, there is a need to further synthesize the existing field data on crop water use that has been collected throughout the entire country over the years to develop simple user-friendly tools that can be used for irrigation scheduling, irrigation planning, and irrigation system designs to improve water use efficiency.

The Food and Agricultural Organization (FAO) developed clear and robust guidelines on the derivation of accurate crop coefficients ( $K_c = ET/ET_o$ ) for various crops (Allen et al., 1998). ET is the actual evapotranspiration and  $ET_o$  is the reference evapotranspiration, calculated using readily available weather data (Allen et al., 1998). Crop coefficients are examples of how the existing water use and weather data can be distilled to provide reliable information which can be used by the farmers to guide their irrigation decisions. The extensive network of automatic weather stations owned by the Agricultural Research Council (ARC), South African Weather Services (SAWS), and individual farmers make daily weather data to be readily accessible to fruit farmers. Therefore, a comprehensive and accurate database of crop coefficients can provide valuable information for irrigation decision making. The focus of the database developed in this study is on the unstressed crop coefficients to minimize the complexities arising from incorporating water stress in the calculations. Currently there is an existing crop coefficient database which was developed for sugarcane (Olivier and Singels, 2001) and there is need to expand this to cover other irrigated crops throughout South Africa.

## **1.2 THE PROPOSED SOLUTION**

Crop coefficients are not readily transferable between fields even planted to the same crop as these vary with; i) crop growth stage, ii) wetted soil fraction, iii) canopy and orchard floor management, iv) planting density, v) irrigation system, etc. The envisaged database will: 1) include the major irrigated fruit tree crops, mainly fruit tree crops for which a substantial volume of data has been collected over the years; 2) be developed on a platform that is readily accessible, quick and easy to use by irrigation decision makers, and; 3) be easy to update when new data becomes available. The

target users of this database are irrigation farmers for irrigation scheduling and water allocation planning, irrigation boards, and catchment water managers.

Two approaches were used to develop the database. The first was to use existing field data collected from completed studies. So, the availability and accessibility of these data was critical on the range of crops included in the database and extent of validation of the crop coefficients. However, these crop coefficients were applicable only to those fields where the data were collected. The second approach was to investigate the possibility of implementing a procedure for deriving the crop coefficients from readily available data supplied by the user to match their specific field situation. Successful evaluation and improvement of this approach also depended on the availability of reliable measured data to derive the parameters for each crop.

### **1.3 AIMS AND OBJECTIVES**

The main aim of the study was to develop an online database (in the form of an APP) of crop coefficients for major irrigated fruit tree crops in South Africa for which water use data has been collected. The specific objectives were to; 1) Conduct a detailed knowledge review to document the crop coefficients from water use information derived in various studies and to identify missing crop coefficients; 2) Gather historical weather data to calculate the reference evapotranspiration and to develop a simple but accurate method to derive missing crop coefficients using readily available information; 3) Estimate the crop coefficients following the FAO's four stage crop coefficient approach, and; 4) Develop an interactive crop coefficient database with a user-friendly graphical user interface for a smartphone.

## CHAPTER 2: KNOWLEDGE REVIEW

### 2.1 INTRODUCTION

South Africa is a major global player in the export of crops, mostly fruit and vegetables (Hortgro, 2020). Given the importance of water in a country where nearly 90% of horticultural crops are produced under irrigation, there have been rapid advancements in the development of irrigation infrastructure over the years (Reinders et al., 2013). This has been necessitated, not only to maintain the country's competitiveness on the export market, but also by the increasing demand on the limited water resources. The increasing pressure on the water resources in the country is due to the growing population, increasing industrial and recreational activities, water needs for the environment, according to the country's Water Act, and droughts linked to climate variability and change (Gush et al., 2019; Ntshidi et al., 2021a).

South Africa's average annual rainfall (~495 mm) is lower than the global average (~840 mm). With agriculture consuming approximately 62% of the available water resources, there is need for equitable sharing of the resource among different sectors of the country's economy. The agricultural sector is very sensitive to climatic variability and to extreme events such as droughts whose frequency and severity is expected to increase in most parts of the country (Abiodun et al., 2019). Therefore, it is essential to invest in building the resilience of farmers, e.g. through increasing the area under irrigation to mitigate against the effects of climate variability and change as outlined in the National Development Plan (2030). However, with about 98% of the surface water already allocated (Le Maitre et al., 2019), it is essential that water is used efficiently for the sustainability and growth of the country's agricultural sector.

The second National Water Resources Strategy for South Africa (NWRS 2, 2013) cites irrigated agriculture as one of the most inefficient sectors with respect to water use. It has been reported that water allocated for irrigation is wasted either through leakages, poor irrigation scheduling, or other non-beneficial uses. These levels of water losses are clearly unsustainable in water scarce country like South Africa. According to the Irrigation Strategy for South Africa, the expansion of irrigated agriculture is critical for the future food security of the country. But with the available water resources almost fully allocated, water for future irrigation expansions can only be derived from existing allocations. This calls for more accurate information on crop water use and for precise irrigation strategies to increase water use efficiency. This need is compelling water resources managers to find solutions to alleviate the pressure on the water resources.

Significant research on crop water use has been initiated and funded by the Water Research Commission and its industry partners in recent years. The overarching aim of these projects has been to provide information on crop water requirements and to develop tools for its accurate determination. Tools, mostly models have been developed using some of these data as summarized by Annandale et al. (2011). Irrigation scheduling, i.e. deciding when to irrigate and with how much water is critical to efficient irrigation management. This can be done using atmospheric, soil or plant-based approaches. Detailed reviews of these methods were done by (Jones, 2004; Gu et al., 2014). In this Chapter we provide a brief review of the FAO 56  $K_c$ - $ET_0$  approach which is subsequently used to develop the crop coefficients database in the later chapters.

## **2.2 CROP COEFFICIENTS FOR IRRIGATED CROPS**

### **2.2.1 Single and dual crop coefficient concepts**

The FAO 56 method (Allen et al., 1998) is one of the most widely used irrigation scheduling approaches globally. And in South Africa it is no different. Recognizing the growing need for good quality weather data to, among others improve irrigation decision-making, various organizations have established weather station networks, both automatic and manual. The Agricultural Research Council (ARC), for example, maintains an agro-climate network of about 500 weather stations nationally. They have a databank of data collected at hourly and daily intervals. Other custodians of weather data are the South African Weather Service (SAWS), and the South African Sugar Research Institute (SASRI). The later covers mostly the sugarcane growing areas in the KwaZulu-Natal and Mpumalanga Provinces. Many individual farmers also have their own weather stations, so access to weather data has improved considerably in recent years.

The climate data is mostly used for irrigation scheduling, i.e. deciding when to irrigate and with how much water. For this, accurate information on evapotranspiration (ET) is required to estimate the crop water requirements (Pereira et al., 2021a). The simplicity, repeatability, and accuracy of the FAO 56 ( $K_c - ET_o$ ) approach is the main reason for the widespread use of this method which has been successfully tested on a range of crop types under different growing conditions. These include fruit tree crops (Garcia and Castel, 2007; Paco et al., 2019., Volschenk, 2017), cereals (Gontia and Tiwari, 2010; Trout and DeJonge, 2018) and root crops (Jayanthi et al., 2007), among others. According to this method, crop evapotranspiration ( $ET_c$ ) is obtained as the product of

a reference evapotranspiration and a crop coefficient (Allen et al., 1998). Reference evapotranspiration is defined as evapotranspiration from a hypothetical crop that is short (~ 12 cm tall), healthy, actively growing, uniformly covering the ground and, not short of water (Allen et al., 1998). This crop has a surface resistance of approximately  $70 \text{ s m}^{-1}$  and an albedo of about 0.23.

The reference crop evapotranspiration is a measure of the atmospheric evaporative demand since the crop is well watered and healthy and evaporation is only limited by the available energy. While  $ET_o$  has been calculated using various methods in literature, for the transferability of crop coefficients between locations, it is recommended that  $ET_o$  (in  $\text{mm d}^{-1}$ ) be calculated following the modified Penman-Monteith equation as:

$$ET_o = \frac{0.408\Delta(R_n - G) + \gamma \frac{900}{T + 273} u_2 (e_s - e_a)}{\Delta + \gamma(1 + 0.34u_2)} \quad (1)$$

where  $R_n$  (in  $\text{MJ m}^{-2} \text{ d}^{-1}$ ) is the net radiation on a short grass surface,  $G$  (in  $\text{MJ m}^{-2} \text{ d}^{-1}$ ) is the soil heat flux.  $R_n - G$  represents the energy that is available for evaporation and for conversion to sensible heat flux (energy used to warm up the air).  $\Delta$  ( $\text{kPa K}^{-1}$ ) is the slope of the saturation vapour pressure vs air temperature curve,  $\gamma$  ( $\text{kPa K}^{-1}$ ) is the psychrometric constant,  $T$  is the air temperature in degrees Celsius measured at 2.0 m height,  $e_s$  and  $e_a$  are the saturation and actual vapour pressure of the air (kPa), respectively.  $U_2$  ( $\text{m s}^{-1}$ ) is the windspeed, also measured at 2.0 m height.

The crop coefficient ( $K_c$ ), calculated as the ratio of the actual crop evapotranspiration ( $ET_c$ ) and the reference crop evapotranspiration ( $ET_o$ ), is a correction factor that

adjusts for the differences in evaporation between the actual crop and the reference crop since the characteristics of the two are different. The characteristics of the actual crop differ from those of the reference crop, e.g. through variations in planting density, vegetation height, wetted soil surface fraction, etc. Using the big leaf Penman-Monteith equation to model  $ET_c$ ,  $K_c$  is mathematically given by:

$$K_c = \frac{ET_c}{ET_o} = \frac{\frac{\Delta(R_{nc}-G_c)+\rho_a c_p(e_{sc}-e_a)/r_{a,c}}{\Delta+\gamma(1+\frac{r_{s,c}}{r_{a,c}})}}{\frac{\Delta(R_{no}-G_o)+\rho_a c_p(e_{so}-e_a)/r_{a,o}}{\Delta+\gamma(1+\frac{r_{s,o}}{r_{a,o}})}} \quad (2)$$

where  $R_{nc}$  and  $R_{no}$  are the net radiation absorbed by the crop and reference surface while  $G_o$  and  $G_c$  are the ground heat fluxes for the crop and reference surface, respectively.  $\rho_a$  is the density of air ( $\text{kg m}^{-3}$ ),  $c_p$  is the specific heat capacity of the air at constant pressure ( $\text{J kg}^{-1} \text{K}^{-1}$ ),  $e_{sc}$  (kPa) is the saturation vapour pressure at the canopy temperature. So,  $e_{sc} - e_a$  is the canopy to air vapour pressure deficit, and  $e_{so} - e_a$  is the vapour pressure deficit of the air.  $r_{a,c}$  and  $r_{a,o}$  represents the aerodynamic resistance ( $\text{s m}^{-1}$ ) to water vapour and heat transport for the crop of interest and the reference surface, respectively.  $r_{s,c}$  and  $r_{s,o}$  are the bulk surface resistance for the crop and the reference surface. Crop evapotranspiration, calculated in this way assumes no water stress. But in reality, field crops experience different kinds of stresses. These range from water deficit stress due to inadequate rainfall or irrigation, stress from excess water in the root zone under waterlogging conditions, salinity stress, heavy metals, and biotic stresses due to pests and diseases, etc. So, the FAO 56 define actual evapotranspiration ( $ET_a$ ) as:

$$ET_a = K_s K_c ET_o \quad (3)$$

Where  $K_s$  is a stress response factor with values between 0 and 1. A value of 1.0 depicts no stress. In the case of soil water deficit, calculation of  $K_s$  is often done through a soil water balance assessment. Examples of the calculation procedures are given in Allen et al. (1998; 2005).

In sparse crops such as orchards where the surface is highly heterogenous due to wide spacings between trees, the dual crop coefficient approach is often adopted wherein  $K_c$  is split into a basal crop coefficient ( $K_{cb} = T/ET_o$ ) and a soil evaporation crop coefficient ( $K_e = E_s/ET_o$ ) where  $T$  is the crop transpiration, and  $E_s$  is soil evaporation. In this case

$$K_c = K_{cb} + K_e \quad (4)$$

In the presence of stress, this expression can be rewritten as

$$K_c = K_s K_{cb} + K_e \quad (5)$$

The stress factor is applied only to the basal crop coefficient which is dependent on plant transpiration.

### **2.2.2 The crop coefficient curve**

The FAO 56 approach identified four stages that describe the growth cycle of crops. These include the initial phase when canopy cover is in the range 0 to 10%. The crop coefficient for this phase is often denoted  $K_{c\_ini}$ . This is followed by the phase of rapid development or simply the development phase with crop coefficient  $K_{c\_dev}$ . This stage

is characterized by increasing canopy cover and height of the crop until maximum values are reached. The phase corresponding to maximum canopy cover is the mid-season phase with crop coefficient  $K_{c\_mid}$ . During this stage, very little changes in canopy cover occurs and the crop coefficient is maximum. This stage is followed by the maturity phase of the crop. Canopy cover again starts to decline towards or post harvesting as the leaves senesce. This represents the end or late season stage ( $K_{c\_end}$ ). All these phases can be represented by the segmented four stage crop coefficient curve shown in Figure 2.1. The shape and phases of the  $K_c$  curve are similar to those of the  $K_{cb}$  curve although they obviously differ in magnitude.

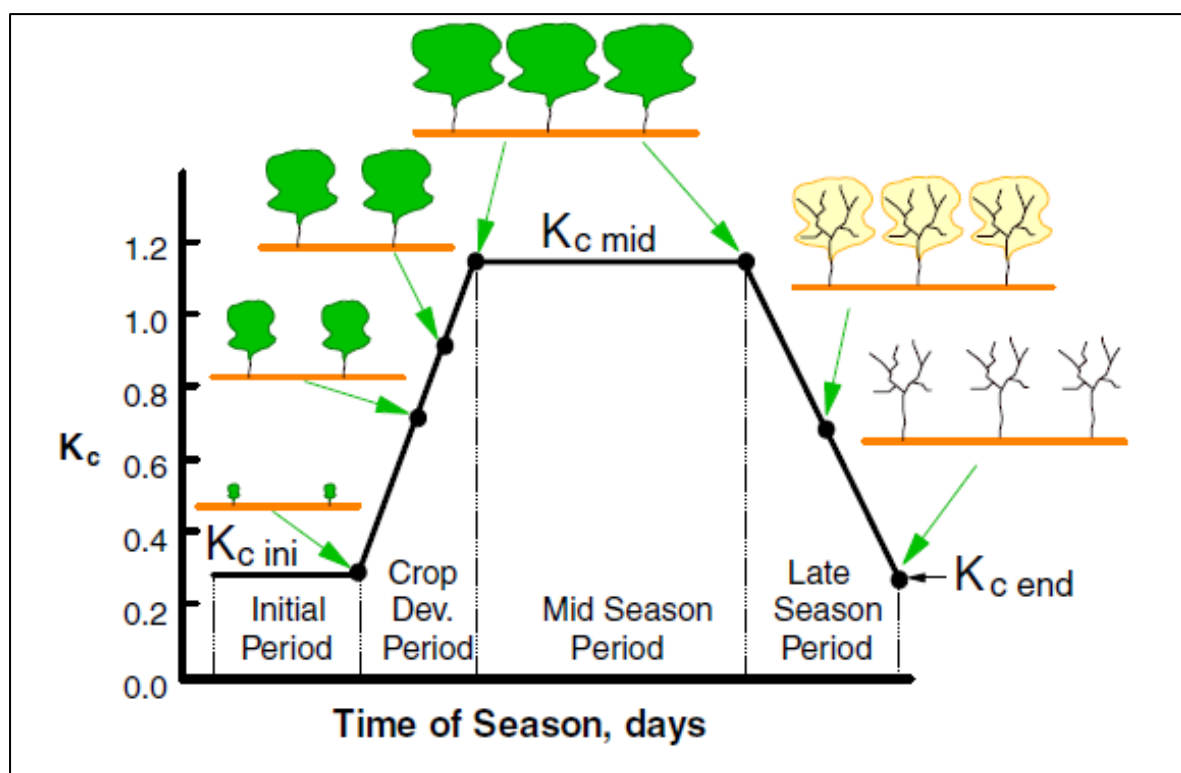


Figure 2.1: The four-stage segmented crop coefficient curve (after Allen and Pereira, 2009).

In published literature the crop coefficient curves have been presented in various forms, mostly as polynomials (Ibraimo et al., 2016; Dzikiti et al., 2018a). The challenge with this way of presenting is that it is difficult to reproduce the curves outside the area where they were produced. However, reproducibility is the main advantage of the FAO 56 four stage crop coefficient curve. To produce the full curve, only three points are needed at the initial ( $K_{c\_ini}$ ), mid-season ( $K_{c\_mid}$ ) and at the late ( $K_{c\_end}$ ) stage. If the length of each growth stage is known, then the curve can be drawn by interpolation between the successive stages. Given the huge variability in the length of the various phenological stages due to differences in growing conditions, it is recommended that the length of the growth stages be determined at each site or growing region. If the growth curve is produced under standard climatic conditions, then adjustments for local conditions that affect the aerodynamic properties of the crop namely the windspeed, minimum relative humidity and vegetation height are required as detailed in the FAO 56 and other sources (Allen et al., 1998; Pereira et al., 2020).

### **2.2.3 Limits of maximum crop coefficients**

The maximum values for crop coefficients reported in literature vary greatly as a function of numerous factors and Pereira et al. (2021) gives a comprehensive review of these. Some of the causes of unusually high or unrealistic crop coefficients include; 1) inaccurate actual evapotranspiration measurements, 2) different methods for calculating the reference evapotranspiration, 3) inappropriate experimental designs, e.g. using microclimatic methods to measure  $ET_a$  in fields with insufficient fetch leading to the so-called clothesline effect, 4) inadequate or lack of post processing of high frequency data, especially with methods such as the eddy covariance technique,

among others. Evapotranspiration from a crop field is driven by the available energy ( $R_n - G$ ) and can be represented by the shortened surface energy balance equation:

$$R_n - G = H + LE \quad (\text{W m}^{-2}) \quad (6)$$

where  $H$  is the sensible heat flux, and  $LE$  is the energy equivalent of evapotranspiration. Under normal circumstances,  $LE$  is not expected to exceed the available energy. But when this happens, the extra energy must be supplied in the form of  $H$  leading to very low or even negative sensible heat values (Pereira et al., 2021b). The negative sensible heat can be supplied by descending air parcels during convective energy transfer or by advection. The descending sensible heat flux is supplied by the wind, so it is dependent on the aerodynamic properties of the field, and this imposes an upper limit by which  $LE$  can exceed the available energy based on the principle of conservation of energy. Pereira et al. (2021b) gives a detailed review of the role of advection in the surface energy balance and in the resulting  $K_c$  values. According to this review, the maximum  $K_c$  values are usually around 1.2, but these can rise to about 1.3. Under exceptional circumstances, this can even get to 1.4. So generally, the peak values of  $K_c$  can be anywhere in the range 1.2-1.4, and not higher. Otherwise, the principle of conservation of energy is violated. High values of crop coefficients can be expected using micrometeorological methods in fields with small size where the boundary layer equilibrium is not well established above the field. Therefore, adequate fetch is a critical consideration to ensure accurate results that can be compared between sites.

## 2.2.4 Transferability of crop coefficients and adjustment to standard conditions

The FAO 56 method uses crop coefficients that are derived using reference evapotranspiration calculated using the standardized Penman-Monteith equation. However, alternative methods for calculating  $ET_o$  are also available. However, the use of  $K_c$  values derived this way are only acceptable for local conditions (Pereira et al., 2021a). They cannot be readily transferred outside the area where they were derived. For the transferability of crop coefficients from one region to another, there is need to convert these to standard  $K_c$  values. Allen et al. (1998) defined standard  $K_c$  as values that represent the relative fraction of  $ET_o$  that is governed by the amount, type and condition of a given crop type under standard pristine conditions. Standard climatic conditions are defined to resemble a temperate sub-humid climate where the FAO 56 crop coefficients were derived. These conditions are characterized by mean daily wind speeds of approximately  $2.0 \text{ m s}^{-1}$  and minimum relative humidity around 45% (Allen et al., 1998). Any deviations from these conditions require that the crop coefficients be corrected for these under local conditions of the user.

Standard  $K_c$  values are generally regarded as transferable among regions subject to adjustment for local climate under the assumption that the  $ET_o$  accounts for nearly all weather related  $ET_c$  variations (Pereira et al., 2021a). For example, if a specific location has average windspeed at 2.0 m height of  $U_2 \text{ m s}^{-1}$  and minimum relative humidity of  $RH_{min}$  (%), and if the observed crop coefficients are  $K_{c\_obs}$ , then the standard crop coefficients ( $K_{c\_std}$ ) can be calculated by rearranging the equation:

$$K_{c_{obs}} = K_{c_{std}} + [0.04(u_2 - 2) - 0.004(RH_{min} - 45)](h^{0.3}/3^{0.3}) \quad (7)$$

where  $h$  is the average height of the crop. The same mathematical representation can be used to derive standard basal crop coefficients ( $K_{cb\_std}$ ) from locally observed values ( $K_{cb\_obs}$ ) as:

$$K_{cb_{obs}} = K_{cb_{std}} + [0.04(u_2 - 2) - 0.004(RH_{min} - 45)](h^{0.3}/3^{0.3}) \quad (8)$$

To obtain the crop coefficients for a given crop at any other site, the user converts the standard  $K_c$  values to estimates for their region by adjusting for the local microclimate according to equations 7 and 8.

## **2.3 SOURCES AND ACCURACY OF FIELD DATA FOR DERIVING CROP COEFFICIENTS**

### **2.3.1 Evapotranspiration measurements**

Accurate measurements of crop evapotranspiration ( $ET_c$ ) are key to the derivation of accurate crop coefficients ( $K_c = ET_c/ET_o$ ). Earlier estimates of the water requirements of irrigated crops in South Africa were done mostly using Class A evaporation pans and lysimeters (Green, 1985; Dent, 1988). However, significant uncertainties were observed, especially with the Class A pan (Annandale et al., 2011). This has necessitated further research to update the crop water use information using more recent measurement and modelling techniques (Gush and Taylor, 2014). Several methods have been developed in recent years to quantify evapotranspiration in crop fields and the natural environment. Most widely used techniques include micrometeorological methods such as the eddy covariance technique (also called eddy correlation), scintillometers, surface renewal system, and the Bowen Ratio Energy Balance method.

Other methods include sap flow monitoring techniques, but these measure only the transpiration component of  $ET_c$  (Steppe et al., 2010; Dzikiti et al., 2010). Remote sensing methods have also been developed and tested on various crops in South Africa with products such as the Surface Energy Balance for Land (SEBAL) (Bastiaanssen et al., 1998) and ET from Fruitlook (Bastiaanssen et al., 2012) being most popular with farmers. The soil water balance method, using a range of soil moisture sensors that include neutron probes, time domain reflectometers and capacitance probes remains the widely used method both in research and for practical irrigation management. A detailed review on the advantages and disadvantages of the various  $ET_c$  estimation methods was published by Allen et al. (2011a). They further provided details on critical information for the reporting of  $ET_c$  data to allow users to discern between good and bad quality data (Allen et al., 2011b). These techniques differ in their level of complexity, operating principles, and the assumptions behind them. In the next section we summarize only those methods that have been used on South African crops. More complete details can be found in the references cited. The most widely used methods include the eddy covariance, surface renewal, soil water balance, sap flow and remote sensing approaches.

### ***2.3.1.1 Eddy Covariance Method***

The open path eddy covariance technique (Figure 2.2) is the most widely used micrometeorological technique for quantifying evapotranspiration over large fields (Dzikiti et al., 2018a&b; Paco et al., 2019; Ntshidi et al., 2021a). It also measures atmospheric  $CO_2$  concentration and other trace gases such as Ozone and methane ( $CH_4$ ). So, it is a valuable tool for studying ecosystem exchanges and can be used climate change studies. The eddy covariance technique is based on the principle that fluxes of momentum, heat and mass over crop canopies are due to the swirling

movement of small pockets of air called eddies that cause air turbulence (Campbell and Norman, 1998). These fluxes can be determined by taking measurements of air temperature ( $T_a$ ) and vertical wind speed ( $\omega$ ) at high frequencies, typically at 10-20 Hz, and by calculating the covariance between them:

$$H = \rho C_p \sum (\omega - \bar{\omega})(T_a - \bar{T}_a) \quad (9)$$

where  $H$  is the sensible heat flux (in  $W m^{-2}$ ),  $\rho$  is the density of air,  $C_p$  is the specific heat capacity of air at constant pressure, and  $T_a$  is the air temperature. The wind speed  $\omega$  and  $T_a$  are measured using sonic anemometers and there are various types that are commercially available. The latent heat flux (LE), which is the energy equivalent of evapotranspiration (ET), can be calculated in two ways. Firstly, as a residual of the surface energy balance equation (equation 6) if all other terms are known. The disadvantages of this approach are that; (a) the calculation assumes energy balance closure (Burba and Anderson, 2010) which is often problematic, and (b) the net radiation ( $R_n$ ) and soil heat flux ( $G$ ) must be accurately measured (Allen et al., 2011a).

Secondly, direct measurement of ET using the eddy covariance method can also be done through the covariance of the vertical wind speed and the atmospheric water vapor concentration ( $e$ ) measured using an infrared gas analyser (IRGA) as:

$$LE = \lambda \frac{M_w/M_a}{P_a} \rho_a \overline{\omega' e'} \quad (10)$$

where  $M_w$  and  $M_a$  are the molar masses of water vapor and air ( $g mol^{-1}$ ),  $P_a$  is the atmospheric pressure (kPa),  $\omega'$  is the instantaneous deviation of the vertical wind

speed, and  $e'$  is the air's vapor pressure and  $\lambda$  is the latent heat of vaporization. The eddy covariance equipment is quite complex, and it requires trained personnel in the field of biophysics, atmospheric sciences, and electronics for its proper operation. According to Allen et al. (2011a), inappropriate use of the equipment can lead to misleading information with errors in the range 30-50%. So, great care is required in the installation of the equipment, data collection, and processing.

A major requirement for appropriate use of the eddy covariance are fields that are large in spatial extent to ensure adequate fetch (Monteith and Unsworth, 1990). Typically for every one-meter height of the infrared and sonic sensors above the crop, an upwind fetch of at least 100 m is required. Use of this method on small fields can lead to errors associated with the so-called clothesline effect which may produce unrealistically high ET values thus producing very high crop coefficients. In addition, in small fields, the atmospheric boundary layer is unlikely to have developed to the equilibrium layer which may influence the results. The sensors must also be a considerable distance above the canopy roughness sublayer to reduce the direct effects of the canopy artefacts on the turbulent fluxes (Pereira et al., 2021b).

Another major requirement for the eddy covariance method is that the IRGA and the sonic anemometer should measure the same air parcel. So, the sensors must be as close to each other as possible, otherwise a correction for sensor separation must be implemented. Post processing of the high frequency data is critical to reduce the measurement errors.



*Figure 2.2: Schematic representation of an eddy covariance micrometeorology*

Mandatory corrections include corrections for air density fluctuations (Webb et al., 1980), coordinate rotations to account for the lack of sensor levelness, spectral corrections, etc., as detailed by Burba and Anderson, (2010) are required. Another source of error are the disturbances to the normal air patterns due to the presence of the flux tower and other artefacts, e.g. solar panels, data loggers, etc. These generate extra turbulence which is not related to the natural evaporative process.

### 2.3.1.2 Surface renewal

Another micrometeorological technique that has been used to quantify crop water requirement in South Africa and elsewhere in the world is the surface renewal method (Paw U et al., 1995). The method is based on estimating the turbulent exchange of sensible heat flux ( $H$ ) between the crop canopy and the atmosphere caused by the instantaneous replacement of air parcels in contact with the surface.

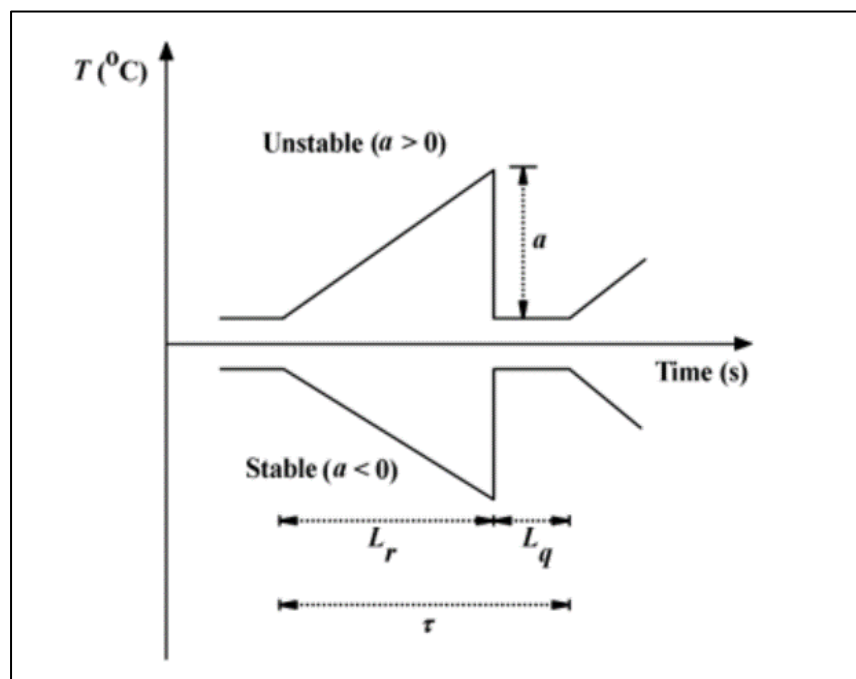


Figure 2.3: An ideal surface renewal analysis ramp model with ramp amplitude for stable ( $a > 0$ ) and unstable ( $a < 0$ ) conditions, ramp period  $L_r$ , quiescent period  $L_q$  – during which there is no change in air temperature (after Mengistu and Savage, 2010).  $\tau = L_r + L_q$  is the total ramp period.

With this technique, air temperature is measured at high frequency at a single point using unshielded and naturally ventilated fine-wire thermocouples. The theory behind the method is that air in contact with a crop surface exchanges heat energy with that

surface. The air becomes warm, expands, becomes less dense and rises (Mengistu and Savage, 2010; Hu et al., 2018). It is subsequently replaced by cooler and dense overlying air thereby changing the temperature characteristics of the surface. Air temperature measurements taken at between 2 and 10 Hz shows characteristics which resemble ramp events as illustrated in Figure 2.3.

According to Paw U et al. (1995) the sensible heat flux can be calculated from the single temperature measurement as:

$$H = \rho C_p \alpha \frac{dT}{dt} \frac{V}{A} \quad (11)$$

where  $\alpha$  is a correction factor that is derived from independent calibration of the surface renewal method usually with the eddy covariance method.  $V/A$  is the ratio of the air volume to area which is essentially the height “z” of the temperature sensor above the ground. So, equation 11 can be written as

$$H = \rho C_p \alpha \frac{dT}{dt} z \quad (12)$$

where H is measured using the surface renewal method which is strongly influenced by the placement height (z) of the sensors above the ground. This parameter must be measured as accurately as possible. If the temperature is measured at canopy height, then z will be equal to the crop height. Pau U et al. (1995) replace  $dT/dt$  with  $a/\tau$  such that equation 12 becomes:

$$H = \rho C_p \alpha \frac{a}{Lr+Lp} z \quad (13)$$

Complex functions have been developed to accurately determine the ramp amplitude “a” and total period “τ”. Details of these can be found in Paw U et al. (1995), Mengistu and Savage (2010), and Hu et al. (2018), among others.

The advantages of the surface renewal method is that it is; 1) cheaper as very little instrumentation is needed, 2) very economic on power, so it is ideal for use at remote sites and 3) accurate if carefully calibrated. The disadvantages of the method are that; i) it requires a large fetch like the other micrometeorological techniques, ii) data reduction and analysis are very complex, iii) it requires accurate measurement of vegetation height which can be a problem in fast growing plants, iv) it requires calibration with the eddy covariance method, and v) it measures only one component of the surface energy balance (i.e. H). Therefore, accurate measurements of Rn and G are critical for ET to be calculated as the residual in the surface energy balance equation (equation 6). In South Africa, this method has been used on maize (Mengistu et al., 2014), sugarcane (Jarman et al., 2014) and fruit trees (Gush and Taylor, 2014).

### **2.3.1.3 Soil water balance**

The soil water balance method is one of the most widely used methods to estimate crop water requirements and it is the basis for some of the irrigation scheduling models developed in South Africa (Annandale et al., 1999).

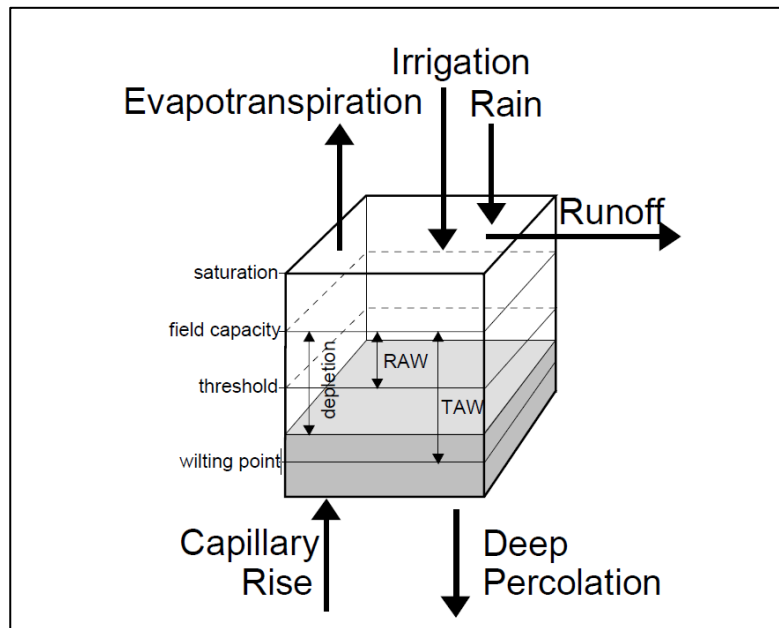


*Figure 2.4: Components of the soil water balance in the root zone of plants (after Allen et al., 1998).*

The use of this method has mostly been spurred by the advent of numerous soil moisture measuring devices such as neutron probes, time domain reflectometers, and capacitance probes (Allen et al., 2011a; Volschenk, 2017). Using the principle of conservation of mass, rainwater and/or irrigation are lost from the field through evapotranspiration (ET), deep percolation (DP), surface run off (RO), and changes in the water stored within the soil profile ( $\pm\Delta\theta$ ) (Figure 2.4).

For simplicity runoff is often assumed to be zero especially for fields on flat terrain with predominantly sandy soils. The method can be inaccurate, e.g. in fields where deep percolation or capillary rise from a shallow water table cannot be account for. For accurate results, fields in which the water table is substantially lower than the root depth is often recommended. Other sources of uncertainty for the soil water balance method include use of non-calibrated sensors. According to Allen et al. (2011a) some types of soil moisture sensors, e.g. capacitance probes work best in sandy soils, but

they may require calibration in clayey soils. Typical error margins for the soil water balance approach are in the range 10-30% although they may rise to about 40% if due care is not taken in the installation, operation, and data reduction processes.

### **2.3.2 Transpiration measurements**

Calculation of the basal crop coefficients ( $K_{cb} = T/ET_o$ ) requires accurate estimation of the transpiration component of  $ET_c$  at the whole field scale. Sap flow monitoring techniques are the most widely used methods that measure transpiration at the branch or whole plant level (Steppe and Dzikiti, 2006). Individual plant sap flow rates are subsequently scaled up to whole field water use using empirical relationships (Gush et al., 2019; Ntshidi et al., 2021a). A common feature of all sap flow monitoring techniques is that they involve the injection of heat into the plant and resolving the resultant temperature gradients to calculate the sap volume flows. According to Smith and Allen (1996) sap flow measuring techniques can be classified into continuous heating and pulsing methods. It is rare to find a sap flow monitoring method that suites all situations. The appropriate sap flow technique depends on the unique circumstances of each experiment, so knowledge of the various methods available is essential when designing experiments. While most sap flow monitoring techniques are quite easy to understand, install and operate, huge errors can easily creep in if due diligence is not exercised. Data reduction can also be quite complicated requiring various corrections, e.g. for wounding created by drilling the trees, determining some parameters to force closure of the energy balance or to zero temperature gradient signals. Allen et al. (2011a) notes that sap flow monitoring methods, while potentially useful in understanding the actual plant water consumption, they can be potential sources of huge errors which can be as much as 100% in poorly designed

experiments. The error can be a major source of uncertainty in the derivation of the basal crop coefficients. In the following sections, we summarize sap flow measurement techniques that have been used to estimate crop water requirements in South Africa.

### 2.3.2.1 Tissue heat balance sap flow gauges

Tissue heat balance (THB) sap flow sensors (Dynamax, Houston, TX, USA) measure the sap flow rate using the principle of conservation of energy (Figure 2.5). They are the most direct method for quantifying sap flow that do not require information on the anatomy of the plant (Baker and Van Bavel, 1987). They are a continuous heating sap flow method that can be used on both woody and herbaceous plants. The THBs can be used on plants with diameters ranging from as small as 2.0 to 130 mm.

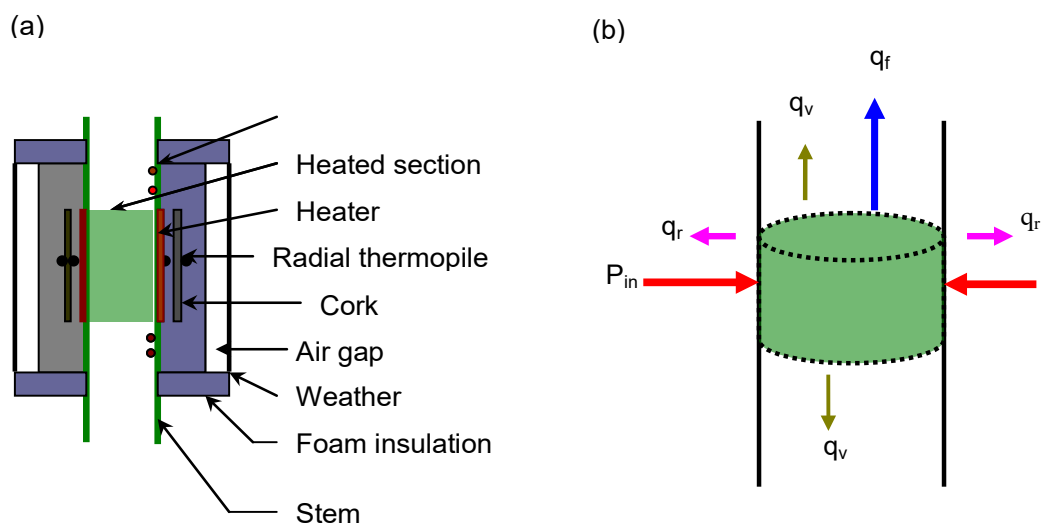


Figure 2.5: Schematic representation of the heat balance sap flow gauge (Dynamax, Houston, TX, USA). (a) Vertical section through the stem heat balance sap flow gauge. (b) Energy balance components of the heat balance sap flow sensor.

In South Africa they have been used to quantify the transpiration dynamics of maize crops (Savage et al., 2000), sugarcane (Ngxaliwe, 2014), young apple trees (Dzikiti et al., 2018b), and on understorey grass species in orchards (Ntshidi et al., 2021a). Elsewhere, they have been used to study complicated physiological responses of tree crops related to the phenomenon of stomatal oscillations (Steppe et al., 2006; Dzikiti et al., 2007). Because the sensors are wrapped around the plant organ of interest, they are also called the collar method. In this technique, a known constant power,  $P_{in}$ , is applied to the plant segment encircled by a small flexible heater (Figure 2.5a), typically a few centimetres in width, wrapped around the organ where sap flow is to be measured (Smith and Allen, 1996). The energy balance equation for that segment is solved for the amount of heat taken up by the moving sap stream under steady state conditions. This energy is then used to calculate the mass flow of sap. Given the need for steady state conditions, it is essential that the heater is the sole source of energy. Thus, insulation of the gauge to cut out energy inputs from the environment is crucial. Suppose the power input to the plant organ (e.g. the stem in Fig 2.5b) is  $P_{in}$ , then the heat balance of the stem according to (Sakuratani, 1981) and (Van Bakel and Van Bavel, 1987) can be written as:

$$P_{in} = q_v + q_r + q_f \quad (W) \quad (14)$$

where  $q_v$  is the rate of vertical heat loss by conduction,  $q_r$  is radial heat loss by conduction through the sensor, and  $q_f$  is heat uptake by the moving sap stream (Figure 2.5b). The value of  $q_f$  is obtained by subtracting  $q_v$  and  $q_r$  from  $P_{in}$  which all can be measured. If  $\Delta T_a$  and  $\Delta T_b$  are the temperature gradients measured by the axial

thermocouples above and below the heater and  $\Delta T_r$  is the radial temperature gradient, then applying Fourier's law for one dimensional heat flow,  $q_v$  is calculated as:

$$q_v = A_{st} k_{st} \left( \frac{\Delta T_b - \Delta T_a}{x} \right) \quad (\text{W}) \quad (15)$$

where  $A_{st}$  is the cross-sectional area of the heated section,  $k_{st}$  is the thermal conductivity and  $x$  is the distance between the two thermocouple junctions on each side of the heater. The radial component of the stem heat balance,  $q_r$ , is determined from  $\Delta T_r$  as:

$$q_r = K_{sh} \Delta T_r \quad (\text{W}) \quad (16)$$

where  $K_{sh}$  is the effective thermal conductance of the sheath of materials surrounding the heater. The value of  $K_{sh}$  is unknown and depends on the thermal conductivity of the insulating sheath and stem diameter. This is determined from the energy balance equation during periods when  $q_f$  is zero. This condition is approached at predawn.

Disadvantages and sources of error in THB sap flow gauges arise from; 1) effects of the stored energy in the gauged area which are not taken into account, 2) thermal gradients, e.g. early in the morning when the sun shines on the exposed parts of the plant tissues. Therefore, thorough insulation of the gauge with shiny reflective material is mandatory. Moreover, the gauges must be installed at least 1.0 m above the ground to minimize the effects of the temperature gradient between cold sap from the soil and warmed plant organs (Steppe and Lemeur, 2004). In addition, the  $K_{sh}$  factor may change over time, and this must be constantly recalculated. Finally, the tissue heat

balance sap flow method is a continuous heating method that requires a lot of power. Therefore, it is not suitable for use at remote sites.

The THB sensors can be installed on the stem of the plant in which whole plant transpiration can be measured. They can also be installed on branches and additional data is required to scale up the branch sap flow to equivalent water depth units in mm per unit time which is required for the calculation of  $K_{cb}$ . For example, if  $SF_i$  is the sap flow (in  $\text{cm}^3/\text{h}$ ) of a single plant stem whose leaf area is  $A_i$ , then the total transpiration ( $T_c$ , in mm) by the field could be calculated as:

$$T_c = \sum_i \frac{SF_i}{A_i} \times LAI_c \quad (\text{mm d}^{-1}) \quad (17)$$

where  $LAI_c$  is the leaf area index ( $\text{m}^2$  of leaf area per  $\text{m}^2$  of ground area) of the crop.

In situations where both  $ET_c$  and  $T$  are measured simultaneously, field floor evaporation ( $E_s$ ) can be estimated as:

$$E_s = ET_c - T \quad (\text{mm d}^{-1}) \quad (18)$$

This relationship can allow the distinction between the beneficial (e.g. transpiration used to grow the crop) and non-beneficial water uses lost as field floor evaporation (Ntshidi et al., 2021a). The crop coefficients can also be calculated if  $ET_o$  is known.

### **2.3.2.2 Thermal dissipation probes**

Thermal dissipation probe (TDPs – also called Granier probes) is another sap flow technique that can be used to estimate water use. These probes are probably the

cheapest type of sap flow sensors (Granier et al., 1985). The probes comprise of a pair of thermocouples installed about 4.0 cm apart (Figure 2.6) and commercial versions can be purchased from companies like Dynamax Inc., Houston, USA although custom made versions are frequently used.



*Figure 2.6: Measurement of transpiration in young orchards using Granier probes.*

The lower probe is just a thermocouple that measures sapwood temperature while the upper probe comprises a thermocouple and a heater. Therefore, there exists a temperature difference ( $\Delta T$ ) between the two probes at any given time. As in the THB method, heat is also applied continuously using a voltage in the range 3 to 8 V depending on the size of the probes. The longer the probes, the higher the voltage is required to apply heat uniformly along the probe length.  $\Delta T$  at a given time is a function

of the sap flow rate. When the sap flow rate is high, as what happens during the daytime,  $\Delta T$  is small and vice versa. Therefore, the time series of the  $\Delta T$  signal over the course of a day is the inverse of the sap flow. To swap the signal around, Granier (1987) defined a parameter  $K$  as:

$$K = \frac{\Delta T_{max} - \Delta T}{\Delta T} \quad (19)$$

where  $\Delta T_{max}$  is the maximum temperature difference between the probes. This is recorded during periods when sap flow is low or zero, typically at predawn. Using data from a range of plant species Granier (1987) related  $K$  to the sap velocity ( $V_s$ , in  $\text{cm h}^{-1}$ ) using the relationship:

$$V_s = 0.0119K^{1.231} \quad (20)$$

where  $V_s$  is equivalent to the sap flux density expressed in  $\text{cm}^3$  of water  $\text{cm}^{-2}$  of sapwood area per unit time. Use of equation 20 is often cited as a major source of uncertainty for this method (Steppe et al., 2010; Dziki et al., 2011; Pasqualotto et al., 2019). Steppe et al. (2010) noted that the sap flow rate can be underestimated by up to 70% using this method, partly due to the empirical nature of the equations used. As a result, most researchers prefer to independently calibrate the TDPs and to derive species-specific parameters in which equation 20 can be rewritten as:

$$V_s = aK^b \quad (21)$$

Where, “a” and “b” are parameters that can be obtained by linearizing equation 21 as a function of the known sap flux density. If the sap velocity is known, the sap flow volume (SF, in cm<sup>3</sup> h<sup>-1</sup>) can then be calculated as:

$$SF = A_s \times V_s \times 3600 \quad (22)$$

where,  $A_s$  is the sapwood area and 3600 is the number of seconds in an hour.

The advantages of the TDPs are that they are cheap, easy to construct and operate. They can be used on both woody and non woody plant species. Their major disadvantage is the low accuracy compared to other methods as detailed by Steppe et al. (2010). The sensors also have high power requirements as heat is applied continuously, then this makes them expensive to operate especially at remote sites. Solar panels can help as a source of power, but they are prone to theft.

### **2.3.2.3 Heat Ratio Method**

The compensation heat pulse velocity (CHP) technique (Green et al., 2003) is by far the most widely used pulsing sap flow monitoring method (Tfwala et al., 2018). Early research in South Africa on the water use of tree species used this technique (Dye et al., 1996). In recent years however, a modification of the CHP called the heat ratio method (HRM) has gained prominence (Burgess et al., 2001). This has, in many instances replaced the CHP and over 90% of the sap flow data on tree crops in the country were collected using this technique. The HRM comprises of two thermocouples installed into the sap wood of the stem at equal distances (~ 0.5 cm) up and downstream of a central heater (Figure 2.7). These thermocouples are marked

as  $T_1$  and  $T_2$  in Figure 2.7. This method is suitable for use on woody species with a diameter of at least 4.0 cm (Allen et al., 2011a).

In a typical measurement cycle, all the thermocouples are read to record the reference sapwood temperatures, say  $T_1$  and  $T_2$ . This is immediately followed by the injection of a pulse of heat ( $\sim 30\text{-}50\text{ W}$ ) for between 1 and 2 seconds. Thereafter a waiting period in the region of 60 to 90 s is observed to allow the heat to distribute within the tissues. The manner of the heat distribution depends on the rate of sap flow. In the last stage of the measurement cycle, post heating temperatures of the thermocouples (e.g.  $T_1'$  and  $T_2'$ ) are read and recorded. These measurements are usually repeated a few times per sensor to ensure that the peak temperature is recorded.

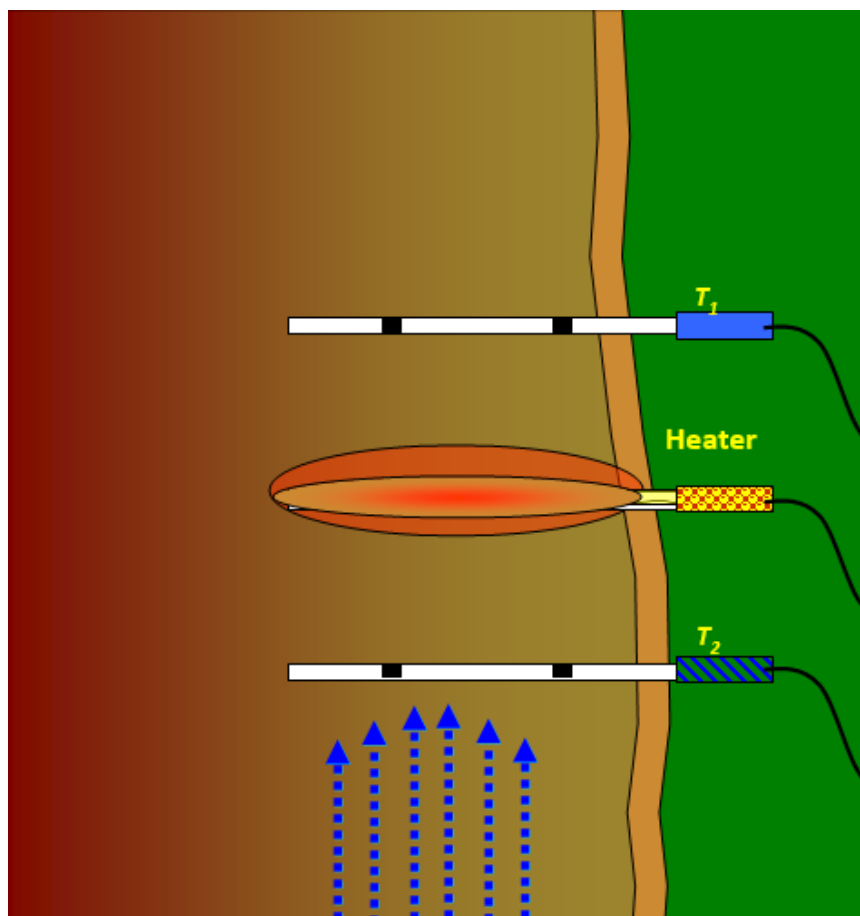


Figure 2.7: Schematic diagram of the heat ratio method (HRM) of monitoring sap flow (after Rafael Oliveira).

According to Burgess et al. (2001), the heat pulse velocity ( $V_h$ , in  $\text{cm h}^{-1}$ ) is then calculated as:

$$V_h = \frac{k}{x} \ln \left( \frac{\Delta T_1}{\Delta T_2} \right) \quad (23)$$

where  $k$  is the thermal conductivity of the wood,  $x$  is the distance of each thermocouple from the heater ( $\sim 0.5$  cm),  $\Delta T_1$  and  $\Delta T_2$  are the changes in temperature recorded by the upper and lower thermocouples, respectively. Additional data required include the wood density, moisture fraction and the wound width to correct for the effects of wounding created by drilling and the presence of probes in the transpiration stream. Details of the wounding corrections can be found in Burgess et al. (2001).

The advantages of the HRM technique are that it is a pulsing method and requires low power requirements making it ideal for use at remote sites. Furthermore, it is accurate for both low and high flows and it can measure reverse sap flows. As a result, it is a valuable tool for ecohydrological studies to understand processes such as hydraulic redistribution in plants (Dzikiti et al., 2013; 2017). Sources of error arise from probe misalignments; therefore, careful drilling and installation of the thermocouple probes must be done as carefully as possible. The wounding correction and wood density have a very large effect on the outputs of the method. These corrections must be implemented as carefully as possible. Sap velocity varies radially from the bark to the heartwood (Wullschlegel and King, 2000). The flow is fastest in the younger xylem located close to the cambium and slowest towards the heartwood where there is old collapse, cavitared and/or occluded vessels (Lambers et al., 2006). Therefore, measurements at several locations along the radial length of the stem cross section are needed to obtain a representative average of the sap velocity. This requires more

sensors which may raise costs. Moreover, the method requires knowledge of the extent of the sapwood area where xylem vessels are actively involved in water transport. In addition, inaccurate estimates of the sapwood area can be a source of significant uncertainty in the water use data measured by this method.

## **2.4 CONCLUSIONS**

In this Chapter we have provided a summary of the irrigation scheduling practices in South Africa with a special focus on the weather-based FAO 56 approach. This approach requires accurate crop coefficients and weather data to estimate  $ET_c$ . For simplicity, we did not include the effects of soil water deficit stress, but details can be found in Allen et al. (1998). Accurate, representative weather data is essential for the calculation of  $ET_o$ . The FAO recommends a standardized approach for the calculation of  $ET_o$  based on the modified Penman-Monteith equation. They also describe conditions for standard weather stations so that comparisons can be made for data collected from different locations. We also summarize key methods that have been used to estimate crop water requirements in South Africa. While there has been tremendous progress on the development of these methods, there are uncertainties associated with each method. Inaccurate  $ET_c$  or  $ET_o$  data inevitably leads to inaccurate crop coefficients. Therefore, due diligence should be exercised to ensure good quality data. In the next Chapter we describe an approach for calculating crop coefficients from readily available input data. This approach is subsequently incorporated into a Smartphone based application (hereafter called APP) for ease of calculation of the crop coefficients by the end users.

## **CHAPTER 3: DERIVATION OF CROP COEFFICIENTS FROM TREE HEIGHT AND VEGETATION COVER**

### **3.1 INTRODUCTION**

The publication of the FAO 56 Irrigation and Drainage paper in 1998 produced crop coefficients for a wide range of irrigated crops that have been used for water resources management globally (Casa et al., 2000; Allen, 2000; Lascano, 2000; Xiang et al., 2016; Kadam et al., 2020). These tabulated crop coefficients were mostly derived under temperate sub-humid climatic conditions (Allen et al., 1998). But they have been used in other climatic regions, e.g. in the arid and semi-arid regions where growing conditions are significantly different (Pereira et al., 2021a). Therefore, it is not surprising that much research that followed the publication of the FAO 56 has focused on establishing the validity of these coefficients under local conditions. In South Africa, for example, most studies on crop water use have produced crop coefficients as an end product one way or the other (Gush and Taylor, 2014; Volschenk, 2017; Dziki et al., 2018a, b; Taylor et al., 2021). The goal of the present study is to attempt to consolidate these crop coefficients into a database that can be used anywhere in the country.

An important research question has been to establish whether the crop coefficients derived in one field can be transferred to another field even with the same crop type but with different growing conditions, e.g. microclimate, soil type, irrigation method, plant density, row orientation, etc. In 2009 Allen and Pereira sought to extend the FAO 56 approach by further developing a method that was initially proposed in the FAO 56 to derive crop coefficients from readily available information. This information includes the average crop height, fraction of ground covered, and a stomatal sensitivity factor.

The purpose of the stomatal sensitivity factor is to differentiate the transpiration

response of one crop type from another (Mobe et al., 2020). This ensures that even if the crops may have the same height and canopy cover, they will have different water use rates, and hence different crop coefficients.

In recent years, this method has been extensively tested on a range of crops that include fruit orchards (Paco et al., 2019, Taylor et al., 2015; Pereira et al., 2020a, Mobe et al., 2020; Mashabatu et al., 2023), cereals (Jiang et al., 2014), vegetable crops (Pereira et al., 2020), among others. While the performance has been quite good in cereal and vegetable crops, there have been substantial errors with tree crops (Taylor et al., 2015; Paco et al., 2019; Mobe et al., 2020a&b; Mashabatu, 2023). Different solutions have also been proposed to improve the performance of the model, but these have focused on a single crop type at a time. In this Chapter, we give the details of the Allen and Pereira (2009) method (hereafter called the A&P method). We suggest changes that can improve its performance on different types of fruit tree crops building on the observations by Taylor et al. (2015), Paco et al. (2019) and Mobe et al. (2020), among others. The A&P method for deriving and transferring crop coefficients has several advantages over other methods. Firstly, it is simple and requires readily available data as inputs, so it is potentially usable by farmers, water resources managers and researchers. Secondly, the method can readily be incorporated into a Smartphone application or computer-based model thereby availing information to users on the go using modern communication platforms.

### 3.2 CALCULATION OF THE BASAL CROP COEFFICIENT (K<sub>cb</sub>)

According to the FAO 56 paper, the basal crop coefficient ( $K_{cb}$ ), also referred to as the transpiration crop coefficient, is given by:

$$K_{cb} = \frac{T}{ET_o} \quad (24)$$

where  $T$  is the crop transpiration (in mm d<sup>-1</sup>). Given that  $K_{cb}$  is dependent on the amount of vegetation (Allen and Pereira, 2009). These authors proposed a dimensionless quantity called a density coefficient ( $K_d$ ) to calculate the basal crop coefficient which they defined as:

$$K_d = \frac{K_{cb} - K_{cmin}}{K_{cbfull} - K_{cmin}} \quad (25)$$

where  $K_{cmin}$  is the minimum basal coefficient for bare soil taken as 0.15,  $K_{cbfull}$  is the estimated basal crop coefficient under conditions of nearly full ground cover (LAI  $\geq$  3.0). According to the A&P method, the density coefficient can be estimated from the effective vegetation cover ( $f_{ceff}$ ) and the mean crop height ( $h$ ) as:

$$K_d = \min\left(1, M_L f_{ceff}, f_{ceff} \left(\frac{1}{1+h}\right)\right) \quad (26)$$

where  $M_L$  is a multiplier on  $f_{ceff}$  describing the effect of canopy density on shading. It has values of  $M_L=2.0$ , e.g. for mature orchards with canopies covering much of the

orchard floor, and 1.5 for rather sparse crops, e.g. young orchards or other sparsely populated crops. The relationship between the effective fractional vegetation cover ( $f_{ceff}$ ) used in the calculations, and that input by the user ( $f_c$ ) are shown in Figure 3.1.

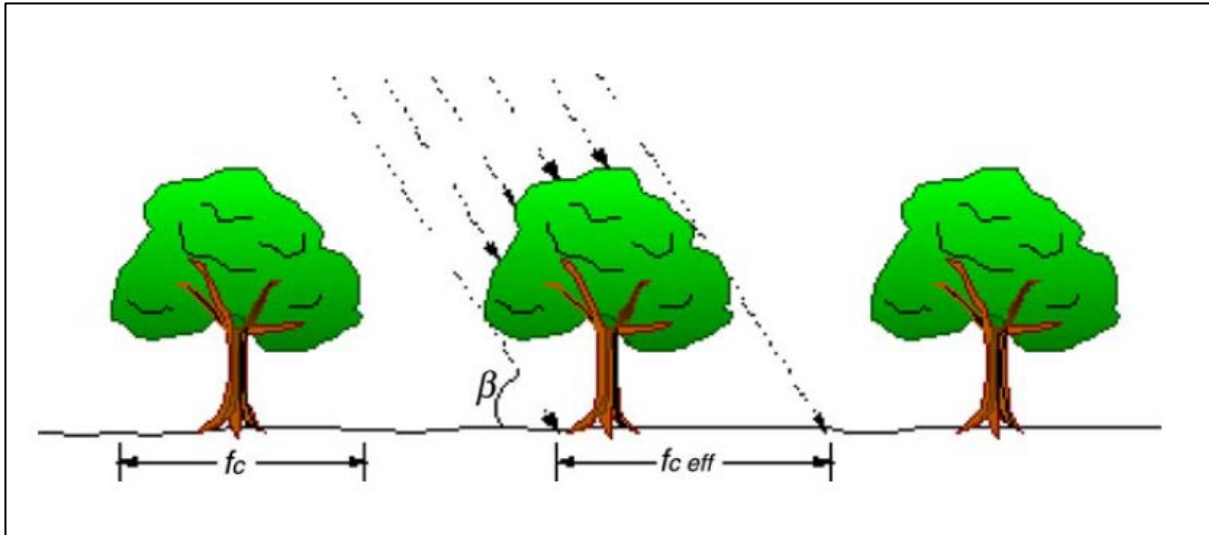


Figure 3.1: Schematic illustrating the fractional cover ( $f_c$ ) and the effective fractional cover (after Allen and Pereira, 2009).

$f_c$  is the fraction of the surface covered by the vegetation as measured from directly overhead. The equations relating  $f_c$  and  $f_{ceff}$  are detailed in Allen and Pereira (2009) and in Allen et al. (1998); so, they will not be repeated here.

In situations where  $K_{cbfull}$  is not measured, Allen et al. (1998) and Allen and Pereira (2009) suggested that it can be estimated from:

$$K_{cb\ full} = F_r \left( \min(1.0 + 0.1h, 1.20) + [0.04(u_2 - 2) - 0.004(RH_{\min} - 45)] \left( \frac{h}{3} \right)^{0.3} \right) \quad (27)$$

where  $u_2$  is the mean wind speed measured at 2.0 m height and  $RH_{\min}$  is the minimum relative humidity (%) and  $h$  is the crop height (m). The parameter  $F_r$ , which can be

considered as a  $K_{cb}$  adjustment factor through crop stomatal control, has values in the range 0 to 1. It is estimated using the following equation according to the A&P method:

$$F_r = \frac{\Delta + \gamma(1 + 0.34u_2)}{\Delta + \gamma(1 + 0.34u_2 \frac{r_l}{100})} \quad (28)$$

where  $\Delta$  is the slope of the saturation vapour pressure vs temperature curve ( $\text{Pa } ^\circ\text{C}^{-1}$ ),  $\gamma$  is the psychrometric constant ( $\text{Pa } ^\circ\text{C}^{-1}$ ) and  $r_l$  is the mean leaf resistance for the vegetation in question ( $\text{s m}^{-1}$ ). So, the method requires accurate measurements of the mid-season leaf stomatal resistance. The value of  $100 \text{ s m}^{-1}$  in the denominator of equation (28) is the mean resistance for annual crops according to Allen and Pereira (2009). In our opinion this could be a source of uncertainty for this approach which has not performed well on perennial crops like fruit tree orchards (Taylor et al., 2015; Paco et al., 2019; Mobe et al., 2020). For example, Figure 3.1 illustrates the performance of the A&P method on apple orchards with varying canopy cover over a typical growing season in the Western Cape Province (Mobe et al., 2020). More than 90% error were observed in the calculated  $K_{cb}$  if the A&P approach was applied using the recommended parameters for apple orchards published in Allen and Pereira (2009). Taylor et al. (2015) observed similar trends on various citrus cultivars in the winter (Citrusdal), and summer (Groblersdal) rainfall areas of the country. Paco et al. (2019) observed similar issues on olive orchards in Portugal and she used trial-and-error to optimize the  $r_l/100$  ratio to get satisfactory results.

In this study we have an opportunity to further evaluate this relationship on a range of fruit tree crops and to establish whether it is possible to establish a general relationship that can possibly work on most fruit tree crops.

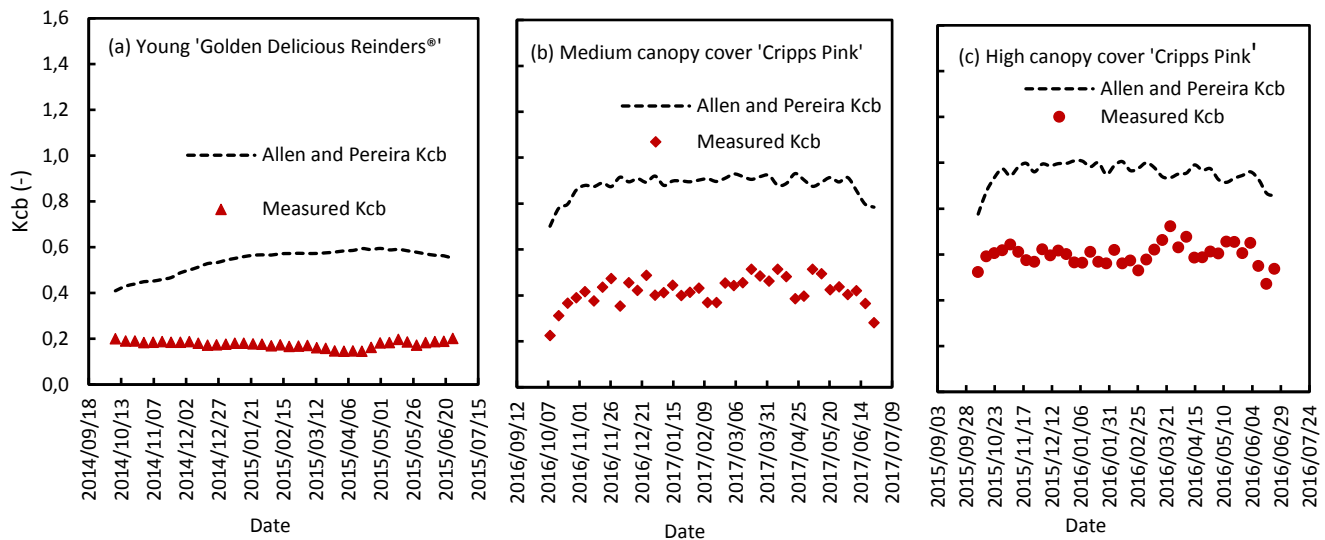


Figure 3.2: Basal crop coefficients for: (a) low, (b) medium and (c) high canopy cover apple orchards in the Western Cape derived using the original Allen and Pereira parameters for apple orchards (after Mobe et al., 2020).

Our proposed approach was firstly to replace the  $100 \text{ s m}^{-1}$  in equation (28) with a empirical parameter  $\alpha$  which can be taken to represent the minimum unstressed surface resistance of the crop in question. Fortunately, data from studies done in South African orchards has all the inputs to equations 27 and 28. So, next we inverted equation 27 using measured values of climatic variables and mean mid-season crop height. We used  $K_{cbfull}$  values calculated from the sap flow derived  $T$ , and  $ET_o$  at full canopy cover on clear days when the crops were well-watered. We then solved for  $\alpha$  for a range of tree crops presented later in this report. We observed  $\alpha$  values in the range 18 and  $37 \text{ s m}^{-1}$  although values for citrus and macadamia fell outside this range. The Bahianinha orchards required a much higher value of  $\alpha$  around  $200 \text{ s m}^{-1}$ , for unclear reasons. Some studies, e.g. Dzikiti et al. (2010) and Dzikiti et al. (2011) showed cultivar-specific transpiration responses for citrus trees. Bahianinha navels for example, showed much tighter stomatal regulation of transpiration through stomatal

oscillations (Steppe et al., 2006; Dziki et al., 2007) while these were not observed on midnight valencias (Dziki et al., 2011). The complex stomatal responses of citrus trees to environmental conditions thus make the application of the A&P method quite difficult on this crop. To solve this problem, Taylor et al. (2015) proposed a variable, leaf resistance which they expressed as a function of the  $ET_o$  and satisfactory results were obtained on the calculation of  $K_{cb}$ . These dynamics should therefore be kept in mind when interpreting the results of the current study.

According to original A&P method, the  $K_{cb}$  can be calculated from the relationship:

$$K_{cb} = K_{cbcover} + K_d \left( \max \left[ K_{cbfull} - K_{cbcover}, \frac{K_{cbfull} - K_{cbcover}}{2} \right] \right) \quad (29)$$

where,  $K_{cbcover}$  is the basal crop coefficient of the understorey vegetation growing between the crop rows. These could be cover crops, weeds, or other plant species. They are quite common in microsprinkler irrigated fields and in the summer rainfall areas where a larger fraction of the soil surface is irrigated. In this study we used generic values of  $K_{cbcover}$  derived in apple orchards in the study by Ntshidi et al. (2021a).

### 3.2.1 Cover crop leaf area index and water use

In their study the seasonal dynamics of the cover crop leaf area index (LAI) were monitored in at least five apple orchards at regular intervals throughout the growing season (September to May) using a destructive sampling technique. In this method, plants in several 50 cm x 50 cm quadrants were harvested and their leaf area

measured manually using a leaf area meter (Model: LI-3000, Li-COR, Inc., Lincoln, Nebraska, USA).

Estimates of cover crop transpiration ( $T_c$ ) were obtained using three to four miniature stem heat balance sap flow gauges (Model: SGA2, Dynamax, Houston, USA) installed on straight portions of individual grass blades on the orchard floor (Figure 3.3).



*Figure 3.3: Stem heat balance sap flow sensor measuring transpiration by grass species on the floor of an apple orchard.*

The sap flow sensors were deployed during short window periods lasting a few days at a time to avoid damage by farm machinery. The transpiration data to determine the maximum basal coefficient for the cover crops ( $K_{cbfullc}$ ) were collected in winter (July 2017) when the apple trees were leafless; there was no shading on the orchard floor

and the grass was well-watered from the winter rains. The sap flow derived transpiration rates of the grasses were confirmed independently using hourly measurements taken using an infrared gas analyser (Model: Li-6400 XT, Li-Cor Inc., Nebraska, USA) over a period of two days as shown in Figure 3.4 (Ntshidi et al., 2021a).

If  $SF_i$  is the sap flow (in  $\text{cm}^3 \text{h}^{-1}$ ) of a single cover crop plant whose leaf area on the exposed part of the sap flow sensor is  $A_i$ , then the cover crop transpiration ( $T_c$ , in  $\text{mm h}^{-1}$ ) expressed over the full orchard surface is given by:

$$T_c = \sum_i \frac{SF_i}{A_i} \times LAI_c \quad (30)$$

where,  $LAI_c$  is the leaf area index of the cover crop. The maximum cover crop basal crop coefficient ( $K_{cbfullc}$ ) was then determined as:

$$K_{cbfullc} = \frac{T_c}{ET_o} \quad (31)$$

The density coefficient for the cover crops ( $K_{dc}$ ) was subsequently derived according to Allen and Pereira (2009) as:

$$K_{dc} = 1 - e^{-0.7 \times LAI_c} \quad (32)$$

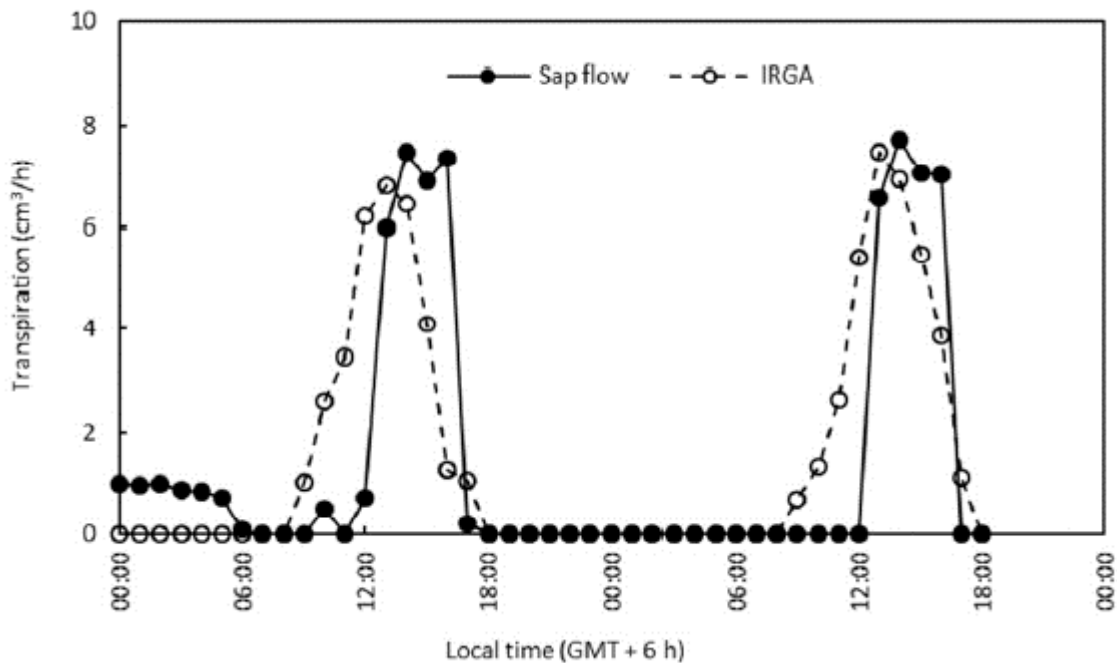


Figure 3.4: Comparison of grass transpiration measured using a stem heat balance sap flow gauge with that measured with an infrared gas analyser (Ntshidi et al., 2021a; published in the *Agricultural Water Management* journal).

The maximum value of  $K_{cbcover}$  measured in the apple orchards was about 0.24. Calculations of  $K_{cb}$  in the tool developed in this study was then calculated using three scenarios based on the information entered by the user.

For example, if the user specifies that the field has a tall cover crop, then  $K_{cbcover}$  is set to 0.24. If they chose the bare ground option, then  $K_{cbcover}$  is zero. If they chose intermediate, well managed cover crop, then a default value halfway between a tall cover crop and bare ground (0.12) is chosen.

### 3.3 SINGLE CROP COEFFICIENT ( $K_c$ )

Allen and Pereira also derived the single crop coefficient ( $K_c$ ) for the whole field using a density coefficient which they defined as:

$$K_c = K_{soil} + K_d \left( \max \left[ K_{cfull} - K_{soil}, \frac{K_{cfull} - K_{soil}}{2} \right] \right) \quad (33)$$

where  $K_{cfull}$  represents  $K_c$  from a fully covered soil with some background evaporation, and it was calculated as:

$$K_{cfull} = \max \left\{ \left[ 1.2 + [0.04(u_2 - 2) - 0.004(RH_{min} - 45)] \left( \frac{h}{3} \right)^{0.3} \right], \{K_{cb} + 0.05\} \right\} \quad (34)$$

$K_{soil}$  in equation (34) represents the average  $K_c$  from the non-vegetated (exposed) portion of the surface and reflects the impact of wetting frequency, and soil type. This was determined, considering evaporation from the wet and dry portions of the field floor as:

$$K_{soil} = K_{ewet} + K_{edry} \quad (35)$$

where,  $K_{ewet}$  was calculated following Allen et al. (2005) as:

$$K_{ewet} = \frac{TEW - (TEW - REW) \exp\left(\frac{-(t_w E_{so} - REW)}{TEW - REW}\right)}{t_w ET_o} f_w \quad (36)$$

where TEW is the total evaporable water which represents the depth of water that can be evaporated from the surface soil layer when the layer has been initially completely wetted. REW represents the readily evaporable water which represents the cumulative evaporation during stage 1 drying (Allen et al., 1998).  $t_w$  is the average time between independent wetting events which we assumed to be on average 2.5 days for wetting due to irrigation.  $E_{so}$  is the potential evaporation rate from a wet soil surface as described in equation (37), and  $f_w$  represents the fraction of the orchard floor that is wetted by irrigation or rain [0-1] and this is an input that the user defines in the tool.

$K_{e\_dry}$  in this study was taken as a constant at 0.06 based on microlysimeter measurements of soil evaporation at some of our study sites in the apple water use project (Dzikiti et al., 2018a).

Generic values of soil parameters, e.g. TEW, REW and the volumetric water content at field capacity and permanent wilting point, respectively were obtained from the data published by Allen et al. (2005) shown in Table 3.1.

**Table 3.1: Typical Readily Evaporable Water (REW), Maximum Total Evaporable Water (TEW) for General Soil Classifications (after Allen et al., 2005)**

Soil texture	Mean value of soil water content limits <sup>a</sup>		Soil texture distribution <sup>b</sup>			REW from Eq. (5) (mm)	REW from other sources (mm)	Estimated maximum TEW from Eq. (4) <sup>c</sup> (mm)
	$\theta_{FC}$ ( $m^3 m^{-3}$ )	$\theta_{WP}$ ( $m^3 m^{-3}$ )	% sand	% silt	% clay			
Sand	0.12	0.04	92	4	4	6	5 <sup>d</sup> ,6 <sup>e</sup>	10–15
Loamy sand	0.14	0.06	84	6	10	9		12–17
Sandy loam	0.23	0.10	65	25	10	9	9 <sup>d,e</sup>	14–27
Loam	0.26	0.12	40	40	20	10	9 <sup>e</sup>	20–30
Silt loam	0.30	0.15	20	65	15	9	12 <sup>d</sup>	23–34
Silt	0.32	0.15	7	88	5	8		25–37
Silty clay Loam	0.34	0.19	10	55	35	11	9 <sup>d</sup>	25–37
Silty clay	0.36	0.21	8	47	45	12		25–38
Clay	0.36	0.21	22	20	58	8	6 <sup>e</sup>	25–38

To account for the presence of tree cover on soil evaporation ( $E_{so}$ ) used in equation (36), we used the expression proposed by Allen et al. (2005) wherein:

$$E_{so} = (K_{c_{max}} - K_{cb})ET_0 \quad (37)$$

where,  $K_{c_{max}}$  is the maximum crop coefficient for the surface under full vegetation and it is equal to  $K_{c_{full}}$  (equation 34);  $K_{cb}$  is the basal crop coefficient calculated according to equation (29).

## **CHAPTER 4: VALIDATION OF CALCULATED CROP COEFFICIENTS FOR TREE CROPS**

### **4.1 INTRODUCTION**

One of the reasons for poor irrigation management in orchards is the lack of appropriate tools for irrigation scheduling (Volschenk et al., 2003; Jones, 2004). The aim of this Chapter was to validate the crop coefficients estimated using the method outlined in Chapter 3 with  $K_{cs}$  derived from the actual measured data. This information was subsequently used to develop the Smartphone APP described in Chapter 5. Given the inaccuracy in the key input data such as the fractional vegetation cover and tree height, detailed goodness of fit statistics on the simulated crop coefficients would be unrealistic. Such a task would require carefully designed experiments in which all the input variables are measured very accurately over much of the growing season. But this was not done in nearly all the studies whose data were used in this project. Rather we attempt to estimate potential errors that would arise if the simulated crop coefficients were used to estimate the orchard water use at the monthly time step.

The species evaluated include deciduous trees, e.g. apples, plums, pecans, nectarines, and peaches. Apple orchards planted to different cultivars with varying canopy cover were used while stone fruit (peach and nectarines) were considered in the summer and winter rainfall areas of the country. Subtropical fruit tree species included macadamia nuts, mango, litchi, and citrus. Data for grapefruit and banana orchards are still being collected and analysed in an ongoing study. While the water use of avocado orchards has been quantified in a recent WRC study, we were not able to access these data.

In this study we report on the crop coefficients presented in previous studies. However, to facilitate the transferability of these coefficients to other locations, we have standardized them following the approach by Pereira et al. (2021b) (see equations 7 and 8). According to the FAO 56 standard crop coefficients are those derived under sub humid temperate climatic conditions (Pereira et al., 2021a, b). This forms the basis for the **Experimental crop coefficients** in the database.

## **4.2 VALIDATION OF CROP COEFFICIENTS AND WATER USE SIMULATIONS**

### **4.2.1 Deciduous fruit tree orchards**

#### ***Nectarine orchards***

##### ***Winter rainfall area***

###### **a) Description of study site and data collection methods**

The data reported in this section was collected by Gush and Taylor (2014) under the project co-funded by the Water Research Commission (WRC K5/1770//4) and the Department of Agriculture Forest and Fisheries and here we summarize key aspects of the study. Data were collected in a mature KS nectarine orchard (Figure 4.1) at Ou Stasie Farm in Wolseley over the 2010 to 2012 growing seasons. Key properties of the orchard are summarized in Table 4.1. The orchard was 8 to 10 years old over the course of the study planted to the Alpine nectarine cultivar on a SAPPO778 rootstock. Plant spacing was 4.0 m x 1.5 m giving a tree density of 1 667 trees per hectare. Irrigation was done via a micro sprinkler system with one sprinkler per tree each delivering water at a rate of 32 L h<sup>-1</sup>. Soil type were the deep sandy soils of the Fernwood soil form, and the trees were planted on ridges (see Figure 4.1).



*Figure 4.1: Alpine nectarine orchard at Ou Stasie Farm in Wolseley, Western Cape (after Gush and Taylor, 2014).*

*Table 4.1: Attributes of the mature nectarine orchard at Wolseley in the Western Cape.*

Age	8-10 years
Block size	2.8 ha
Planting density	1 667 trees per ha
Cultivar	Alpine (nectarine)
Rootstock	SAPO778
Height	3.2 m
Irrigation	Micro sprinkler producing 32 L h <sup>-1</sup>
Soils	Sandy (80-100 cm rooting depth)
Yield	32-35 t ha <sup>-1</sup> (harvested late November to early December)

Tree transpiration data was measured using the heat ratio method (HRM) of monitoring sap flow on four instrumented trees with different stem diameters. The sap flow data were collected over two growing seasons from July 2010 to June 2012. Further details about the tree attributes, data processing for sap flow are presented in Gush and Taylor (2014). Whole orchard evapotranspiration (ET) was measured using an open path eddy covariance system over short window periods lasting a few days to one and half weeks at most. The exact dates of ET data collection are again summarized in Gush and Taylor (2014).

Weather data were collected using an automatic weather station which was located within 1.0 km of the study site. The station collected the maximum and minimum temperatures, maximum and minimum relative humidity, wind speed (at 2.0 m height), solar irradiance and rainfall. These data were collected hourly throughout the duration of the study. Soil water content was monitored at several depths in the rootzone of the trees at hourly intervals. Irrigation volumes were also monitored using water flow meters. Reference evapotranspiration was calculated for a short grass reference as defined earlier in this report.

#### **b) Observed vs standardized crop coefficients for nectarine orchards.**

The observed basal crop coefficients, which strictly speaking should be called transpiration coefficients because of the occurrence of water stress are shown in Table 4.2. For consistency, we will use the phrase basal crop coefficients in this report

although these are strictly transpiration coefficients. The  $K_{cb\_obs}$  values are monthly averages over a two-year period as presented in Gush and Taylor (2014).

The  $K_c$  values are presented in Table 4.3 only for months when ET was measured. These data show a clear seasonal trend, as expected, given that nectarine trees are deciduous. In the last column in Tables 4.2 and 4.3 we converted the observed values into the standard values using equations 7 and 8, following the approach explained by Pereira et al. (2021b). In the Smartphone APP that will be described in the next Chapter, only the standardized values are presented. When the user enters the coordinates of their orchard, the APP links up with the 50-year weather database and calculates the actual crop coefficients for the specific site using equations 7 and 8.

*Table 4.2: Observed and standardized basal crop coefficients for a mature nectarine orchard at Wolseley, Western Cape (Gush and Taylor, 2014).*

<b>Month</b>	<b>Kcb_obs</b>	<b>Kcb_std</b>
<b>Jul</b>	0.01	0.00
<b>Aug</b>	0.14	0.14
<b>Sep</b>	0.32	0.32
<b>Oct</b>	0.45	0.47
<b>Nov</b>	0.41	0.44
<b>Dec</b>	0.32	0.36
<b>Jan</b>	0.27	0.27
<b>Feb</b>	0.24	0.29
<b>Mar</b>	0.31	0.35
<b>Apr</b>	0.45	0.45
<b>May</b>	0.40	0.38
<b>Jun</b>	0.05	0.01

*Table 4.3: Observed and standardized crop coefficients on a mature nectarine Alpine orchard at Wolseley, Western Cape (Gush and Taylor, 2014).*

Month	Kc_obs	Kc_std
Jul	-	-
Aug	0.74	0.82
Sep	-	-
Oct	-	-
Nov	-	-
Dec	-	-
Jan	0.71	0.65
Feb	0.58	0.55
Mar	-	-
Apr	-	-
May	-	-
Jun	-	-

The four stage  $K_{cb}$  curve for the nectarines at Wolseley is shown in Figure 4.2. The curve was constructed using growth stage length data extracted from SAPWAT (see Appendix A). According to the phenological data presented by Gush and Taylor (2014), budbreak for the nectarines was around mid-July with flowering and fruit set occurring between the first and second week of August. Harvesting was done around mid-November. Irrigation was highly infrequent after harvest only to be ramped up again in March/ April before leaf drop. Figure 4.2 shows that the weekly  $K_{cb}$  values during the initial and development phases fitted the crop coefficient curve. However, there is a massive deviation during most of the mid-season stage due to water stress arising from lack of irrigation as explained above.

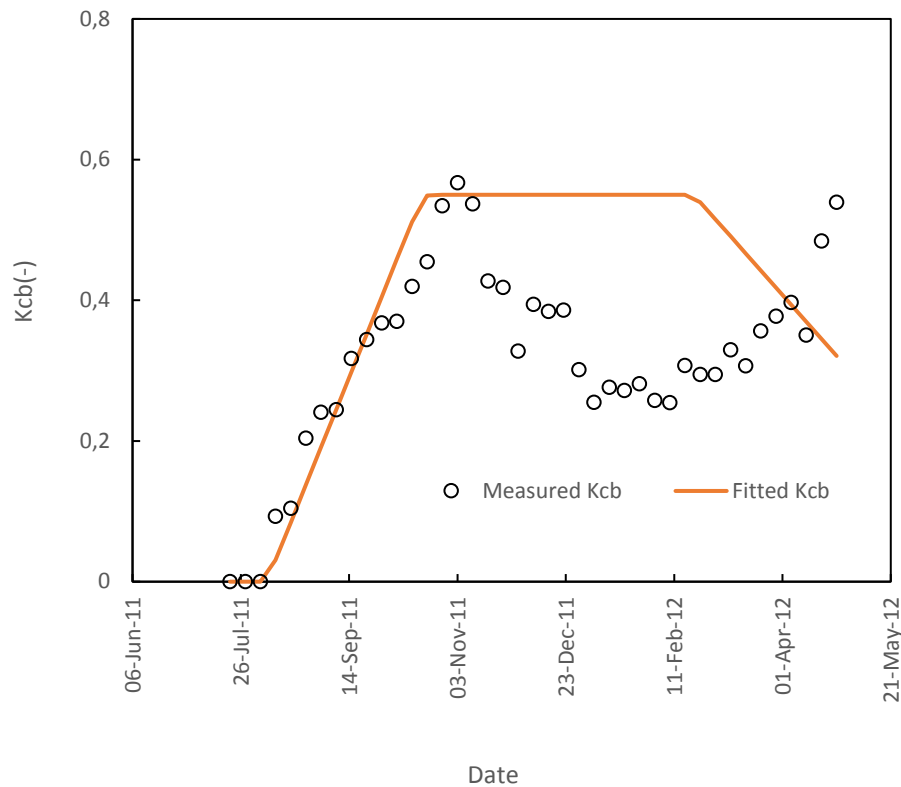


*Figure 4.2: Comparison of the observed  $K_{cb}$  (open circles) and the 4-stage  $K_{cb}$  curve (orange line) for a mature Alpine nectarine orchard in Wolseley, Western Cape.*

For simplicity, the crop coefficients reported in this study do not consider the effects of water stress due to either over or under irrigation. The effect of water stress is also apparent in Figure 4.3 where there is a clear deviation between the measured and simulated  $K_{cb}$  during the mid-season stage. The simulated  $K_{cb}$  in Figure 4.3 were calculated using the procedure described in Chapter 3. Gush and Taylor (2014) present an interpolated leaf area index (LAI) curve for the orchard. Accurate fractional vegetation cover ( $f_c$ ) data were not measured. So, we estimated this variable from the LAI curve by inverting Beer's Law using an extinction coefficient of 0.65. This gave  $f_c$  values in the range 0, at the start of the season and 0.7 at harvest.

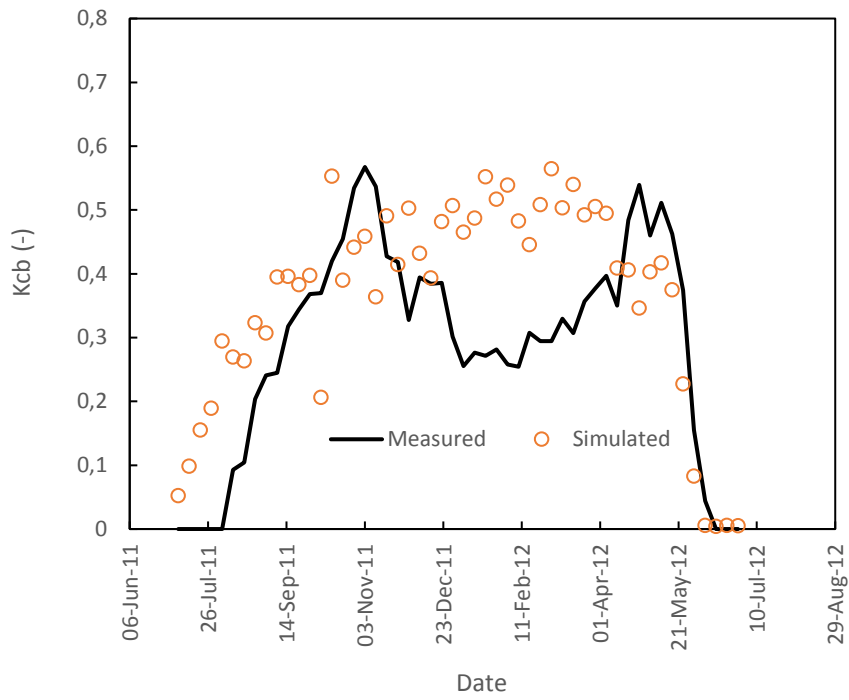


Figure 4.3: Comparison of the measured and simulated weekly  $K_{cb}$  for a mature Alpine nectarine at Wolseley, Western Cape.

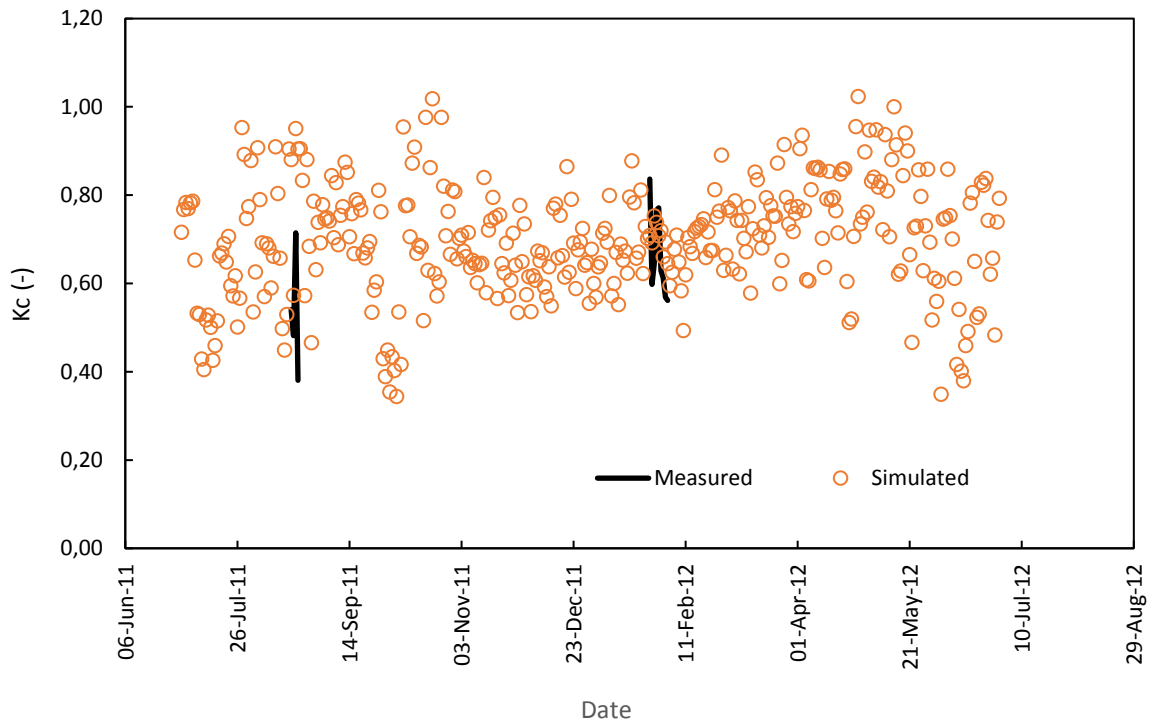


Figure 4.4: Measured vs simulated daily  $K_c$  for a mature Alpine nectarine orchard in Wolseley, Western Cape.

The leaf stomatal resistance was also not measured in the Gush and Taylor study. So, we used a value of  $\sim 400 \text{ s m}^{-1}$  obtained by inverting the Penman-Monteith (PM) equation at peak canopy cover. This value was close to the  $320 \text{ s m}^{-1}$  measured by Paudel et al. (2015) on nectarine trees in Israel. The inversion was done following the approach by Zhang et al. (1997) that used the canopy microclimate, canopy dimensions, and whole tree sap flow data to calculate  $r_l$ . According to this method (also used in Dzikiti et al., 2011 and Dzikiti et al., 2022a), the entire canopy is considered as a single big leaf whose net radiation is about 50% of that absorbed by a reference crop surface. Detailed equations can be found in Zhang et al. (1997), Dzikiti et al. (2011) and Dzikiti et al. (2022a). This calculation was done using data for a clear day in early November 2011 when the trees were at full canopy cover and under well-watered conditions.

A comparison of the observed and simulated  $K_c$  values is shown in Figure 4.4 for days when eddy covariance ET measurements were available. Unfortunately, the eddy covariance data was quite patchy. But it appears the simulated values were of the same order of magnitude as the observed values. The simulated daily changes in the crop coefficients for the nectarine orchard over the entire growing season are shown in Figure 4.5. The soil evaporation coefficient,  $K_e$  was calculated as the difference between  $K_c$  and  $K_{cb}$ . The simulated peak  $K_c$  value was around 1.16 while  $K_{cb}$  had a maximum value of 0.91. The soil evaporation coefficient was highest during the winter months when the soil was wet due to the winter rains and when canopy cover was zero.

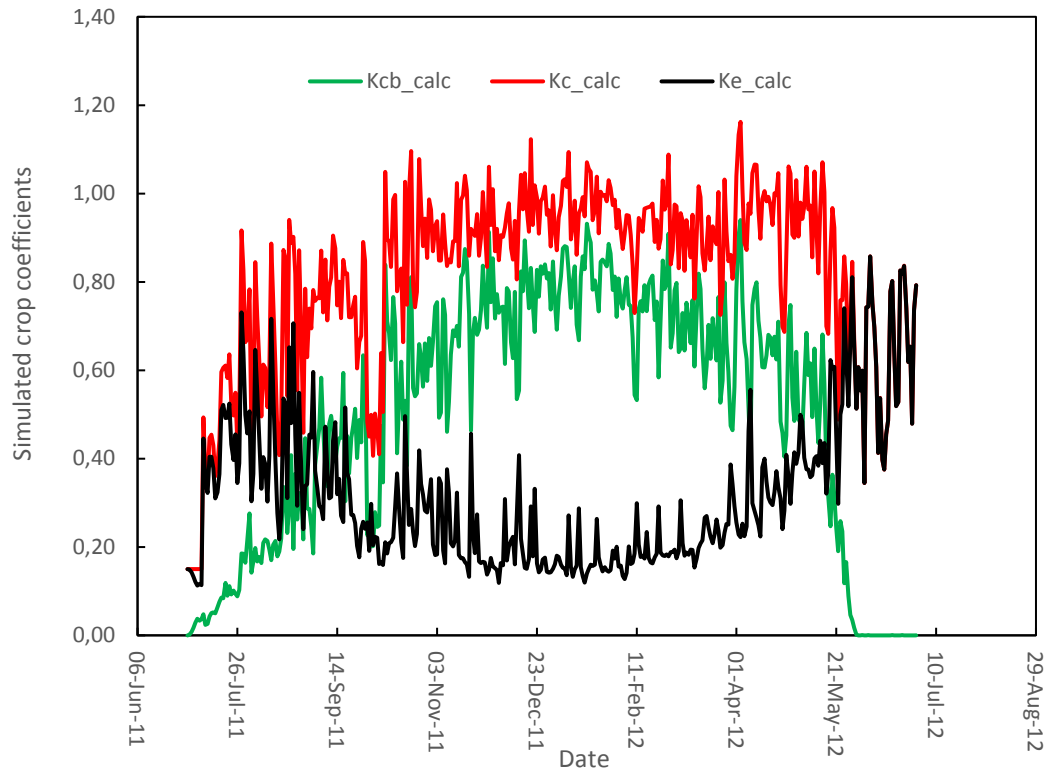
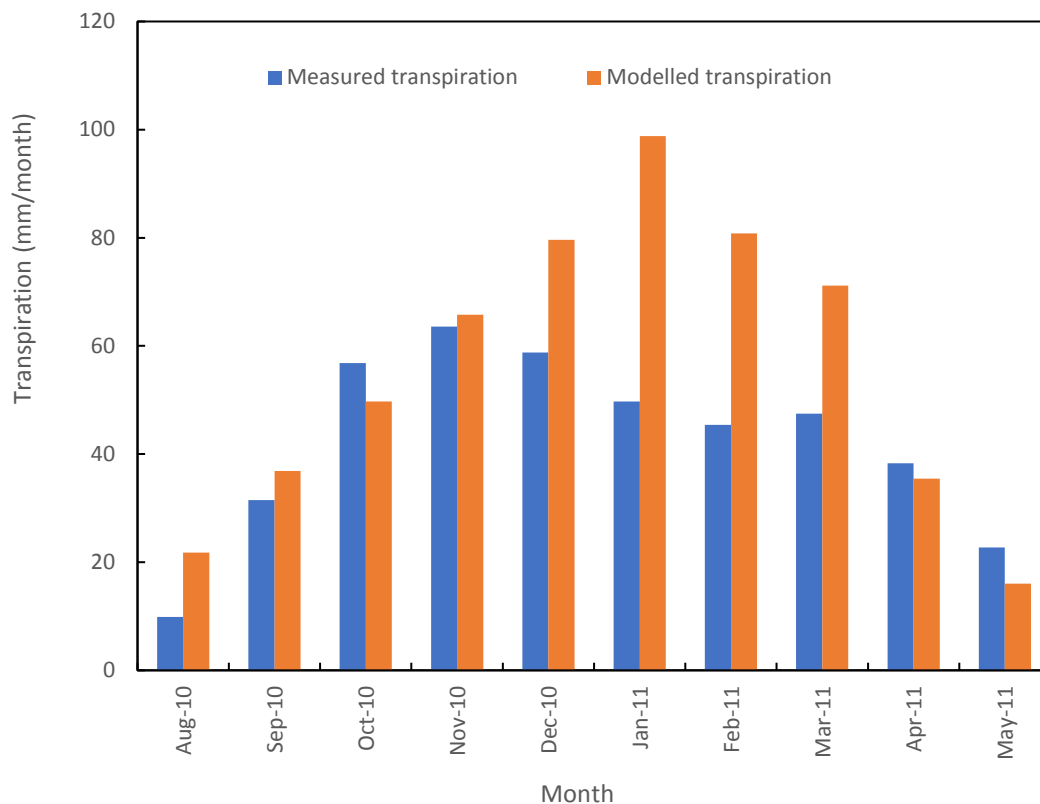


Figure 4.5: Seasonal changes in the simulated daily crop coefficients for a mature Alpine nectarine orchard at Wolseley in the Western Cape.

### c) Observed vs simulated monthly transpiration rates for a nectarine orchard in the winter rainfall areas

A comparison of the measured monthly transpiration with that simulated using the  $K_{cb}$  derived for nectarines and the monthly total  $ET_o$  ( $T = K_{cb} \times ET_o$ ) is shown in Figure 4.6. During the first four months (August to November) when the trees were irrigated there was a good agreement between the measured and simulated values. We used the coefficient of determination ( $R^2$ ), mean absolute error (MAE) and root mean square error (RMSE) as measures of agreement between the measured and estimated monthly transpiration. For the period August to November,  $R^2 \sim 0.94$ ; MAE  $\sim \pm 6.6$  mm/month and RMSE  $\sim \pm 4.3$  mm/month. The accuracy of the simulations is poor

beyond November because of water stress which is not accounted for in the calculations.



*Figure 4.6: Comparison of measured and modelled monthly total transpiration for the Alpine nectarine orchard at Wolseley, Western Cape.*

## **Summer rainfall area, Rustenburg, Northwest Province**

### **a) Description of study site and data collection methods**

The second Alpine nectarine orchard was in Rustenburg in the Northwest Province which is a summer rainfall area. These data were also collected by Gush and Taylor (2014) over one growing season from mid-2008 to mid-2009. The cultivar was also Alpine nectarine on a SAPPO 778 root stock. Tree spacing was 5 m x 2 m giving a lower plant density of 1000 trees per hectare than at Wolseley. Irrigation at Rustenburg was through a drip system delivering about 1.8 L h<sup>-1</sup> with the emitters spaced about

1.0 m apart. No details are given about the soils, but these appear to be dark red clayey loam soils. There was a very active ground cover in between the rows as shown in Figure 4.7 possibly as a result of rainfall that occurs during the fruit growing period. These trees also appear to be somewhat smaller than the ones in Wolseley and the details are summarized in Table 4.4.



*Figure 4.7: An Alpine nectarine orchard at Rustenburg, in the Northwest Province (after Gush and Taylor, 2014).*

*Table 4.4: Attributes of the mature nectarine orchard at Rustenburg in the Northwest Province (after Gush and Taylor, 2014).*

Age	unknown
Block size	unknown
Planting density	1 000 trees per ha
Cultivar	Alpine (nectarine)
Rootstock	SAPO778
Height	Unknown
Irrigation	Drip irrigation (1.8 L h <sup>-1</sup> spaced every 1.0 m)
Soils	Clayey loam
Yield	Unknown

## b) Observed vs standardized crop coefficients for nectarine orchards

The observed and standardized  $K_{cb}$  curves for the nectarine orchards are shown in Table 4.5. The values at Rustenburg are somewhat lower given that the trees were also clearly smaller than in Wolseley. However, the data in Figs. 4.8 and 4.9 suggests that these trees were also not frequently irrigated after harvest, similar to Wolseley.

*Table 4.5: Observed and standardized basal crop coefficients for a mature Alpine nectarine orchard in the summer rainfall area in Rustenburg, Northwest Province (Gush and Taylor, 2014).*

Month	Kcb_obs	Kcb_std
Aug	0.12	0.02
Sep	0.15	0.05
Oct	0.17	0.10
Nov	0.18	0.17
Dec	0.13	0.16
Jan	0.15	0.21
Feb	0.14	0.18
Mar	0.18	0.20
Apr	0.11	0.08
May	0.10	0.07
Jun	0	0

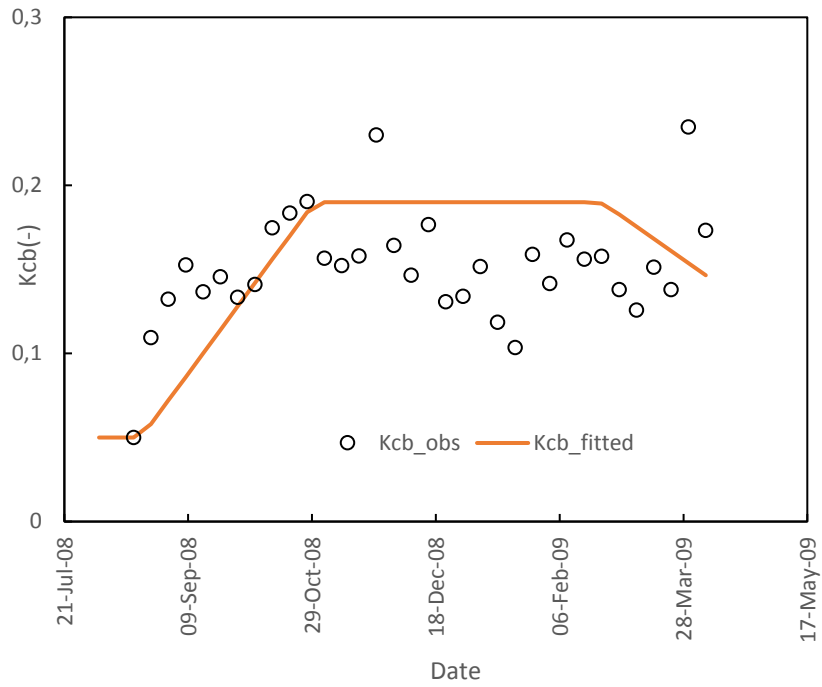


Figure 4.8: Comparison of the measured  $K_{cb}$  of the nectarine orchard at Rustenburg against the four stage  $K_{cb}$  curve.

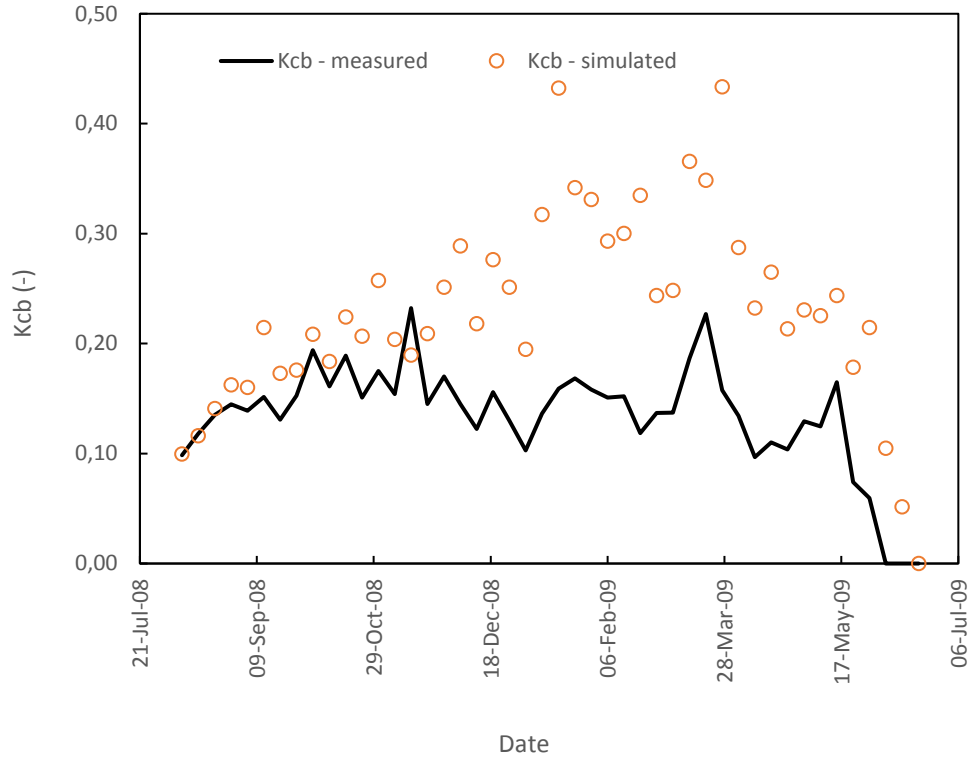


Figure 4.9: Comparison of the measured and derived  $K_{cb}$  values for an Alpine nectarine orchard in Rustenburg, Northwest Province.

The huge discrepancy between the observed and simulated  $K_{cb}$  after harvest (around November) in Figure 4.9 can also be attributed to the effects of water stress which was probably more pronounced in the drip irrigated orchards. The ET data were not collected in this orchard, so no  $K_c$  values are included.

### c) Monthly transpiration rates for a nectarine orchard in the summer rainfall areas

The trend in the monthly total transpiration from the sap flow measurements and calculated from the derived  $K_{cb}$  and  $ET_o$  followed a similar trend to that at Wolseley (Figure 4.10). This is expected since the same cultivar is used between the two sites, the orchards are likely managed in the same way. The  $R^2$  between the measured and modelled transpiration between August and November was 0.97, but this drops to 0.45 when the ten months are considered.

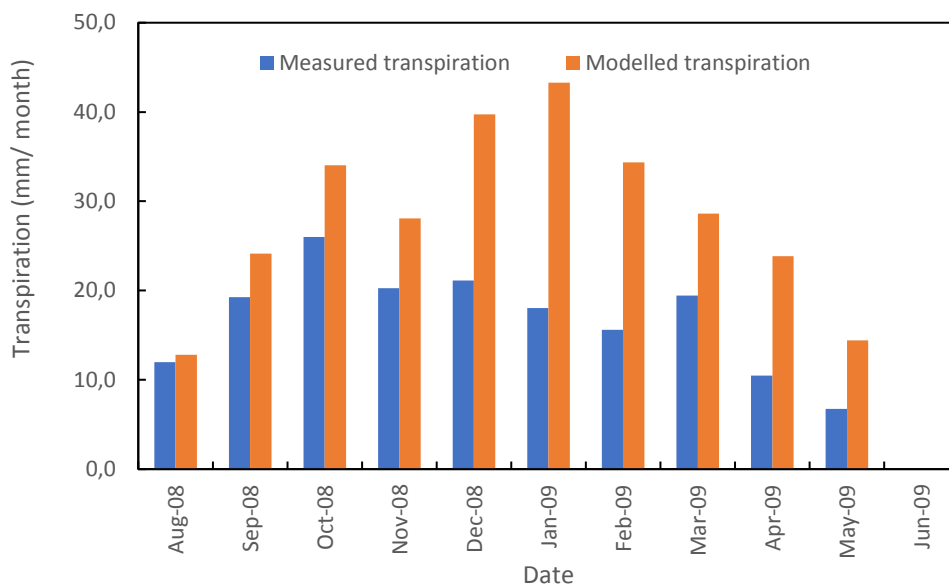


Figure 4.10: Comparison of the measured and modelled monthly transpiration by an Alpine nectarine orchard in Rustenburg, Northwest Province.

The MAE during the irrigation period from August to November was  $\sim \pm 5.4$  mm/month, but it was more than doubled to  $\pm 11.4$  mm/month when the whole period is considered. The RMSE was  $\sim \pm 3.5$  mm/month up to November increasing to about  $\pm 4.5$  mm/month if the whole ten months period is considered.

## **PEACH ORCHARDS**

### **Winter rainfall area, Ceres, Western Cape Province**

#### **a) Description of study site and data collection methods**

Data were collected in a 4-year-old Juliepretty peach orchard during the 2013-2014 growing season in a study funded by the WWF-SA in partnership with Marks & Spencer. The Juliepretty cultivar is a long season cultivar, so it has one of the highest water use rates. The trees were planted on ridges on the SAPP0 778 rootstock (Figure 4.11).



*Figure 4.11: Four-year-old Juliepretty peach orchard at Denou Farm in Ceres, Western Cape (after Dzikiti and Schachtschneider, 2015).*

Tree height was about 3.0 m, and the orchard was planted in a north-south row orientation with a very active ground cover (see Figure 4.11). Irrigation was via a microsprinkler system with one sprinkler per tree delivering about 32 L h<sup>-1</sup>. The soils were clayey loam with a high stone content; further details can be found in Dzikiti and Schachtschneider (2015).

*Table 4.6: Properties of the Juliepretty peach orchard in Ceres (after Dzikiti and Schachtschneider, 2015).*

Age	4 years
Block size	4.0 ha
Planting density	1 667 trees per ha
Cultivar	Juliepretty
Rootstock	SAPO778
Height	3.0 m
Irrigation	Microsprinkler (32 L h <sup>-1</sup> )
Soils	Clayey loam
Yield	21.0 t ha <sup>-1</sup>

Tree transpiration data were collected using the HRM on four instrumented trees. Data collection started in October 2013 and ended in May 2014. Whole orchard evapotranspiration was measured using an eddy covariance system over a 12-days period in summer from 28 February to 11 March 2014. Harvesting was done in late March 2014.

#### **b) Observed vs standardized crop coefficients for peach orchards**

The monthly  $K_{cb}$  and  $K_c$  values for this orchard are summarized in Tables 4.7 and 4.8, respectively. The  $K_{cb}$  values did not vary significantly between October and May as the trees maintained a high canopy cover for longer.

*Table 4.7: Observed and standardized basal crop coefficients for a mature peach orchard in the Western Cape Province (Dzikiti and Schachtschneider, 2015).*

<b>Month</b>	<b>Kcb_obs</b>	<b>Kcb_std</b>
<b>Oct</b>	0.58	0.54
<b>Nov</b>	0.55	0.51
<b>Dec</b>	-	-
<b>Jan</b>	0.59	0.55
<b>Feb</b>	0.51	0.46
<b>Mar</b>	0.62	0.59
<b>Apr</b>	0.73	0.71
<b>May</b>	0.51	0.45

*Table 4.8: Observed and standardized crop coefficients for a mature peach orchard in the Western Cape.*

<b>Month</b>	<b>Kc_obs</b>	<b>Kc_std</b>
<b>Oct</b>	-	-
<b>Nov</b>	-	-
<b>Dec</b>	-	-
<b>Jan</b>	-	-
<b>Feb</b>	0.77	0.70
<b>Mar</b>	0.71	0.69
<b>Apr</b>	-	-
<b>May</b>	-	-

Since a large portion of the early growth stages was missing due to the late start of the project, the 4-stage crop coefficient curve was not constructed. A comparison of the measured vs simulated  $K_{cb}$  values shows a good agreement (Figure 4.12). Data were missing for a large part of the mid-season due to equipment malfunctioning.

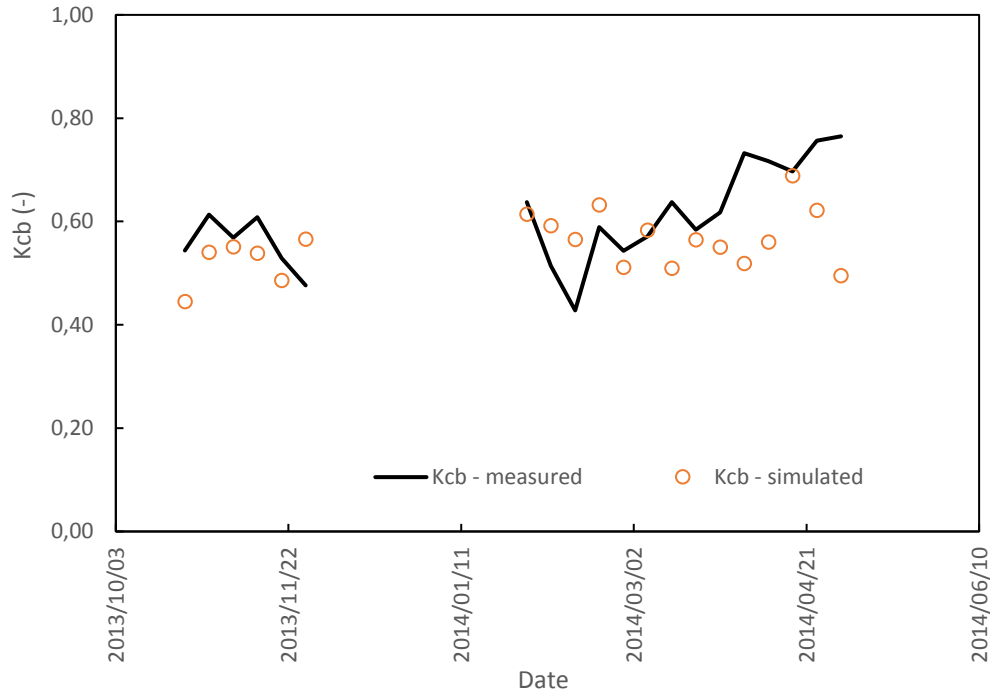


*Figure 4.12: Comparison of the measured and modelled weekly  $K_{cb}$  for a mature peach orchard at Ceres, Western Cape Province.*

For the  $K_{cb}$  simulations,  $f_c$  was derived from the LAI by inverting the Beer's law. LAI values ranged from a peak around 2.0 in summer to zero during winter. The leaf resistance was set at  $280 \text{ s m}^{-1}$  obtained by inverting the Penman-Monteith equation at full canopy cover. The value of  $\alpha$  was  $\sim 20 \text{ s m}^{-1}$ . The simulated  $K_c$  tended to be slightly higher than the measured values for unclear reasons (Figure 4.13). The small dataset was not very helpful in showing the behavior of the simulated  $K_c$  values over a range of conditions.

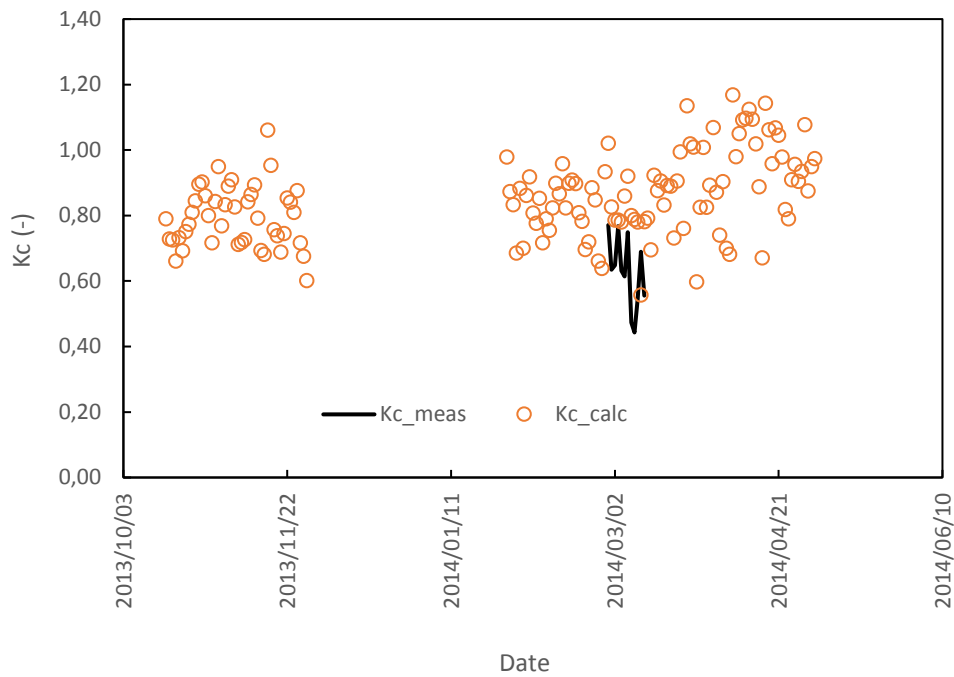


*Figure 4.13: Comparison of the  $K_c$  values from actual measurements (black continuous line) with the simulated values (orange circles).*

The simulated  $K_c$  peak at around 1.18 while  $K_{cb}$  reached a maximum of 0.81 in late summer (Figure 4.14). The soil evaporation coefficient hovered around 0.20 for most of the growing season. Because of the small data set available, weekly total transpiration were compared in Figure 4.15. Even though the simulated transpiration was of the same order of magnitude as the measured values, the  $R^2$  between the two variables was quite low ( $<0.2$ ). Generally, there tended to be a better agreement in the long-term (one month or more) water use estimates than the short-term values.

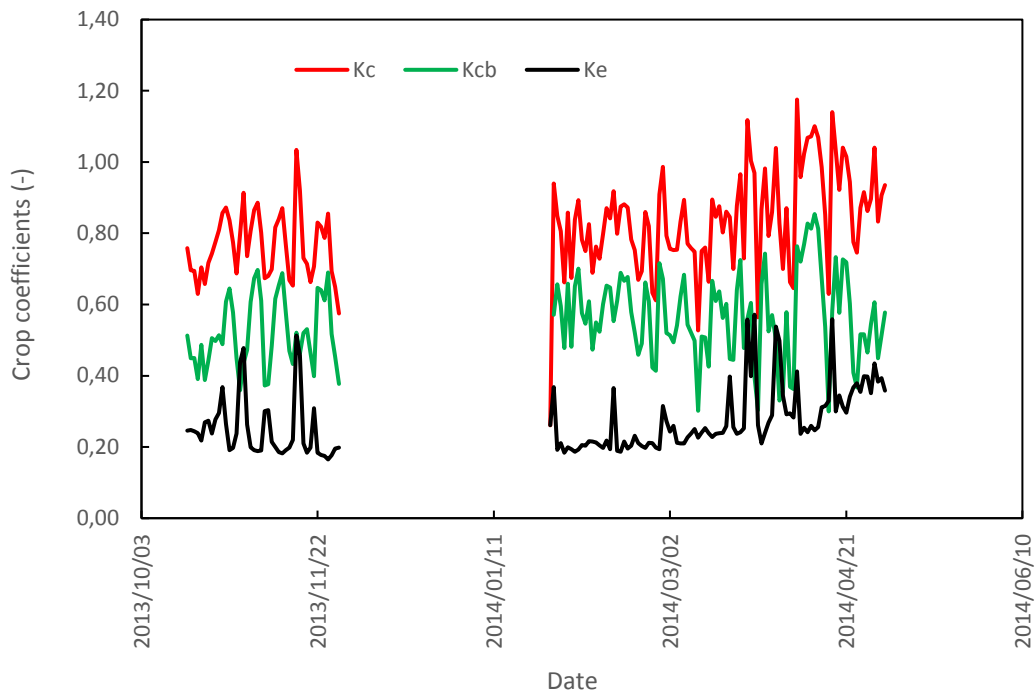


Figure 4.14: Seasonal changes in the crop coefficients for a peach orchard in Ceres simulated using the modified A&P method.

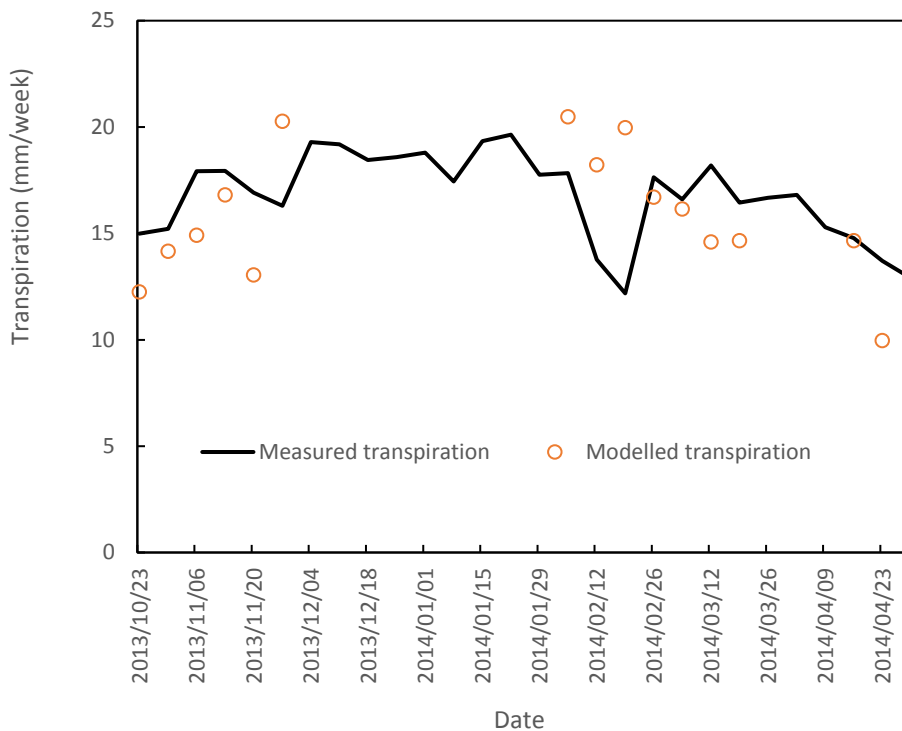


Figure 4.15: Comparison of the measured vs simulated weekly transpiration for the peach orchard at Ceres.

## Summer rainfall area, Rustenburg, Northwest Province

### a) Description of study site and data collection methods

The peach orchard studied at Rustenburg was planted to the Transvalia cultivar, also on the SAPPO 778 rootstock (Gush and Taylor, 2014). This orchard was located adjacent to the nectarine orchard described earlier. Not much information was given about the irrigation system, but this appears to be under drip irrigation from Figure 4.16. The soil type appears to be dark red clayey loams and the trees were planted on ridges.



*Figure 4.16: Transvalia peach orchard at Rustenburg in the Northwest.*

As with the other orchards, tree transpiration was measured using the HRM sap flow monitoring technique. According to Gush and Taylor (2014), three trees with different

stem sizes were instrumented with the sap flow sensors. An automatic weather station collected standard weather variables next to the orchard. Rootzone soil water content was measured at different depths using soil moisture probes. Data collection spanned over 327 days (August 2008 to June 2009). Whole orchard evapotranspiration was not measured.

### **b) Observed vs standardized crop coefficients for peach**

The  $K_{cb}$  values followed a clear seasonal trend (Table 4.9) with low values close to zero in late winter to a peak around 0.27 in summer for both the observed and standardized values.

*Table 4.9: Observed and standardized basal crop coefficients for a peach orchard in the summer rainfall areas (Gush and Taylor, 2014).*

Month	Kcb_obs	Kcb_std
Aug	0.01	0.07
Sep	0.14	0.06
Oct	0.24	0.19
Nov	0.27	0.27
Dec	0.20	0.13
Jan	0.22	0.27
Feb	0.23	0.26
Mar	0.20	0.21
Apr	0.06	0.04
May	0.05	0.03
Jun	0.03	0.06

The observed weekly average  $K_{cb}$  values for the peach orchard at Rustenburg closely followed the four-stage crop coefficient curve as shown in Figure 4.17. The stage length data were obtained from the SAPWAT database. The simulated weekly  $K_{cb}$  in Figure 4.18 closely followed the course of the measured values. But as with the other stone fruit discussed earlier, the accuracy of the simulated  $K_{cb}$  values decreased late

in the season likely when irrigation was reduced, although we do not have this information in the case of the peach orchard.

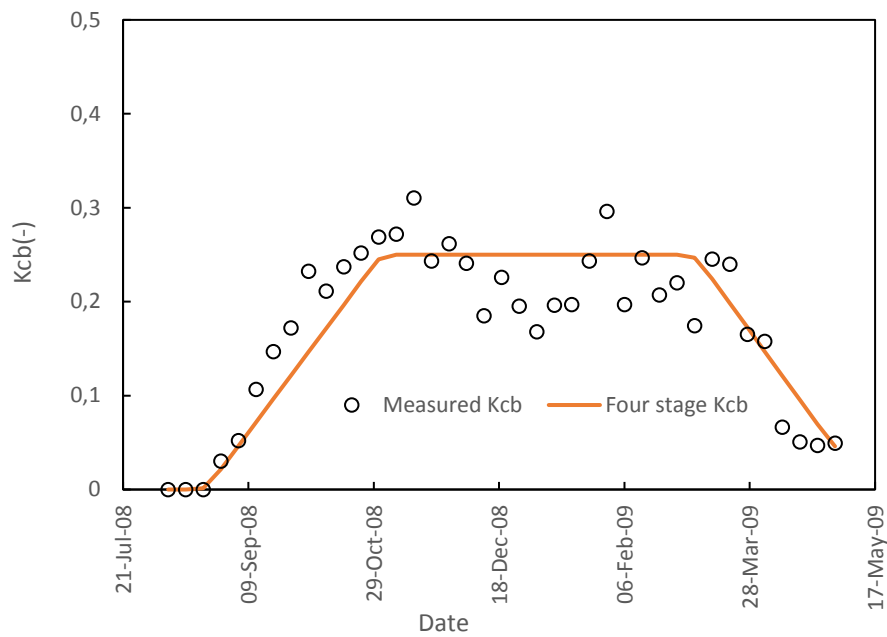


Figure 4.17: Weekly  $K_{cb}$  values for a peach orchard at Rustenburg, Northwest Province in relation to the four-stage curve.

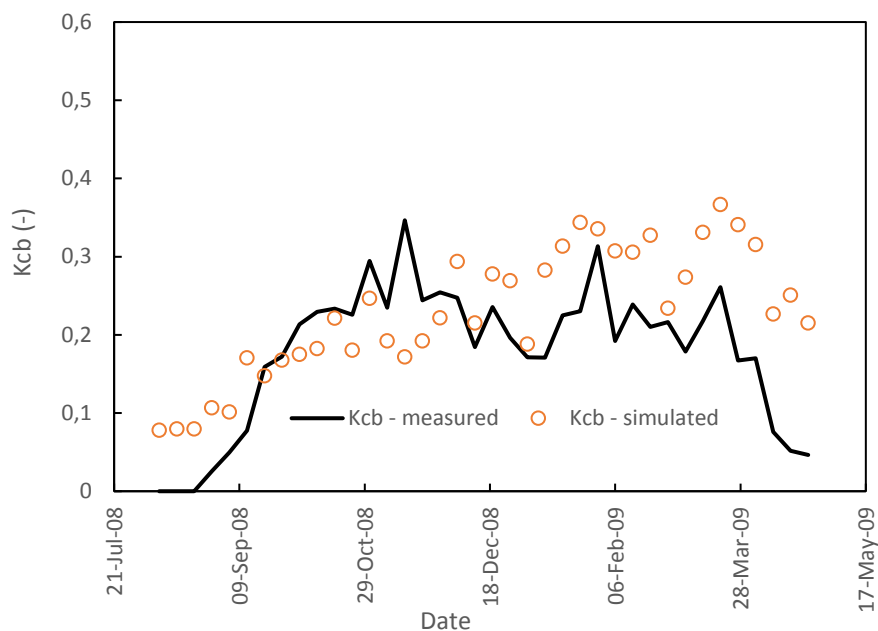
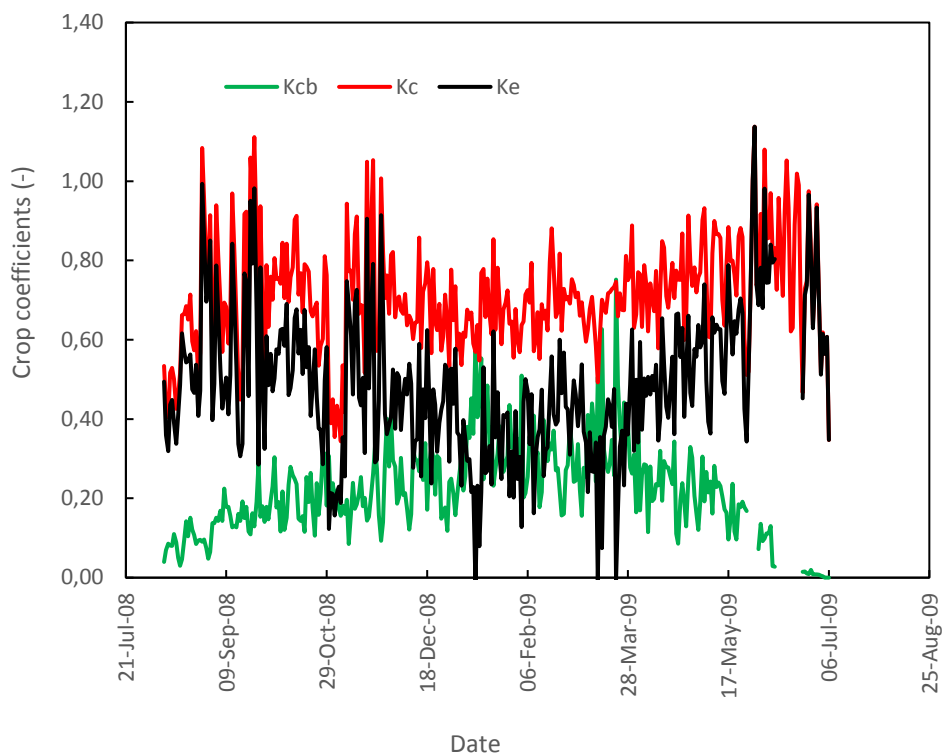


Figure 4.18: Comparison of the actual weekly  $K_{cb}$  (black line) measured in a mature peach orchard in Rustenburg, Northwest Province with simulated values (orange circles).

The seasonal changes in the simulated crop coefficients are summarized in Figure 4.19. The soil evaporation coefficient was higher than  $K_{cb}$  early and late in the growing season when canopy cover was low. The low  $K_{cb}$  values can be attributed to the rather sparse canopies with a peak LAI of 1.8 reached in summer. The reduction in simulated  $K_c$  values during mid-season are not expected. These could be attributed to the increased frequency of cloud cover in the summer rainfall area.



*Figure 4.19: Crop coefficients for a peach orchard at Rustenburg, Northwest Province.*

### **c) Monthly transpiration rates for a peach orchard at Rustenburg, Northwest Province**

The simulated monthly transpiration closely matched the measured values in the first five months from August to December (Figure 4.20). These are likely the irrigated periods before harvest. Later in the growing season the simulated monthly water use

exceeded the measured values, consistent with the observations made in the nectarine orchards. The simulated monthly transpiration could explain about 84% of the observed values during the first five months, but this figure dropped to only 57% when all the ten months were considered. The MAE was around  $\pm 5.3$  mm/month translating to less than  $\pm 0.2$  mm d<sup>-1</sup> during the first five months from August to December. The RMSE was  $\pm 2.8$  mm/month during the first five months rising to  $\pm 3.9$  mm/month. The increasing errors after the irrigation season can be explained by the occurrence of significant water stress when irrigation was stopped, and this is not accounted for in the calculations.

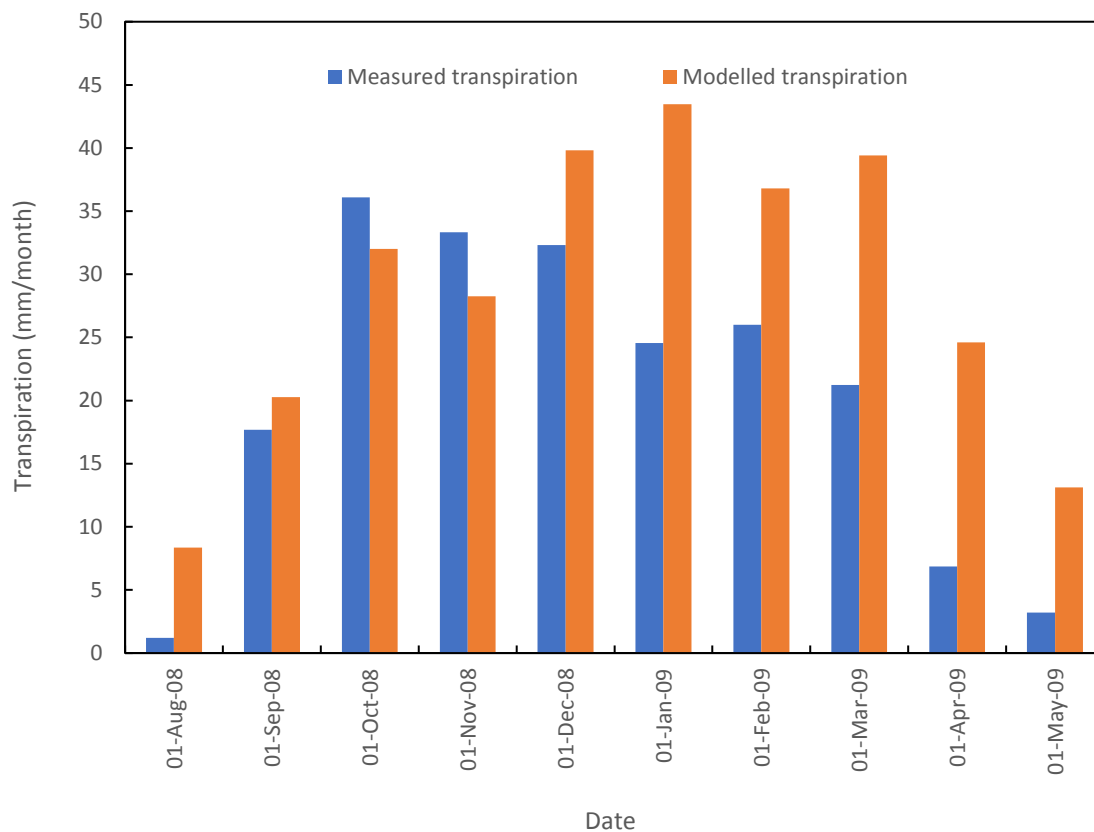


*Figure 4.20: Comparison of the measured vs modelled monthly transpiration of a peach orchard in Rustenburg, Northwest Province.*

## **PLUM ORCHARDS**

### **a) Description of study site and data collection methods**

Water use data in the plum orchard were collected at Sonskyn farm in Robertson from October 2013 to May 2014. The study was funded by WWF-SA in partnership with Marks & Spencer, UK. The orchard was a 3.5 ha block planted to the African Delight plum cultivar (Figure 4.21). The trees were on a V-trellis training system with a plant density of about 2000 trees per hectare. Irrigation was via a drip irrigation system with drippers delivering  $1.4 \text{ L h}^{-1}$  spaced 1.0 m along the drip line. There was one drip line per tree row.



*Figure 4.21: An African Delight plum orchard at Sonskyn farm in Robertson, Western Cape (after Dzikiti and Schachtschneider, 2015).*

*Table 4.10: Summary of the characteristics of the plum orchard at Robertson, Western Cape (after Dzikiti and Schachtschneider, 2015).*

Age	5 years
Block size	3.5 ha
Planting density	2000 trees per ha
Cultivar	African Delight on V-trellis training system
Rootstock	SAP0778
Height	3.0 m
Irrigation	Drip irrigation delivering 1.4 L h <sup>-1</sup> at 1.0 m spacing
Soils	Clayey loam with a high stone content
Yield	35.0 t ha <sup>-1</sup>

Tree transpiration was measured using an HRM sap flow system and six trees with different stem sizes were instrumented. Orchard evapotranspiration was measured using an open path eddy covariance system (Figure 4.21) over just four days from six to nine February 2014. The leaf area index ranged from 1.5 to 2.7 in the period October 2013 to May 2014. A unique characteristic of this orchard is that it maintained a high leaf area well into the winter months in late June 2014. Volumetric soil water content was measured at different depths in the root zone using CS616 soil moisture probes. Simulations of the crop coefficients were done with a mid-season stomatal resistance of 250 s m<sup>-1</sup> and  $\alpha = 20$  s m<sup>-1</sup>.

#### **b) Observed vs standardized crop coefficients for plum orchards**

Because of the late start to the data collection campaign (October 2013), the four-stage crop coefficient curve was not constructed as much of the data for the early parts to the season were missing. The observed and standardized basal and single crop coefficient are shown in Tables 4.11 and 4.12. The  $K_{cb}$  remained above 0.5 for most of the season as the trees retained their leaves through much of the winter season. This was partly because irrigation was applied for a large part of the season resulting

in high water use rates over a longer period. A comparison of the weekly observed and simulated  $K_{cb}$  are shown in Figure 4.22 while the daily crop coefficients are in Figure 4.13. The simulated values are of the same order of magnitude as the measured values. However, the small ET, and hence  $K_c$  data set restricts us from drawing firm conclusions about the accuracy of the derivation.

*Table 4.11: Observed and standardized basal crop coefficients for a plum orchard in Robertson, Western Cape (Dzikiti and Schachtschneider, 2015).*

Month	Kcb_obs	Kcb_std
Oct	0.53	0.53
Nov	0.56	0.53
Dec	0.52	0.48
Jan	0.58	0.57
Feb	0.59	0.57
Mar	0.61	0.61
Apr	0.68	0.69
May	0.71	0.68
Jun	0.69	0.68

*Table 4.12: Observed and standardized crop coefficients for a plum orchard in Robertson, Western Cape (Dzikiti and Schachtschneider, 2015).*

Month	Kc_obs	Kc_std
Oct	-	-
Nov	-	-
Dec	-	-
Jan	-	-
Feb	0.92	0.89
Mar	-	-
Apr	-	-
May	-	-
Jun	-	-

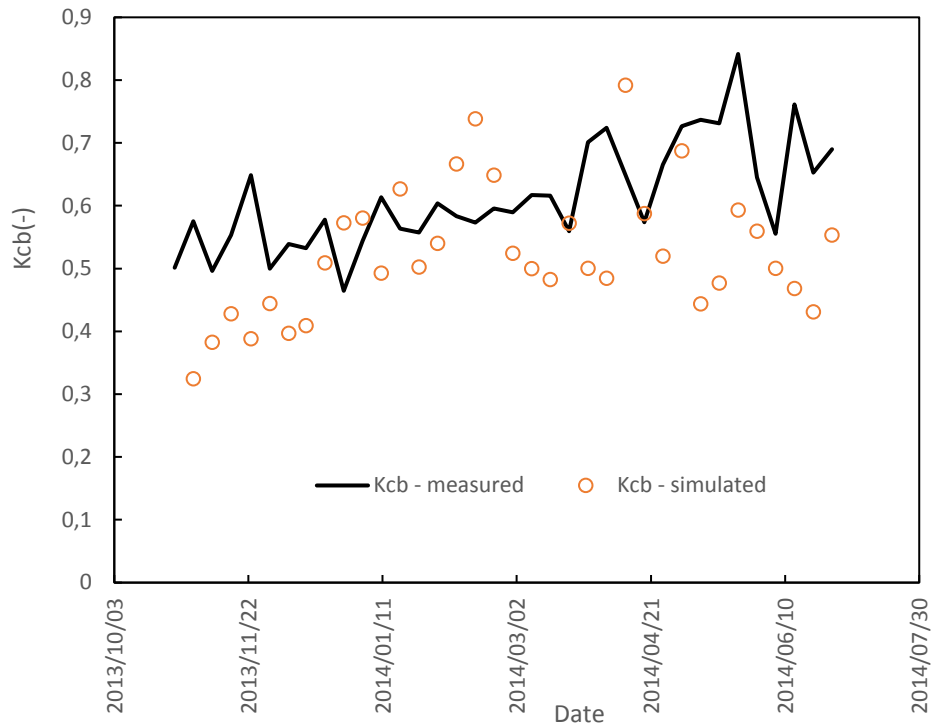


Figure 4.22: Comparison of the measured and simulated  $K_{cb}$  for a mature plum orchard in Robertson, Western Cape Province.

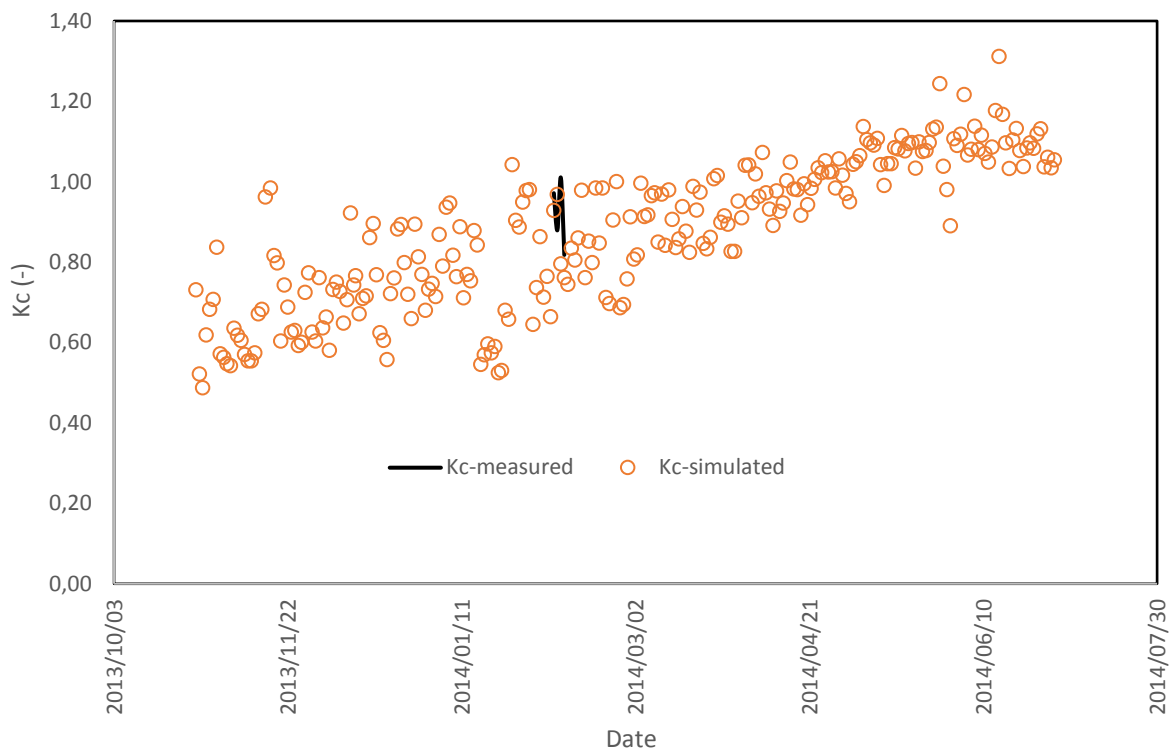
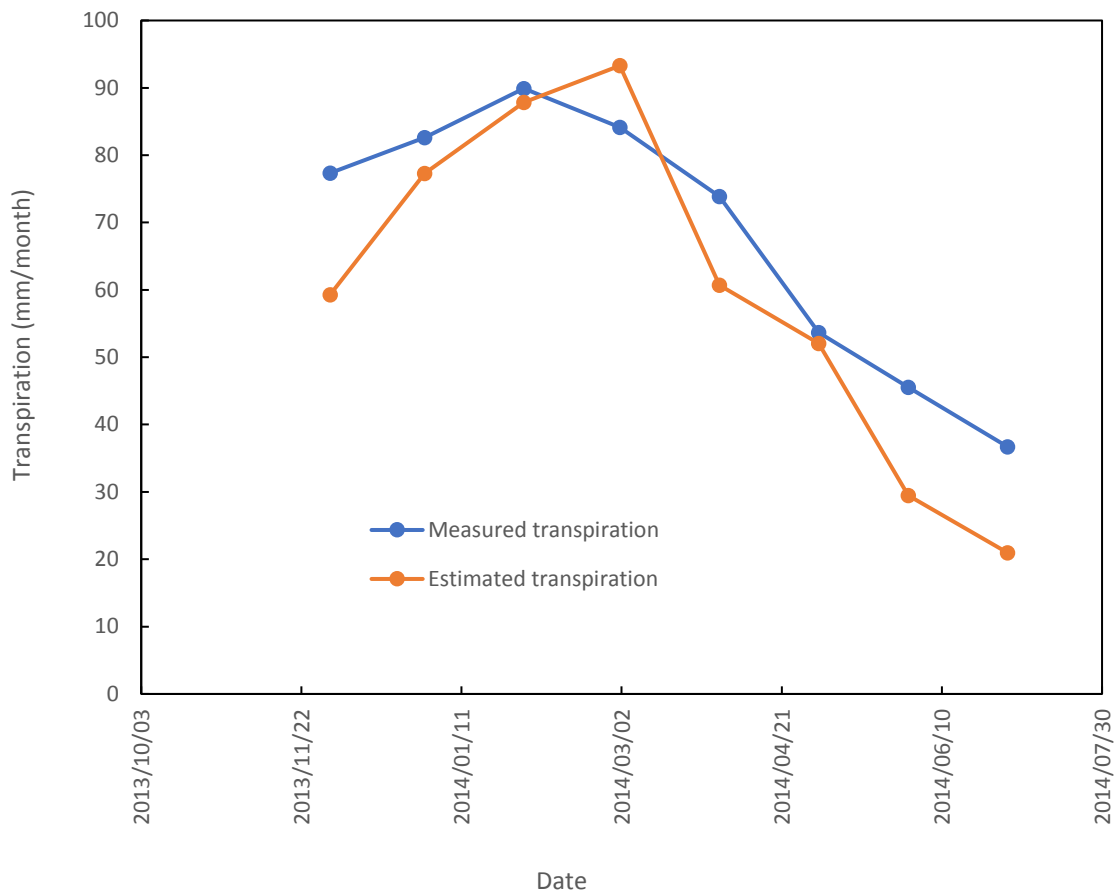


Figure 4.23: Validation of the calculated  $K_c$  values (orange circles) with measured data in a plum orchard at Robertson, Western Cape.

**c) Monthly transpiration rates for a plum orchard in Robertson, Western Cape.**

A comparison of the measured and simulated monthly total transpiration for the plum orchard is shown in Figure 4.24. The simulated transpiration closely matched the observed values over the entire 8 months period from November 2013 to June 2014. About 90% of the variation in transpiration in the monthly total transpiration could be explained by the simulated values ( $R^2 \sim 0.90$ ). The mean absolute error was about  $\pm 10$  mm/month translating to less than  $\pm 0.3$  mm  $d^{-1}$ . The root mean square error was even smaller at about  $\pm 4.5$  mm/month translating to less than  $\pm 0.15$  mm  $d^{-1}$ .



*Figure 4.24: Comparison of the actual measured transpiration by the plum orchard at Robertson with the simulated values.*

## **PECAN ORCHARDS**

### **a) Description of study site and data collection methods**

Pecan orchards present a unique challenge to the crop coefficient derivation approach described here given its different aerodynamic properties. This is because the trees were much taller than most conventional orchard crops and they are more sparsely populated. The data reported here was collected by Gush and Taylor (2014) in the WRC/DAFF funded project. The experiment was done in Cullinan, about 50 km to the northeast of Pretoria from October 2009 to April 2012. The orchard details are summarized in Table 4.13. The trees were between 34 and 37 years old during the trial planted to a Choctaw cultivar on Barton rootstock. They were about 13 m tall with about 140 trees per hectare. Irrigation was via a microsprinkler system delivering about 90 L h<sup>-1</sup>.



*Figure 4.25: Pecan orchard at Cullinan, Gauteng (after Gush and Taylor, 2014).*

*Table 4.13: Characteristics of the pecan orchard at Cullinan, Gauteng.*

Age	34-37 years
Block size	22 ha
Planting density	142 trees per ha
Cultivar	Choctaw
Rootstock	Barton
Height	13.0 m
Irrigation	Micro sprinkler delivering 90 L h <sup>-1</sup> at 1.0 m spacing
Soils	Sandy to sandy loam
Yield	1.9 t ha <sup>-1</sup>

Tree transpiration was monitored using the HRM sap flow system installed on five trees with different stem diameters. Whole orchard evapotranspiration was measured using an open path eddy covariance system and the data were collected over short window periods. Volumetric soil water content was monitored at different depths down the soil profile. Irrigation volumes were also monitored, and an automatic weather station was mounted close to the orchard. According to the report by Gush and Taylor (2014), there are two main highlights from this study. The first relates to the very high volumes of daily water consumed by the trees exceeding 400 L per tree per day on some occasions. The second highlight is that these orchards have a unique crop coefficient curve which appears to have six stages compared to the four that are widely reported in literature. Details of the six-stage crop coefficient curve were published by Ibraimo et al. (2016). Because of this unique behavior which deviates from the conventional crop coefficient curve, we did not attempt to reconstruct the curve in this study.

The leaf area was also measured at various intervals during the campaign, and this ranged from zero in winter to a peak just over 8.0 in summer. We used these data to

calculate the fractional vegetation cover by inverting Beer’s law. The maximum fractional canopy cover at mid-season was in the range 0.82 to 0.98. The leaf resistance used in the simulations was set at 250 s m<sup>-1</sup> which was at the lower end of the measured leaf resistance range of 200 to 800 s m<sup>-1</sup>. The value of  $\alpha$  was taken as 20 s m<sup>-1</sup>, similar to the other orchard species.

### **b) Observed vs standardized crop coefficients for pecan**

A summary of the monthly observed and standardized  $K_{cb}$  and  $K_c$  values are shown in Tables 4.14 and 4.15, respectively. The mid-season crop coefficients were quite high on occasion exceeding 1.4 which is the theoretical maximum discussed in the knowledge review. In these instances, these values were set to 1.4. We suspect that this is an artefact of the measured data and there is a possibility that we did not get the most accurate data for this exercise. The crop coefficients reported by both Gush and Taylor (2014) and Ibraimo et al. (2016) do not seem to violate the principle of conservation of energy thus supporting the view that our data quality was not good.

*Table 4.14: Observed and standardized basal crop coefficients for pecan orchards (Gush and Taylor, 2014).*

<b>Month</b>	<b>Kcb_obs</b>	<b>Kcb_std</b>
<b>Sep</b>	0.34	0.12
<b>Oct</b>	0.57	0.32
<b>Nov</b>	0.89	0.65
<b>Dec</b>	0.86	0.62
<b>Jan</b>	1.40	1.18
<b>Feb</b>	0.87	0.66
<b>Mar</b>	1.45*	1.24

Table 4.15: Observed and standardized crop coefficients for pecan orchards (Gush and Taylor, 2014).

Month	Kc_obs	Kc_std
Sep	1.05	0.83
Oct	0.81	0.56
Nov	1.16	0.92
Dec	1.18	0.94
Jan	1.84*	1.62*
Feb	0.97	0.76
Mar	1.49*	1.28

Comparisons of the simulated and measured  $K_{cb}$  and  $K_c$  values are presented in Figure 4.26 and 4.27. These data suggest that the simulated crop coefficients were substantially lower than the measured values.

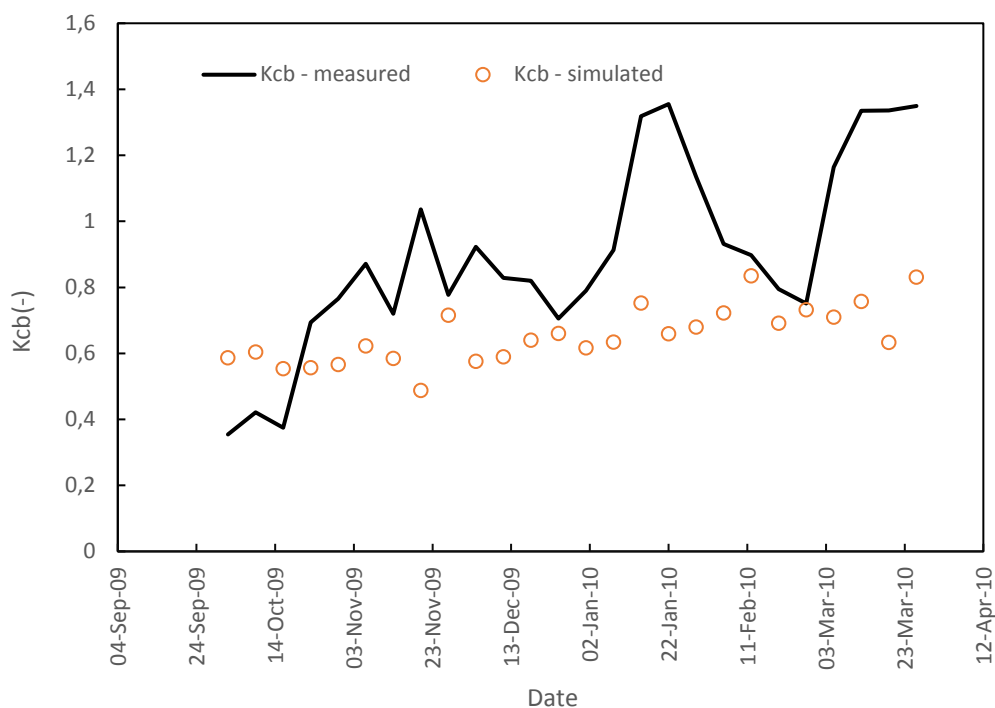


Figure 4.26: Comparison of the measured and simulated  $K_{cb}$  curve for a mature pecan orchard at Cullinan, Gauteng.

However, we are uncertain of the role of the inferior data used in these graphs. The peak  $K_c$  and  $K_{cb}$  values reported by Gush and Taylor (2014) reach a peak of 1.2 while the measured values in Figure 4.26 and 4.27 reach up to 1.4.

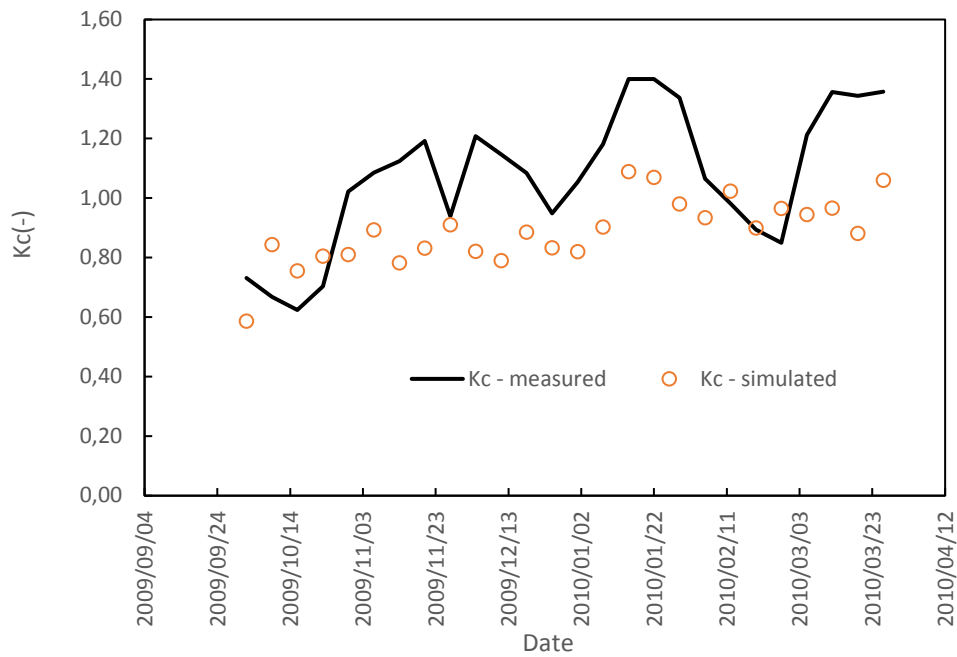


Figure 4. 27: Comparison of the measured and simulated  $K_c$  for a mature pecan orchard at Cullinan, Gauteng.

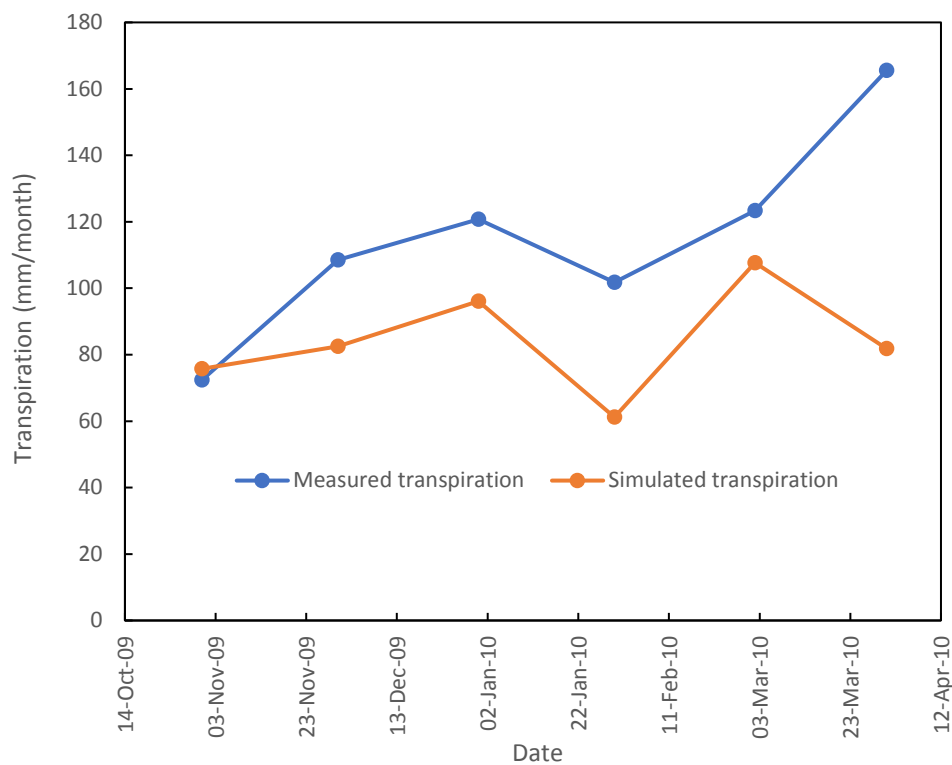
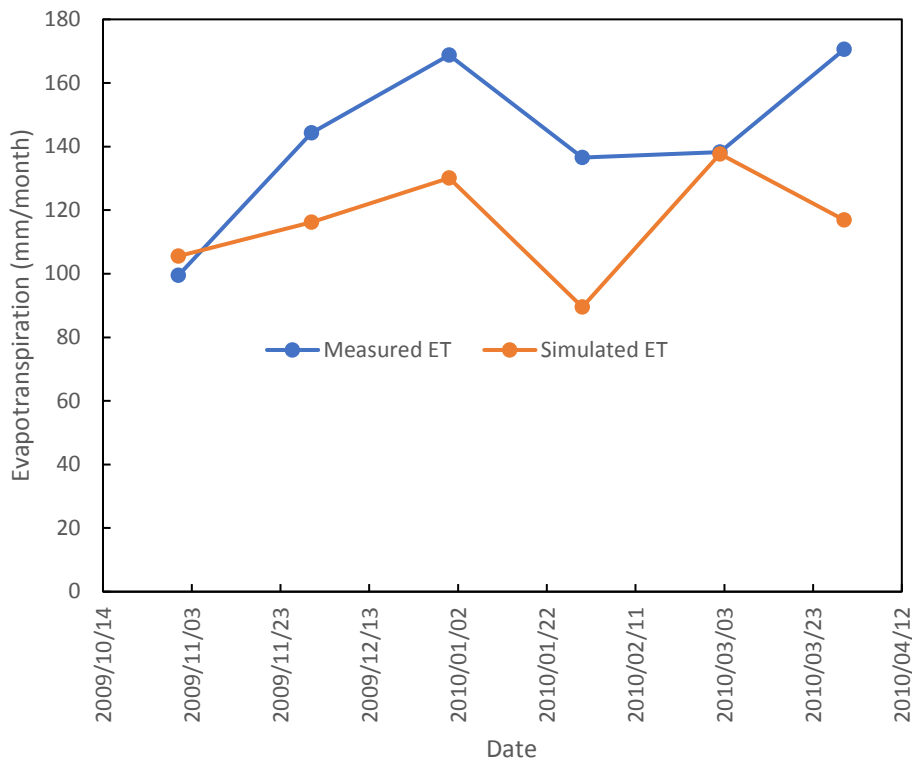


Figure 4.28: Measured vs simulated monthly transpiration for a mature pecan orchard in Cullinan, Gauteng.



*Figure 4.29: Measured vs simulated monthly evapotranspiration for a mature pecan orchard in Cullinan, Gauteng.*

It is not surprising therefore that the monthly total transpiration and evapotranspiration derived using the simulated crop coefficients were much lower than the measured values (see Figs 4.28 and 4.29). There is need for more work to improve the simulations, starting with a thorough assessment of the quality of the data used.

## **APPLE ORCHARDS**

### **a) Description of study sites and data collection methods**

Data used in this section were collected as part of a WRC/ Hortgro Science funded project which ran from April 2014 to March 2018 and Figure 4.30 shows a typical apple orchard on ridges. This experiment was done in 12 different orchards planted to either the blushed apple cultivars (i.e. ‘Cripps’ Pink/ Rosy Glo or Cripps’ Red) and the green cultivars, namely the ‘Golden Delicious’ or ‘Golden Delicious Reinders’. The selected blushed cultivars are late season varieties. Therefore, the argument was that they

consume more water by virtue of them supporting a high crop load over a longer period. The green cultivars were selected because they are the most widely planted, so their water requirements were of interest.

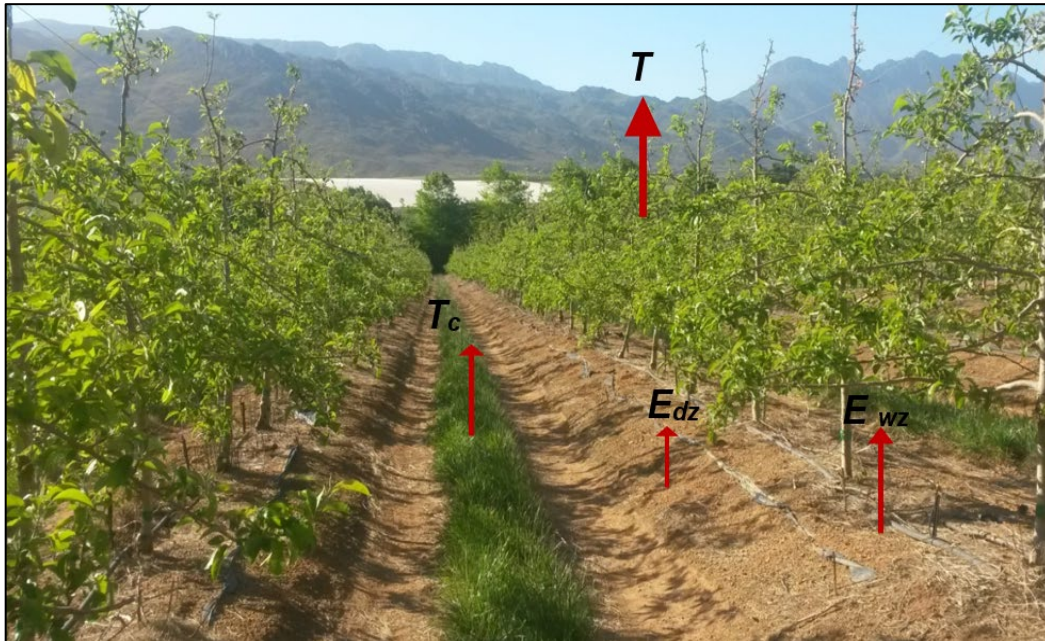


*Figure 4.30: Typical layout of an apple orchard in the Western Cape.  $T$  is transpiration by the trees,  $T_c$  transpiration from the cover crop,  $E_{dz}$  – soil evaporation from the dry zone,  $E_{wz}$  – soil evaporation from the wetted zone (after Dzikiti et al., 2018a).*

*Table 4.16: Details of the 12 orchards used in the Koue Bokkeveld (KBV) and Elgin/Grabouw/Vyeboom/Villiersdorp (EGVV) production regions from 2014-2017. High, medium, and low canopy cover denotes >50%, 20-49% and <20% fractional vegetation cover. LAI = Leaf area index (after Mobe et al., 2020).*

Year	Region	Cultivar	Age (yr.)	Canopy cover	Area (ha)	Planting patterns (m)	Height (m)	LAI
2014/15	KBV	Golden Delicious	22	High	6.0	4 × 1.5 m	4.5	2.38
	KBV	Cripps' Pink	9	High	6.5	4 × 1.5 m	3.8	2.16
	KBV	Golden Delicious	3	Low	3.2	4 × 1.5 m	2.0	0.45
	KBV	Reinders® Rosy Glow	4	Low	4.0	3.5 × 1.25 m	3.0	0.74
2015/16	EGVV	Golden Delicious	29	High	6.5	4 × 2.0 m	4.5	2.13
	EGVV	Cripps' Pink	12	High	5.0	4 × 1.5 m	4.3	1.99
	EGVV	Golden Delicious	3	Low	6.5	4 × 2.0 m	2.5	0.64
	EGVV	Reinders® Cripps' Red	3	Low	5.0	4 × 2.0 m	2.6	0.46
2016/17	KBV	Golden Delicious	5	Medium	3.2	4 × 1.5 m	3.4	1.02
	KBV	Reinders® Cripps' Pink	7	Medium	4.5	4 × 2.0 m	4.0	1.48
	EGVV	Golden Delicious	5	Medium	5.5	4 × 2.0 m	3.0	0.74
	EGVV	Reinders® Cripps' Pink	6	Medium	4.5	4 × 2.0 m	4.0	1.34

Details of the soil properties in the study orchards are summarized in Table 4.17. Data collected include tree transpiration rates measured using the HRM technique for trees whose stem diameters were larger than 4.0 cm. Thermal dissipation probes were used to measure transpiration rates in younger (<4.0 cm) orchards. Whole orchard ET rates were measured using the eddy covariance system and the soil water balance approach. Orchard microclimates, soil water content, irrigation volumes, growth, leaf

area index, etc. were also measured.

*Table 4.17: Typical soil classification analysis for the orchards of different age groups monitored at KBV and EGVV in 2014/15, 2015/16 and 2016/17 growing seasons.  $\theta_{FC}$ = volumetric soil water content at field capacity;  $\theta_{WP}$ =volumetric soil water content at the permanent wilting point; REW= readily evaporable water; TEW= total evaporable water, FBGD= Mature ‘Golden Delicious’, FBCP= Mature ‘Cripps Pink’, NBGR= Non-bearing ‘Golden Delicious Reinders®’, NBRG= Non-bearing ‘Rosy Glow’, NBCR= Non-bearing ‘Cripps’ Red’, BGD= Bearing ‘Golden Delicious’, BGR= Bearing ‘Golden Delicious Reinders®’ BCP= Bearing ‘Cripps Pink’.*

Location	Season	Orchards	Soil texture	Soil water		Soil texture distribution			REW (mm)	TEW (mm)
				$\theta_{FC}$	$\theta_{WP}$	Sand	Silt	Clay		
				(cm <sup>3</sup> cm <sup>-3</sup> )	(cm <sup>3</sup> cm <sup>-3</sup> )	%				
KBV	2014/15	FBGD	Sandy loam	0.171	0.027	83.5	2.9	13.6	7.4	23.6
		FBCP	Sandy loam	0.174	0.049	82.7	4.0	13.3	7.6	22.4
		NBGR	Sandy loam	0.187	0.023	81.0	3.3	15.7	11.9	30.4
		NBRG	Sandy	0.193	0.042	92.0	2.0	6.0	11.9	18.1
EGVV	2015/16	FBGD	Sandy loam	0.189	0.055	80.8	8.7	10.3	7.8	24.2
		FBCP	Clay loam	0.230	0.050	33.8	28.4	37.6	11.0	30.8
		NBGD	Sandy clay	0.230	0.055	15.7	35.4	48.9	7.9	26.3
		NBCR	Sandy loam	0.143	0.045	81.4	6.9	11.7	6.7	25.8
KBV	2016/17	BGD	Sandy loam	0.187	0.023	85.4	8.1	6.5	7.1	26.3
		BCP	Loamy sand	0.190	0.032	83.6	13.7	2.8	7.4	26.
EGVV		BGR	Sandy clay loam	0.230	0.055	58.3	15.3	26.5	10.2	30.4
		BCP	Clay loam	0.195	0.030	35.0	25.3	39.7	11.2	27.0

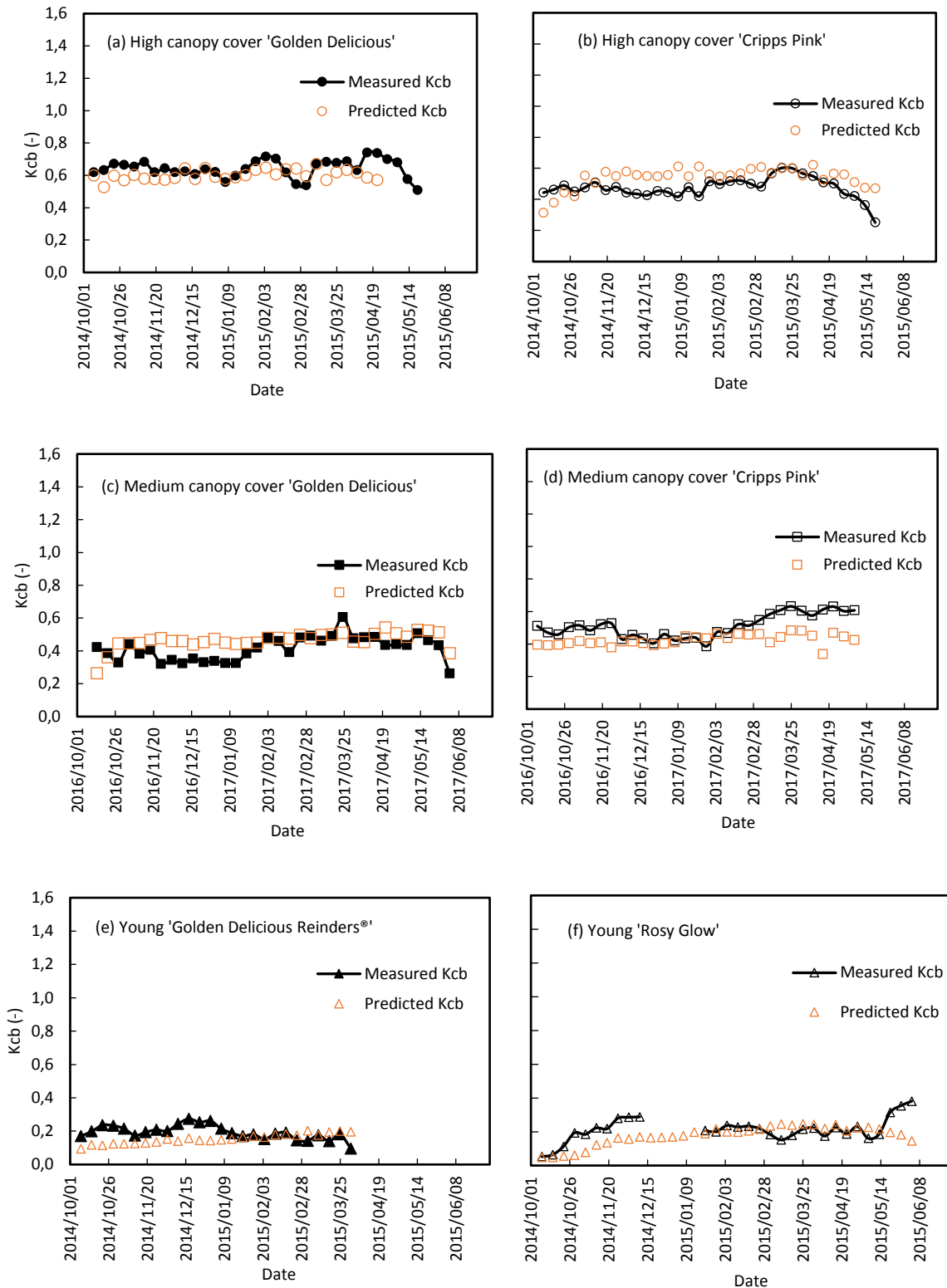
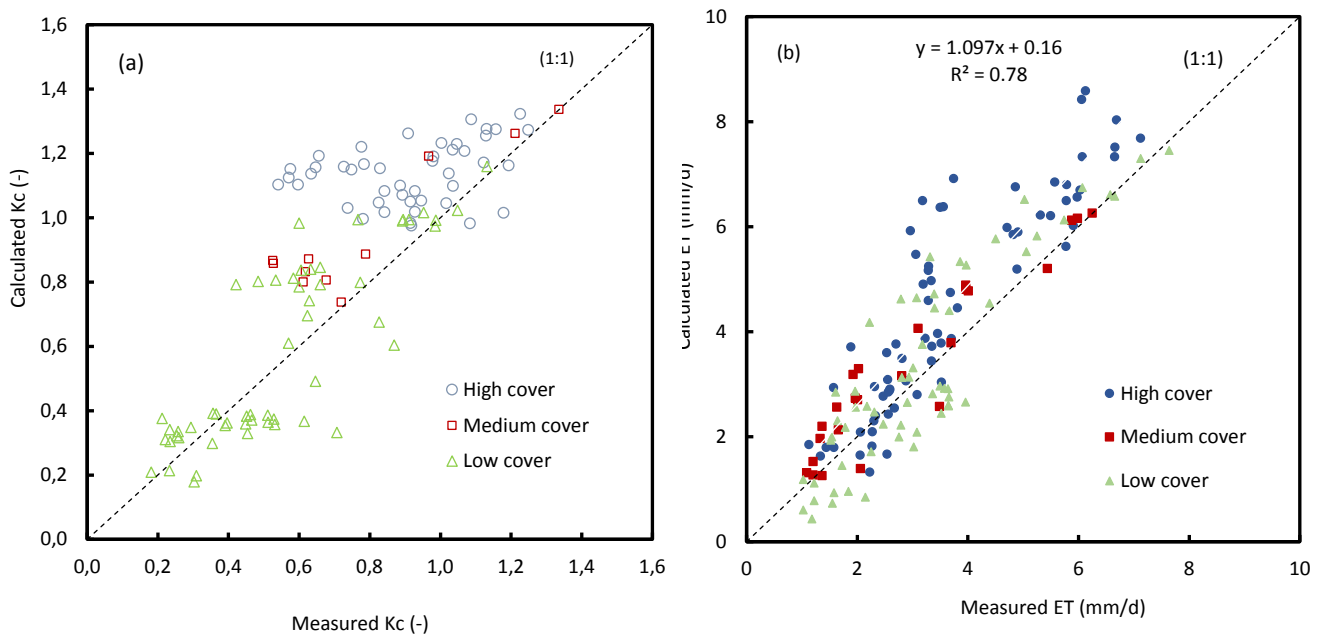


Figure 4.31: Illustration of the performance of the improved Allen and Pereira basal crop coefficient calculation method on ‘Golden Delicious’ and ‘Cripps’ Pink apple cultivars in: (a-b) – high canopy cover, (c-d) – medium canopy cover, and (e-f) – low canopy cover orchards (after Mobe et al., 2020).

Detailed descriptions can be found in the following papers published in the Agricultural Water Management journal (Dzikiti et al., 2018b, Mobe et al., 2020 and Ntshidi et al., 2021a) and in Scientia Horticulturae (Mobe et al., 2021), Water SA journal (Mobe et al., 2020b) and Physics and Chemistry of the Earth journal (Ntshidi et al., 2021b). The average leaf resistance that was used in the calculations for all the 12 orchards was  $212 \text{ s m}^{-1}$  and  $\alpha$  was calculated as  $37 \text{ s m}^{-1}$ . The fractional vegetation cover was derived from the LAI data using Beer's law.

The derived basal crop coefficients clearly closely matched the measured values for orchards of all age groups and cultivars (Figure 4.31). In Figure 4.31 we demonstrate the performance of the calculation procedure on selected orchards although similar results were observed in all orchards.



**Figure 4.32:** (a) Comparison of the crop coefficients determined with the improved A&P method with measured values for 12 apple orchards. (b) Evapotranspiration predicted using the improved crop coefficients and measured by the eddy covariance system.

Because the ET data were also collected over short window periods, we decided to pool together all  $K_c$  data from the 12 orchards as summarized in Figure 4.32a. The corresponding ET estimates of the data pooled from all the orchards are summarized in Figure 4.32b.

***b) Monthly transpiration rates for apple orchards, Western Cape.***

A comparison of the monthly tree transpiration calculated using the simulated  $K_{cb}$  with the measured data for apple trees with varying canopy cover are shown in Figure 4.33. The associated statistics are presented in Table 4.18. It is clear that the improved A&P method can accurately predict the crop coefficients and hence the water use (both transpiration and ET) of apple orchards.

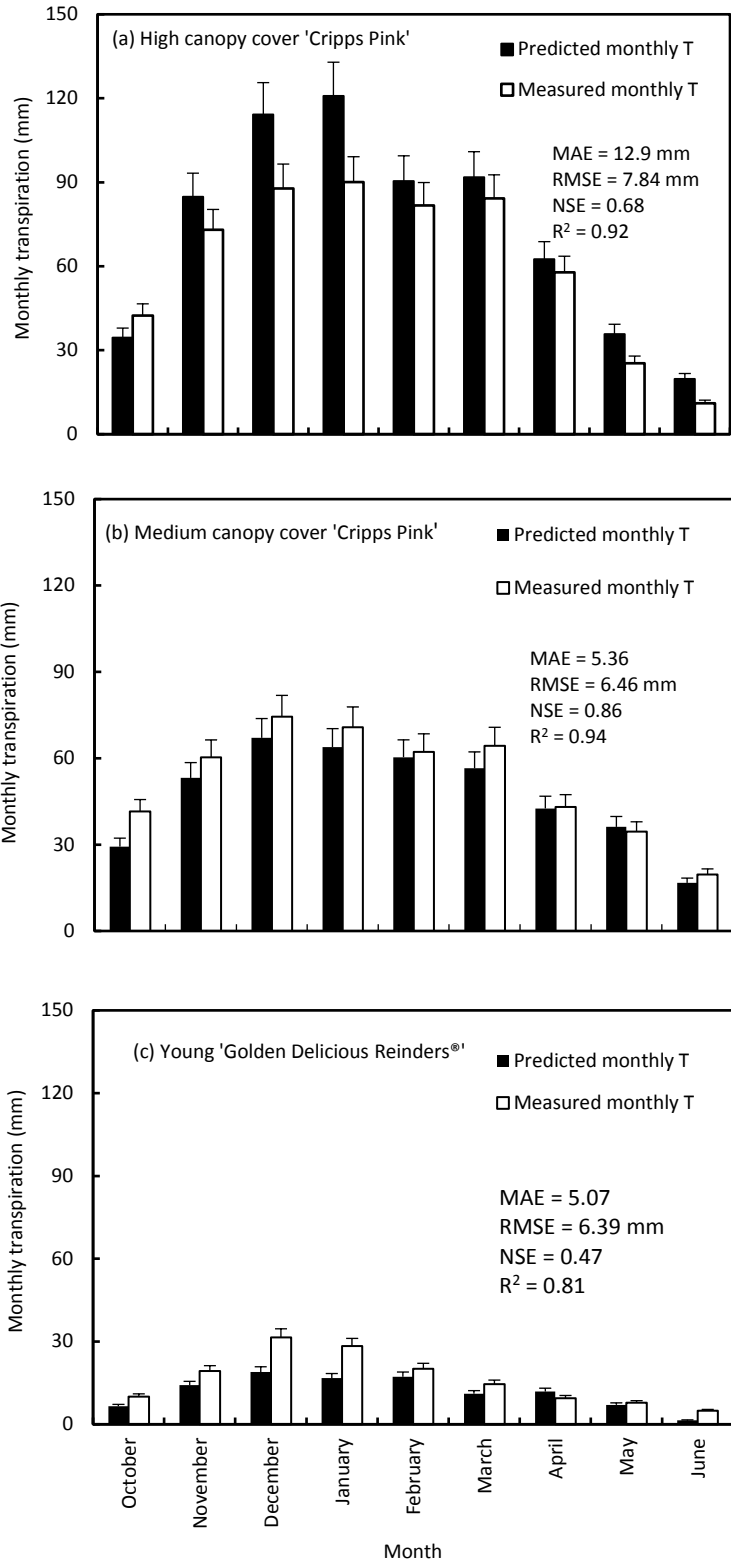


Figure 4.33: Comparison of the measured and calculated monthly total transpiration rates of orchards with high (a), medium (b) and low canopy cover (c) (after Mobe et al., 2020).

Table 4.18: Comparison between monthly predicted and measured transpiration for orchards with varying canopy cover.  $R^2$  is the coefficient of determination, RMSE is the root of the mean square error, MAE is mean absolute error and N is the number of observations.

Month	Full canopy cover					Medium canopy cover					Low (young) canopy cover					
	T_predicted (mm)	T_measured (mm)	$R^2$	RMSE (mm)	MAE (mm)	T_predicted (mm)	T_measured (mm)	$R^2$	RMSE (mm)	MAE (mm)	T_predicted (mm)	T_measured (mm)	$R^2$	RMSE (mm)	MAE (mm)	N
October	47.61	59.22	0.52	14.35	11.61	25.13	38.43	0.43	17.32	13.30	5.01	11.37	-	7.25	6.36	4
November	90.88	89.78	0.37	9.74	8.33	51.92	53.11	0.68	9.71	8.78	15.03	26.71	0.77	12.43	11.68	4
December	116.18	107.66	0.36	14.36	10.96	62.69	61.21	0.55	13.81	12.21	22.23	34.87	0.75	12.65	12.64	4
January	118.01	107.57	0.41	15.68	10.45	61.19	57.88	0.72	10.12	8.43	23.62	33.09	0.80	10.30	9.48	4
February	92.29	92.31	0.62	8.49	7.95	56.68	53.40	0.94	4.94	4.23	21.01	23.83	0.83	4.14	2.94	4
March	82.33	85.57	0.12	8.19	7.00	51.60	54.25	0.93	6.05	5.53	18.65	18.77	0.69	4.34	3.78	4
April	59.62	63.22	0.64	6.72	5.96	36.76	39.66	0.61	10.35	7.20	15.49	14.24	0.68	2.49	2.47	4
May	39.03	45.71	0.12	13.96	11.85	28.63	30.95	0.44	9.43	6.72	9.69	11.46	0.72	2.72	2.33	4

## 4.2.2 Evergreen subtropical fruit tree orchards

### Mango orchards

#### *a) Description of study site and data collection methods*

Water use of commercial mango orchards is being measured in an ongoing study at Riverside farm in Malelane, Mpumalanga Province (Table 4.19). The four-year study (2020-2024) is funded by the Water Research Commission (WRC C2020/2023-00399) and the Inkomati-Usuthu Water Management Area. The cultivar is the widely planted Tommy Atkins on Sambre rootstock. The orchard is about 9.5 ha with a tree density of 303 trees per hectare. The soils are predominantly sandy loam with a high stone content. Irrigation is via a micro sprinkler system delivering 50 L h<sup>-1</sup>. The trees are about 4.0 m high on average and the interrow spacing is covered with indigenous grasses which die off during the dry months (Figure 4.34).



*Figure 4.34: Mature mango orchard at Riverside farm in Malelane, Mpumalanga province.*

Table 4.19: Characteristics of the mature mango orchard at Riverside farm in Malelane, Mpumalanga Province.

ORCHARD CHARACTERISTICS	DESCRIPTION
Block name	M11
Cultivar	Tommy Atkins
Rootstock	Peach/Sabre
Planting date	1984
Plant density (no of trees per ha)	303
Orchard area	9.5 ha
Row orientation	North-South
GPS coordinates	S25°26'51.72"; E31° 33' 18,87"; 321 m asl
Soil texture	Sandy loam
Irrigation system	Microsprinkler
Irrigation delivery rate	50 L/h
Wetted diameter	1.5 m
Tree dimensions	
- Height	4.0 m
- Canopy width	3.5 m
- LAI (Tree & orchard)	2.99 ± 0.13 & 1.89 ± 0.28
Average yield	40 t/ha
Cover crop type and status	Indigenous Vlei Bristle Grass ( <i>Setaria incrassata</i> )

Transpiration is being measured with the HRM sap flow monitoring technique on four trees with different stem diameters. Orchard evapotranspiration is being measured with the open path eddy covariance method during selected window periods. Other data being collected include the orchard microclimate, LAI, soil water content in the root zone, irrigation volumes, canopy temperature, and light interception. Ecophysiological data namely photosynthesis, leaf stomatal resistance, and leaf transpiration are being measured also at selected intervals.

### **b) Observed vs standardized crop coefficients for mango**

Typical observed and standardized basal and single crop coefficients for the mango orchard are shown in Tables 4.20 and 4.21. Since mango is an evergreen tree crop, the crop coefficients remain high throughout the year with  $K_{cb}$  ranging from 0.31 to 0.65 while the  $K_c$  for March 2022 just exceeded 1.0.

*Table 4.20: Observed and standardized basal crop coefficients for mature mango orchards (Dzikiti et al., ongoing).*

<b>Month</b>	<b>Kcb_obs</b>	<b>Kcb_std</b>
<b>Jul</b>	0.37	0.32
<b>Aug</b>	0.31	0.28
<b>Sep</b>	0.39	0.39
<b>Oct</b>	0.39	0.41
<b>Nov</b>	0.51	0.56
<b>Dec</b>	0.45	0.51
<b>Jan</b>	0.46	0.53
<b>Feb</b>	0.49	0.51
<b>Mar</b>	0.65	0.7
<b>Apr</b>	0.54	0.58

*Table 4.21: Observed and standardized crop coefficients for mature mango orchards (Dzikiti et al., ongoing).*

<b>Month</b>	<b>Kc_obs</b>	<b>Kc_std</b>
<b>Jul</b>	-	-
<b>Aug</b>	-	-
<b>Sep</b>	-	-
<b>Oct</b>	-	-
<b>Nov</b>	-	-
<b>Dec</b>	-	-
<b>Jan</b>	-	-
<b>Feb</b>	-	-
<b>Mar</b>	1.03	0.79
<b>Apr</b>	-	-

The crop coefficient curve did not show the characteristic four phenological stages (see Figure 4.35) and we are uncertain at this stage why this is the case. The weekly  $K_{cb}$  values, calculated using a leaf resistance of about  $380 \text{ s m}^{-1}$  closely matched the observed values (Figure 4.36). The daily  $K_c$  results are shown in Figure 4.37.

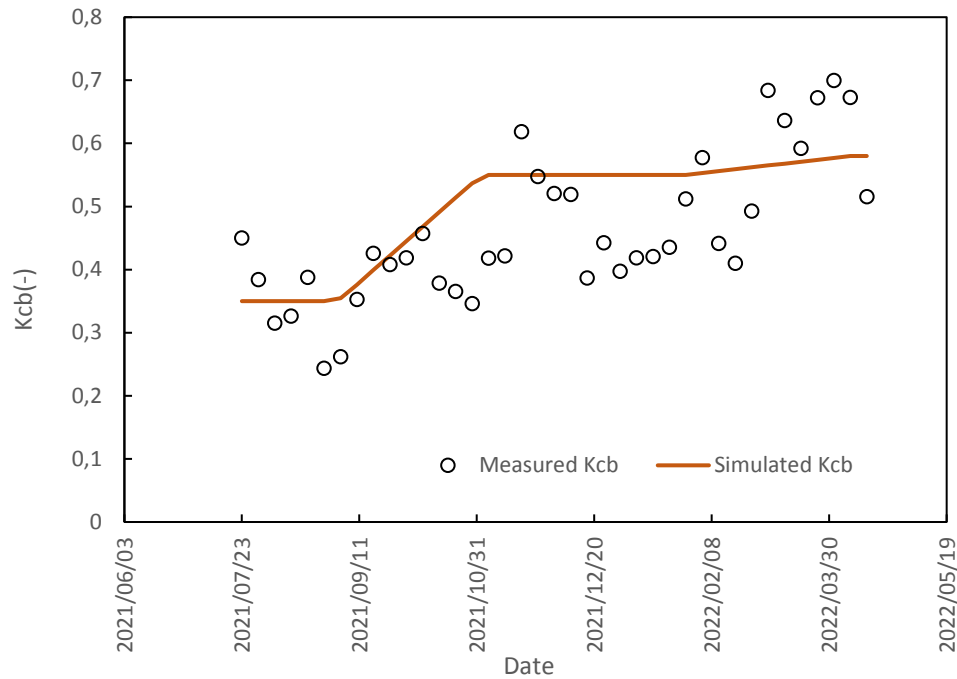


*Figure 4.35: Crop coefficient curve for a mature mango orchard in Malelane, Mpumalanga Province.*

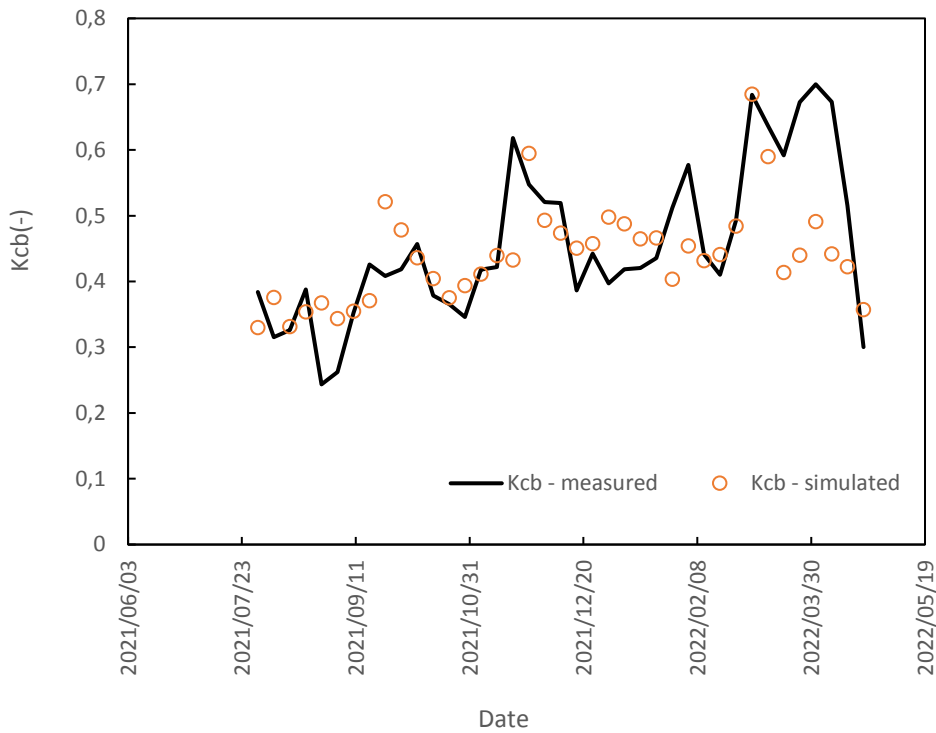


Figure 4.36: Observed vs simulated weekly  $K_{cb}$  for a mature mango orchard in Malelane, Mpumalanga Province.

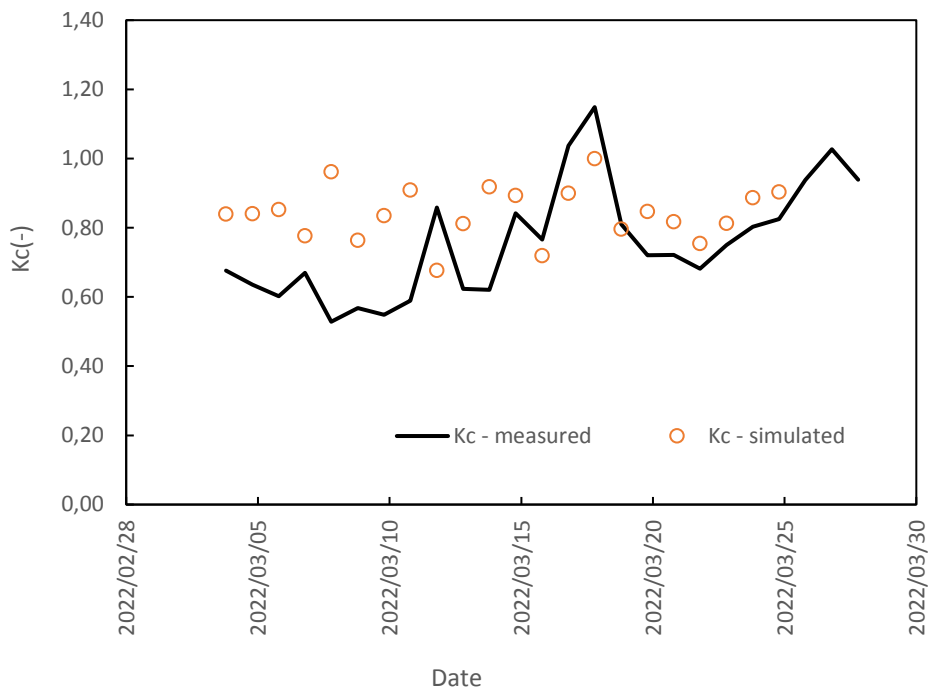
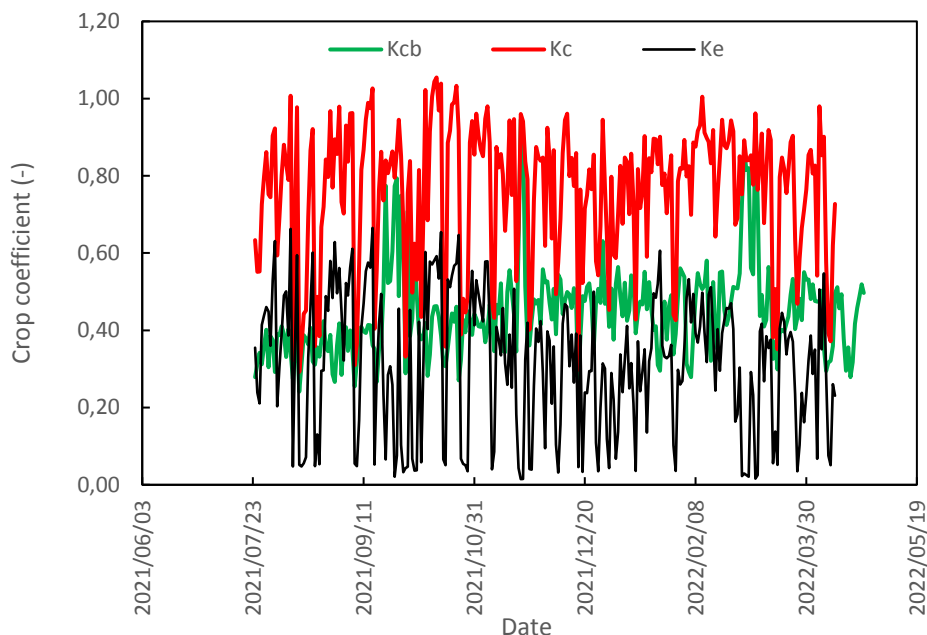


Figure 4.37: Measured vs simulated  $K_c$  values for a mature mango orchard in Malelane, Mpumalanga.

The seasonal changes in the crop coefficients (Figure 4.38) show that the simulated peak  $K_c$  was around 1.05 reached in late spring. The  $K_c$  values decreased in summer likely because of the high incidence of cloud cover which reduced the atmospheric evaporative demand since the area receives summer rainfall. Occasional peaks in  $K_{cb}$  were observed and we are unsure what could be the cause for these. The simulated soil evaporation coefficient was fairly high hovering between 0.30 and 0.40. This is not surprising given the low tree density which created large interrow spacings which result in higher orchard floor evaporation.

**c) Monthly transpiration rates for mango orchards in Mpumalanga**

Figure 4.39 shows that the simulated monthly transpiration for the mango orchard closely matched the actual measured data. The coefficient of determination ( $R^2$ ) was 0.92. The MAE was  $\pm 4.3$  mm/month while the RMSE was  $\pm 1.9$  mm/month. These values translate to less than  $\pm 0.15$  and  $\pm 0.06$  mm  $d^{-1}$  MAE and RMSE which is quite small.



*Figure 4.38: Seasonal changes in the simulated daily crop coefficients for a mango orchard in Malelane, Mpumalanga Province.*



*Figure 4.39: Comparison of the measured vs simulated monthly total transpiration for a mango orchard in Malelane, Mpumalanga Province.*

## **MACADAMIA ORCHARDS**

### **a) Description of study site and data collection methods**

The water use of macadamia orchards has been quantified in two separate studies, first by Gush and Taylor (2014), and secondly by Taylor et al. (2021). In this study we present the details of the Gush and Taylor (2014) campaign, and we refer to Taylor et al. (2021) where necessary. Details of the macadamia orchard at White River, in Mpumalanga are summarized in Table 4.22. The orchard was 7 years old at the time of the study planted to the Beaumont cultivar on the Beaumont rootstock. Plant density was 312 trees per hectare arranged in north-south oriented rows. The trees were 5.0 m tall irrigated with double drippers per tree row with dripper delivering  $1.3 \text{ L h}^{-1}$  spaced about 1.0 m along the dripper line. The soils were deep sandy loam soils.



*Figure 4.40: Macadamia orchard at White River in Mpumalanga Province (after Gush and Taylor, 2014).*

*Table 4.22: Details of the macadamia orchard at White River, Mpumalanga.*

Age	6-7 years
Block size	2.6 ha
Planting density	312 trees per ha
Cultivar	Beaumont
Rootstock	Beaumont
Height	5.0 m
Irrigation	Double line drip @ 1.3 L h <sup>-1</sup> every 1.0 m
Soils	Sandy loam
Yield	5 t ha <sup>-1</sup>

Tree transpiration was measured using the heat ratio method of quantifying sap flow on four trees. Orchard evapotranspiration was measured at selected intervals using an open path eddy covariance system. Other data collected included the orchard

microclimate, volumetric soil water content, irrigation amounts, soil evaporation, and leaf area index. Ecophysiological data, namely the stem water potential, and stomatal conductance were also measured.

**b) Observed vs standardized crop coefficients for macadamia orchards**

The observed and standardized basal and single crop coefficients for the macadamia orchard are summarized in Tables 4.23 and 4.24. The observed  $K_{cb}$  was consistently high throughout the year ranging from 0.41 in mid-summer to a peak around 0.74 in late spring.

These figures suggest that the transpiration rate does not keep up with the atmospheric evaporative demand during the hot summer periods. Both studies (Gush and Taylor, 2014; Taylor et al., 2021) indicate that macadamia have low water use rates due to very active regulation of the stomatal conductance.

*Table 4.23: Observed and standardized  $K_{cb}$  for a mature macadamia orchard in White River, Mpumalanga (after Gush and Taylor, 2014).*

Month	Kcb_obs	Kcb_std
Oct	0.74	0.81
Nov	0.48	0.59
Dec	0.5	0.62
Jan	0.49	0.61
Feb	0.41	0.49
Mar	0.46	0.54
Apr	0.61	0.73
May	0.61	0.76

Another reason for the low crop coefficients in summer could be the high incidence of cloud cover that reduced the atmospheric evaporative demand since the study site

was in a summer rainfall area. Taylor et al. (2021) studied the water use of slightly younger macadamia trees over multiple seasons. Their results are summarized in Tables 4.24 and 4.25.

*Table 4.24: Observed and standardized  $K_c$  for a mature macadamia orchard in White River, Mpumalanga (after Gush and Taylor, 2014).*

<b>Month</b>	<b>Kc_obs</b>	<b>Kc_std</b>
<b>Oct</b>	0.76	0.73
<b>Nov</b>	0.61	0.72
<b>Dec</b>	0.57	0.69
<b>Jan</b>	0.56	0.68

Table 4.25: Observed and standardized  $K_{cb}$  for a mature macadamia orchard in Mpumalanga (Taylor et al., 2021).

Year	Month	Kcb_obs	Kcb_std
2018	Aug	0.25	0.14
	Sep	0.30	0.24
	Oct	0.26	0.20
	Nov	0.27	0.29
	Dec	0.30	0.32
2019	Jan	0.29	0.34
	Feb	0.27	0.31
	Mar	0.32	0.34
	Apr	0.29	0.35
	May	0.30	0.27
	Jun	0.30	0.29
	Jul	0.24	0.21
	Aug	0.24	0.20
	Sep	0.25	0.22
	Oct	0.25	0.28
	Nov	0.25	0.28
	Dec	0.26	0.33
2020	Jan	0.26	0.30
	Feb	0.29	0.39
	Mar	0.29	0.36
	Apr	0.32	0.40
	May	0.24	0.30
	Jun	0.28	0.25
	Jul	0.28	0.27
	Aug	0.25	0.23

Table 4.26: Observed and standardized  $K^c$  for a mature macadamia orchard in Mpumalanga (after Taylor et al., 2021).

Year	Month	Kc_obs	Kc_std
2018	Aug	-	-
	Sep	-	-
	Oct	-	-
	Nov	-	-
	Dec	-	-
2019	Jan	-	-
	Feb	-	-
	Mar	-	-
	Apr	-	-
	May	-	-
	Jun	-	-
	Jul	-	-
	Aug	-	-
	Sep	0.52	0.5
	Oct	-	-
	Nov	-	-
	Dec	-	-
2020	Jan	-	-
	Feb	-	-
	Mar	-	-
	Apr	0.21	0.27
	May	0.59	0.65
	Jun	0.44	0.42
	Jul	0.37	0.36
	Aug	0.32	0.3

Taylor et al. (2021) measured the mean leaf resistance ( $r_l$ ) for macadamia trees of around  $2\ 100\ \text{s m}^{-1}$ . In this study, the best fit between the measured and simulated  $K_{cb}$  values were obtained using a value of  $r_l$  of  $1\ 800\ \text{s m}^{-1}$  and  $\alpha$  was set at around  $200\ \text{s m}^{-1}$ . A comparison of the observed and simulated weekly  $K_{cb}$  for the macadamia orchards is shown in Figure 4.41 while  $K_c$  values are shown in Figure 4.42.

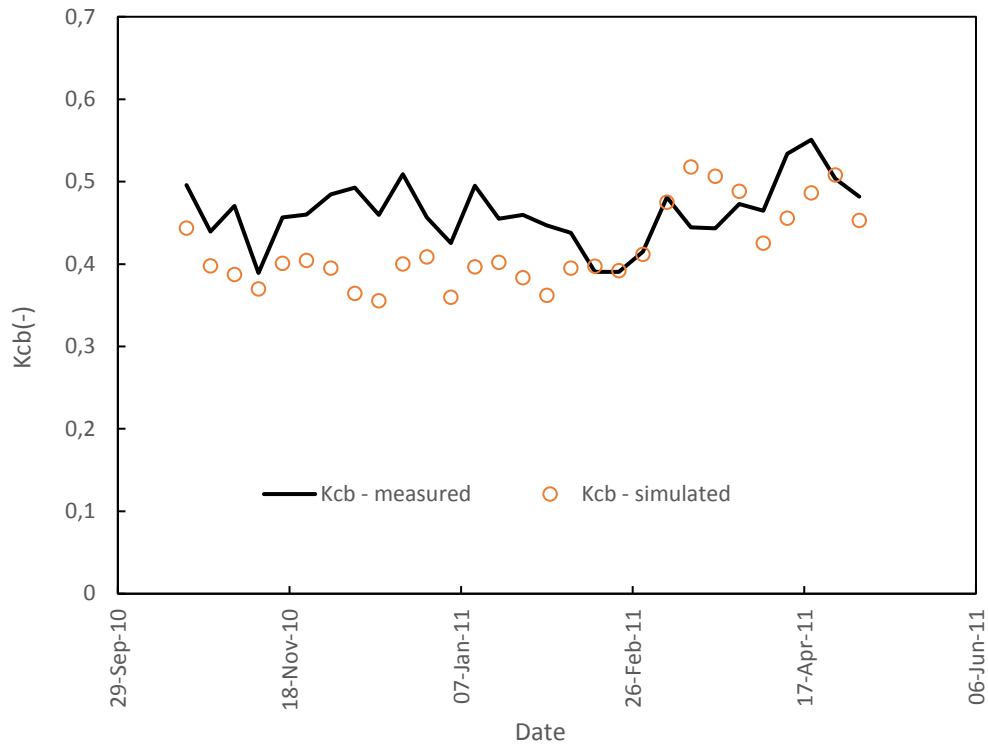


Figure 4.41: Comparison of the measured and simulated  $K_{cb}$  for a mature macadamia orchard in White River, Mpumalanga Province.

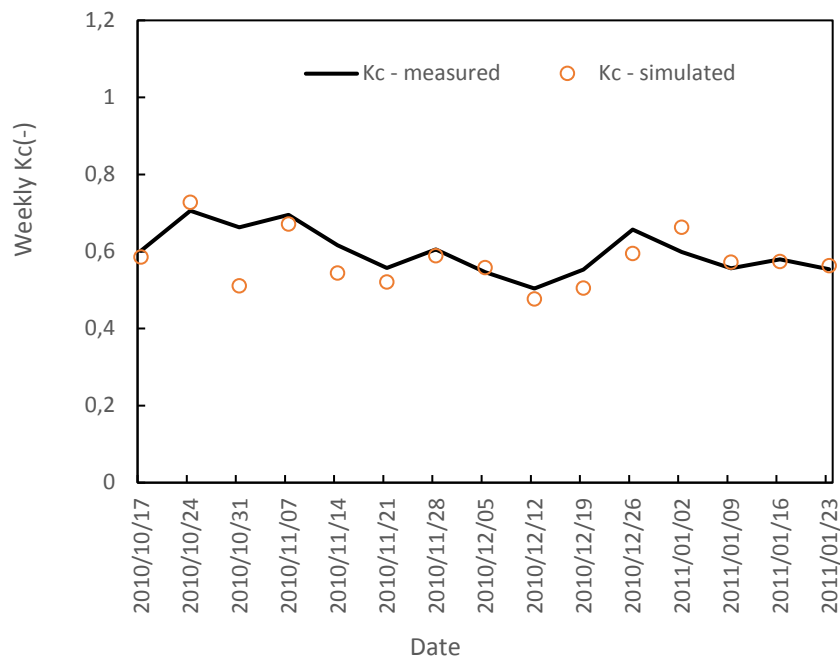
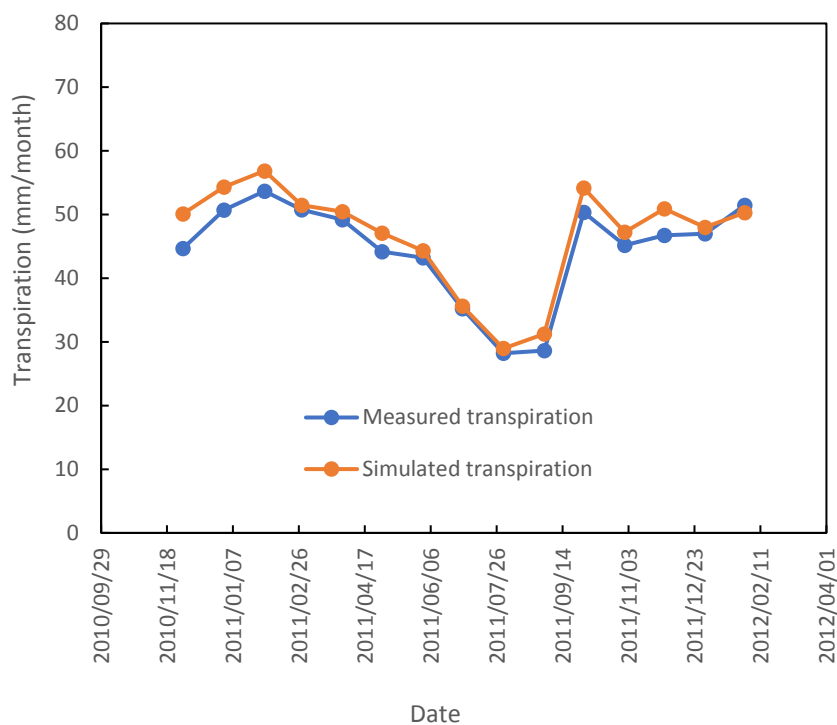


Figure 4.42: Comparison of the measured and simulated  $K_c$  for a mature macadamia orchard in White River, Mpumalanga Province.

### **b) Monthly transpiration rates for macadamia orchards in Mpumalanga**

Figure 4.43 shows that there is a very strong correlation between the simulated and the observed monthly transpiration rates ( $R^2 \sim 0.96$ ). The simulated water use could explain most of the variation in the observed values indicating a strong performance by the modified A&P method. The MAE was 2.3 mm/month while the RMSE was 0.7 mm/month. These observations agree with those by Taylor et al. (2021) although they used a different value of  $\alpha$ .



*Figure 4.43: Comparison of the measured and simulated transpiration for a mature macadamia orchard in White River, Mpumalanga Province.*

## **LITCHI ORCHARDS**

### **a) Description of study site and data collection methods**

Water use and yield data is currently being collected in a mature full bearing orchard at Riverside farm in Malelane (Figure 4.44). This is part of the WRC-IUWMA funded project and detailed characteristics of the orchard are summarized in Table 4.27. The

cultivar is Mauritius on a Mauritius rootstock. The orchard was planted in 1970 with a tree spacing of 11 m x 13 m, giving a tree density of only 70 trees per hectare. The planted area is 13.1 ha, and the trees are irrigated with a microsprinkler irrigation system delivering 50 L h<sup>-1</sup>. Soil type is clayey loam, and the orchard is on gentle sloping terrain. Tree dimensions are shown in Table 4.27. The average yield hovers around 1.5 t ha<sup>-1</sup> per year.



*Figure 4.44: Drone image of the litchi orchard at Riverside farm in Malelane, Mpumalanga.*

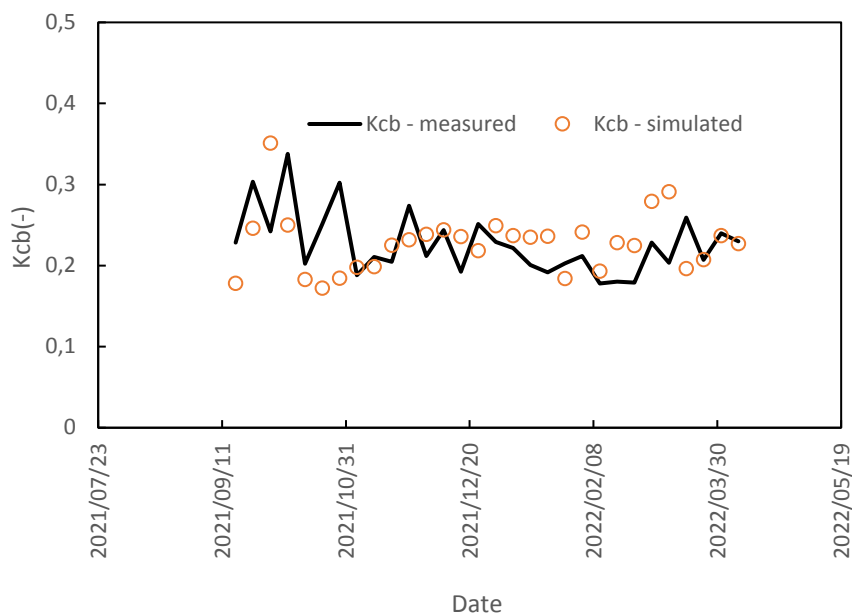
Table 4.27: Characteristics of the litchi orchard at Riverside farm, Mpumalanga.

ORCHARD CHARACTERISTICS	DESCRIPTION
Block name	L7
Cultivar	Mauritius
Rootstock	Mauritius
Planting date	1970
Plant density (no of trees per ha)	70
Tree spacing	11 m x 13 m
Orchard area	13.1 ha
Row orientation	North-South
GPS coordinates	S 25°26'45.49"; E31° 33' 37,21"; 312 m asl
Soil texture	Clayey loam
Irrigation system	Microsprinkler
Irrigation delivery rate	50 L/h
Wetted diameter	1.5 m
Tree dimensions	
- Height	6.0 m
- Canopy width	5.0 m
- LAI (Tree & orchard)	3.14 ± 0.15 & 2.38 ± 0.28
Average yield	1.5 t/ha
Cover crop type and status	Indigenous Vlei Bristle Grass ( <i>Setaria incrasatta</i> )

As like the other orchards, tree transpiration is being measured using the HRM sap flow technique. However, given the huge multiple stems of the trees, up to 8 sap flow probes are installed per tree with the total transpiration calculated as the algebraic sum of the sap flow in the individual branches. Whole orchard evapotranspiration is currently being measured using an open path eddy covariance system. Unfortunately, the data has not been analyzed yet. Other data being collected include the volumetric soil water content, LAI, orchard microclimate, irrigation amounts, canopy temperature, and the intercepted radiation. Ecophysiological data, namely, leaf photosynthesis, transpiration, and stomatal conductance are measured at selected intervals. Continuous data of the tree xylem water potential is being using micro tensiometers embedded into the stems of the trees.

## b) Basal crop coefficients for litchi orchards

The leaf resistance used to calculate the basal crop coefficients shown in Figure 4.45 and was set at  $1000 \text{ s m}^{-1}$ , whilst  $\alpha$  was set to  $20 \text{ s m}^{-1}$ . There appears to be a reasonable agreement between the observed and simulated weekly  $K_{cb}$  values. More data is still being collected, so the trend will be confirmed in the long term. The  $K_{cb}$  values are low given the low water use rates by the trees and the very sparse tree density with large open spaces between the rows. The maximum daily transpiration of the trees can reach up to 220 litres although this is quite low when it is expressed over the entire orchard surface. The  $K_c$  values are not included in this analysis as the ET data is still being collected and analysed. The simulated seasonal changes in the daily crop coefficients are shown in Figure 4.46. The data suggests that  $K_e$  exceeds the basal crop coefficient nearly all the time. This is probable given the wide tree spacing and the active ground cover in the orchard.



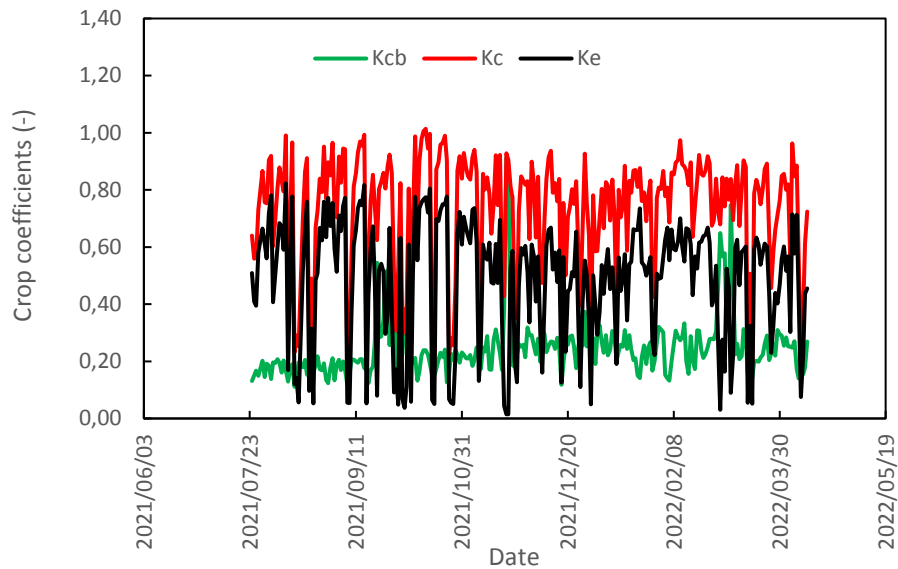


*Figure 4.46: Seasonal changes in the crop coefficients for a mature litchi orchard at Malelane, Mpumalanga Province.*

**c) Monthly transpiration rates for a litchi orchard in Mpumalanga**

The simulated monthly total transpiration by the litchi orchard appears to be consistently greater than the measured values for unclear reasons. The simulated monthly transpiration was up to 7 mm greater than the measured values which translates to an overestimate of close to 0.2 mm d<sup>-1</sup>. It is probable that errors could reside with the weather data used to calculate ET<sub>o</sub>, but this will be further analysed.

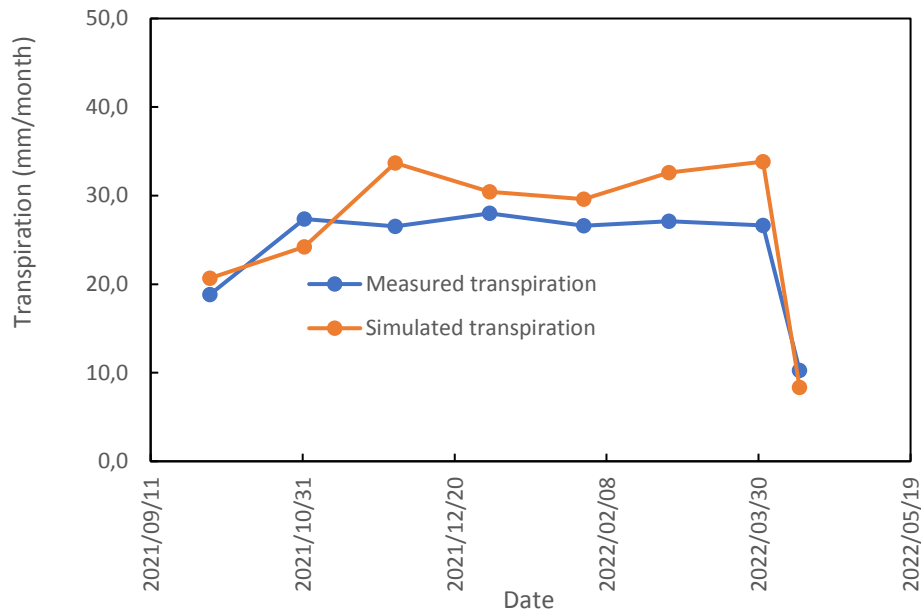


Figure 4.47: Comparison of the measured and simulated monthly transpiration for a mature litchi orchard at Malelane, Mpumalanga Province.

### 4.2.3 Citrus orchards

#### *Rustenburg navel orchards*

##### **a) Description of study site and data collection methods**

The Rustenburg navel orchard was at Patrysberg farm in Citrusdal in the Western Cape. The study was co-funded by the WRC and DAFF and Figure 4.48 shows a side view of the orchard. The trees were 15 years old and data collection occurred during the 2010-2011 season. The data used in this analysis was collected from August 2010 to March 2011 and detailed information about the orchard is presented in Table 4.27. Average tree height was about 3.3 m, and the tree density was 666 trees per hectare. The orchard was under drip irrigation with double drippers per tree row; the drippers were spaced 0.8 m along the irrigation line and the discharge rate of the drippers was about 1.8 L h<sup>-1</sup>. Soils in the orchard were deep sandy loam soils with a very low stone content.



*Figure 4.48: View of the Rustenburg Navel citrus orchard in Citrusdal, Western Cape (after Gush and Taylor, 2014).*

*Table 4.28: Characteristics of the Rustenburg navel citrus orchard at Citrusdal (after Gush and Taylor, 2014)*

Age	15 years
Block size	3.9 ha
Planting density	666 trees per ha
Cultivar	Rustenburg navel
Rootstock	Troyer citrange
Height	3.3 m
Irrigation	2 dripper lines per row; 6 drippers per tree at 0.8 m spacing delivering 1.8 L h <sup>-1</sup>
Soils	Sandy loam
Yield	79 t ha <sup>-1</sup>

Tree transpiration was measured using the heat ratio method of monitoring sap flow and four trees of different stem sizes were instrumented. The details of the installations are given in Gush and Taylor (2014). Whole orchard evapotranspiration was measured using an eddy covariance system which was deployed at selected intervals

representing the different seasons. Additional data collected included the site microclimate, profile soil moisture, irrigation volumes, and the leaf area index. The average leaf stomatal resistance reported by Gush and Taylor (2014) for the Rustenburg navels is around  $2\,500\text{ s m}^{-1}$ . This value was used in the calculation of the crop coefficients. Parameter  $\alpha$  had a value of  $200\text{ s m}^{-1}$  which gave the best fit between the measured and simulated crop coefficients.

***b) Observed vs standardized crop coefficients for Rustenburg navel orange orchards***

Tabulated values of the observed and standardized basal crop coefficients are shown in Table 4.29. As expected, the  $K_{cb}$  values varied over a narrow range between 0.25 and 0.40. For a large part of the data set, the simulated  $K_{cb}$  values matched the observed values except for the period December 2010 to February 2011. The mismatch can be explained by the occurrence of water stress during the peak summer season.

*Table 4.29: Observed and standardized basal crop coefficients for Rustenburg navel citrus at Citrusdal, Western Cape.*

Month	Kcb_obs	Kcb_std
Aug	0.40	0.37
Sep	0.33	0.26
Oct	0.42	0.35
Nov	0.31	0.30
Dec	0.29	0.30
Jan	0.25	0.30
Feb	0.35	0.34
Mar	0.36	0.34

Given the hydraulic resistance of the transpiration stream of citrus trees, it highly probable that water uptake by the trees did not match transpiration leading to transient stress developing.

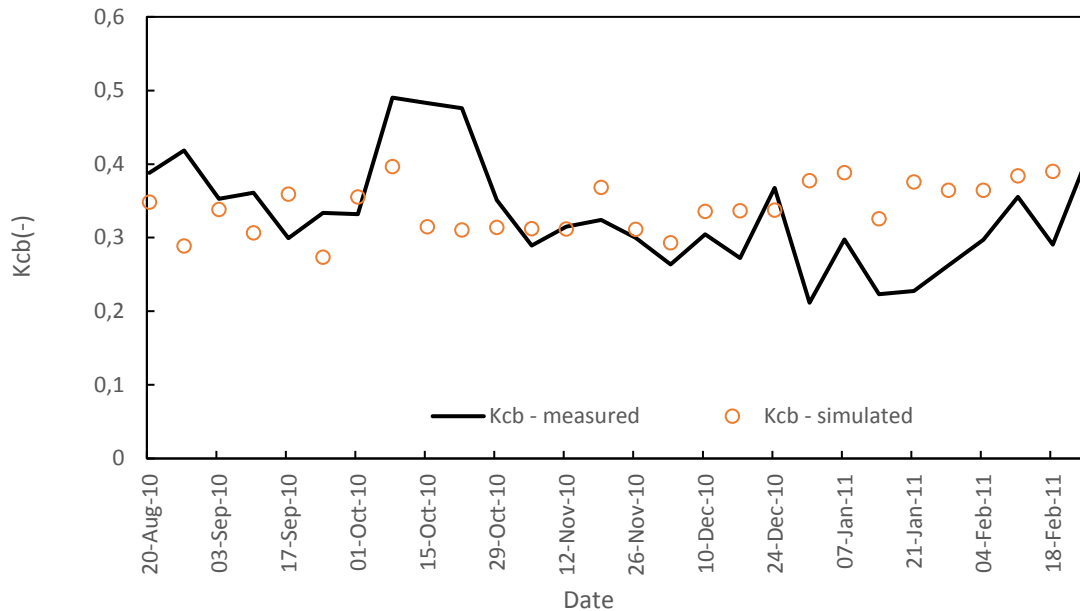


Figure 4.49: Comparison of the observed and calculated  $K_{cb}$  for a Rustenburg navel citrus orchard in Citrusdal, Western Cape.

The simulated seasonal changes in the crop coefficients are shown in Figure 4.50. The peak  $K_c$  approached 1.20 while the  $K_{cb}$  hovered around the 0.40 level. As expected under drip, the  $K_e$  was lower than  $K_{cb}$  except for days after rainfall or heavy irrigation. The trend in  $K_e$  is what is expected in the winter rainfall areas being larger in late winter to early spring due to the greater wetted soil surface by winter rains. The  $K_e$  values decreased towards the summer season when only irrigation was the source of water for evaporation.

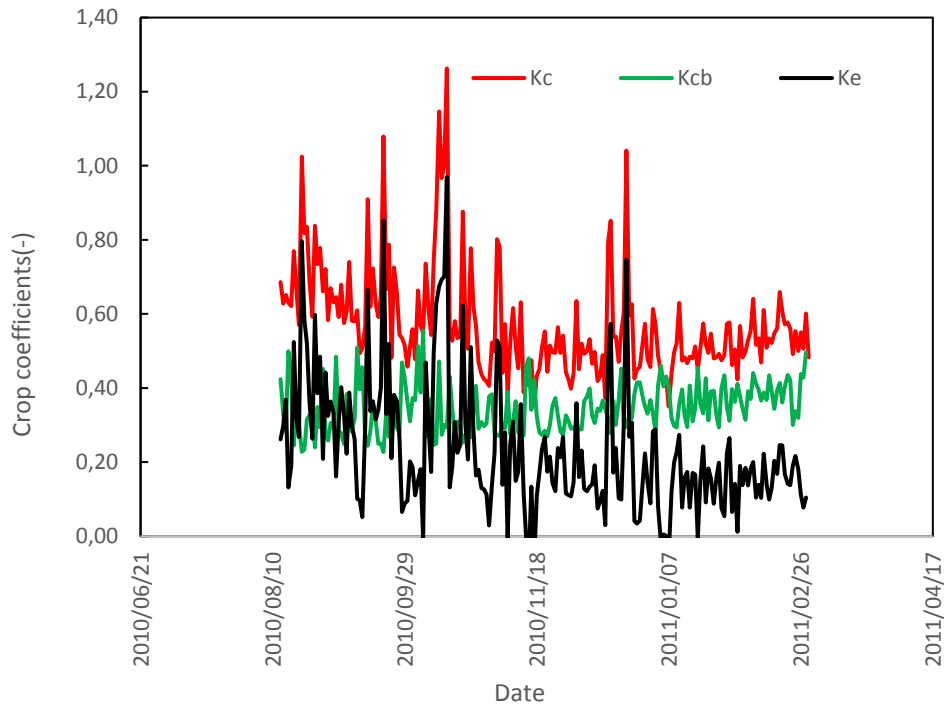


Figure 4.50: Seasonal variations in the crop coefficients for a mature Rustenburg navel citrus orchard in Citrusdal, Western Cape.

**c) Monthly transpiration rates for a Rustenburg navel orange orchard in Citrusdal**

Comparison of the simulated vs measured monthly total transpiration is shown in Figure 4.51. There was good agreement between the two sets of values for the first four months of the year, but the differences became larger towards the summer consistent with the  $K_{cb}$  trend described earlier. The A&P method being evaluated here does not take into account the effect of water stress either due to water deficit or excess water in the rootzone.  $R^2$  between the simulated and measured monthly transpiration 0.87, but this dropped to 0.81 when the whole study period was considered. The MAE was  $\pm 4.7$  mm/month for the first four months, but this doubled to  $\pm 9.7$  mm/month when the whole period was considered. Similarly, the RMSE was

±3.3 mm/month for the first four months, but it increased to ±4.6 mm/month when the whole period was considered.

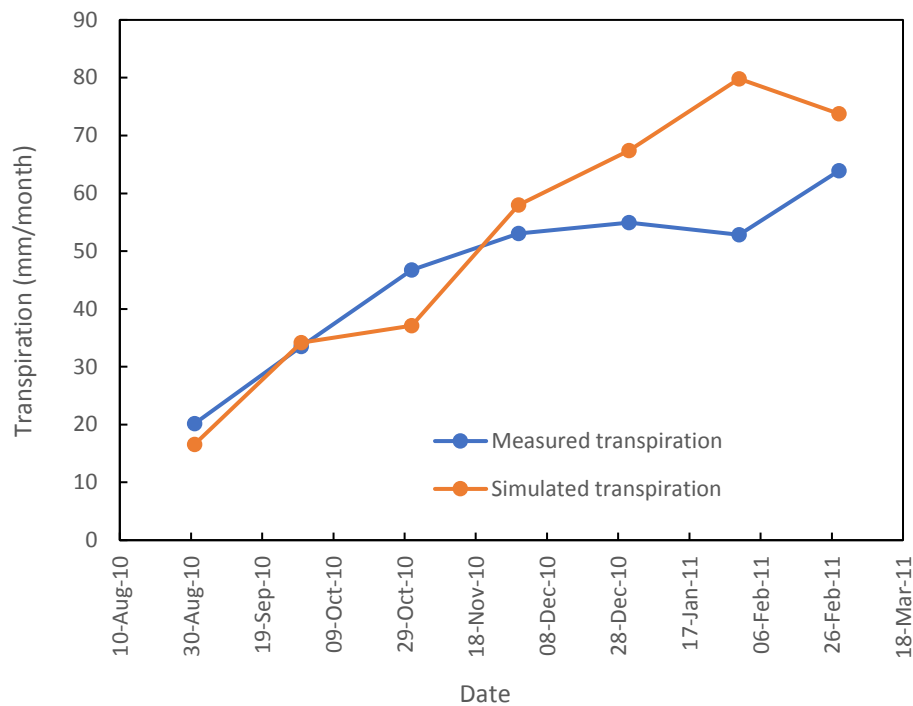


Figure 4.51: Comparison of the measured and simulated monthly transpiration by a mature Rustenburg Navel.

### **Midnight Valencia citrus orchards: Malelane**

#### **a) Description of study site and data collection methods**

The citrus orchard at Malelane (Figure 4.52) was planted to the midnight valencia cultivar on a swingle rootstock. The orchard was 17 years old at the time of the study. Orchard block size was about 7.6 ha, tree density was about 571 trees per hectare. Average height of the trees was about 4.0 m, and the trees were planted in north-south oriented rows. Soil type was sandy loam with a high stone content. Irrigation was through a drip system with two dripper lines per row. The delivery rate of the of the drippers was about 2.0 L h<sup>-1</sup> and these were spaced about 0.6 m along the drip line.

Further details about the orchard are shown in Table 4.30 and in Gush and Taylor (2014).



*Figure 4.52: View of the Midnight Valencia orange orchard in Malelane (after Gush and Taylor, 2014).*

*Table 4.30: Properties of the Midnight Valencia citrus orchard at Malelane.*

Age	16-18 years
Block size	7.6 ha
Planting density	571 trees per ha
Cultivar	Midnight Valencia
Rootstock	Swingle
Height	4.0 m
Irrigation	Double line drip per row @ 2.0 L h <sup>-1</sup> every 0.6 m
Soils	Sandy loam
Yield	30 t ha <sup>-1</sup>

Tree transpiration was measured using the heat ratio method of monitoring sap flow (Burgess et al., 2001). Four trees with different stem diameters were instrumented to capture the variability in water use by trees of different sizes in the orchard. Whole orchard evapotranspiration was measured at selected intervals using the open path eddy covariance system described in detail in Gush and Taylor (2014). Other data collected include volumetric soil moisture content, irrigation volumes, orchard microclimate, leaf area index, and tree dimensions. There was no active ground cover on the orchard floor during the dry season due to the small, wetted area under drip. But natural grasses grew between the tree rows during the summer season following rainfall events.

***b) Observed vs standardized crop coefficients for***

A summary of the observed and standardized basal and single crop coefficients for the Midnight Valencia orchard is shown in Tables 4.31 and 4.32. Unfortunately, we could only access data over three months from November 2011 to January 2012.

*Table 4.31: Observed and standardized basal crop coefficients for Midnight Valencia navel citrus at Malelane, Mpumalanga*

<b>Month</b>	<b>Kcb_obs</b>	<b>Kcb_std</b>
<b>Nov</b>	0.33	0.35
<b>Dec</b>	0.22	0.24
<b>Jan</b>	0.12	0.18

Table 4.32: Observed and standardized crop coefficients for Bahianinha navel citrus at Malelane, Mpumalanga

Month	Kc_obs	Kc_std
Nov	0.70	0.74
Dec	0.71	0.72
Jan	0.65	0.71

A comparison of the observed and simulated weekly crop coefficients for the Midnight Valencia is shown in Figure 4.53. The mean leaf resistance used in the simulations was  $2\ 700\ \text{s m}^{-1}$  and no values are presented for this cultivar in Gush and Taylor (2014). The value of  $\alpha$  was set at  $200\ \text{s m}^{-1}$ . The observed  $K_{cb}$  deviated significantly from the simulated values in early November and in the December-January period. The reasons for this are unclear, but it is possible that stress due to water deficit may have played a role, but this is not clear from the soil water content data. Poor sap flow data quality may also explain the discrepancy although, again, this cannot be independently confirmed.

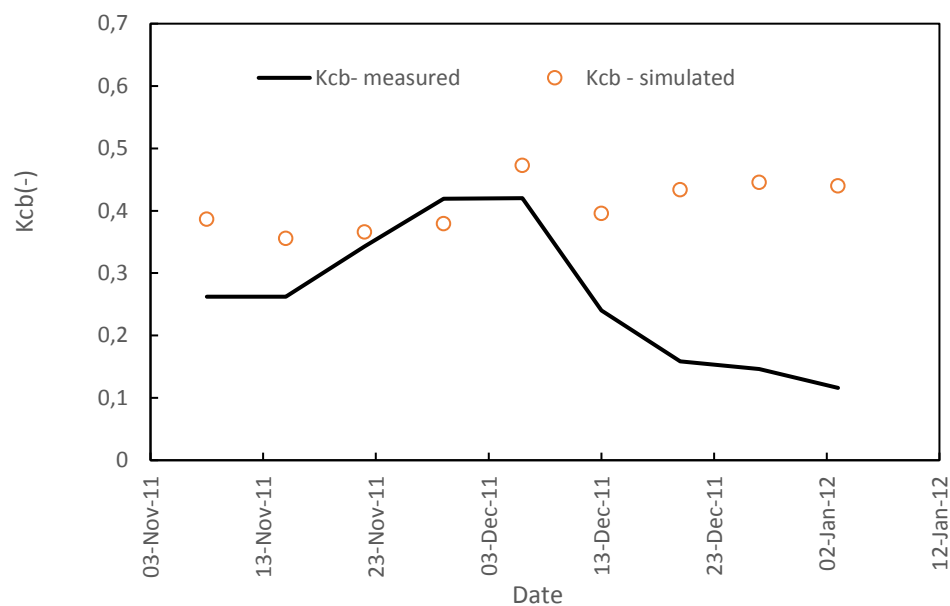
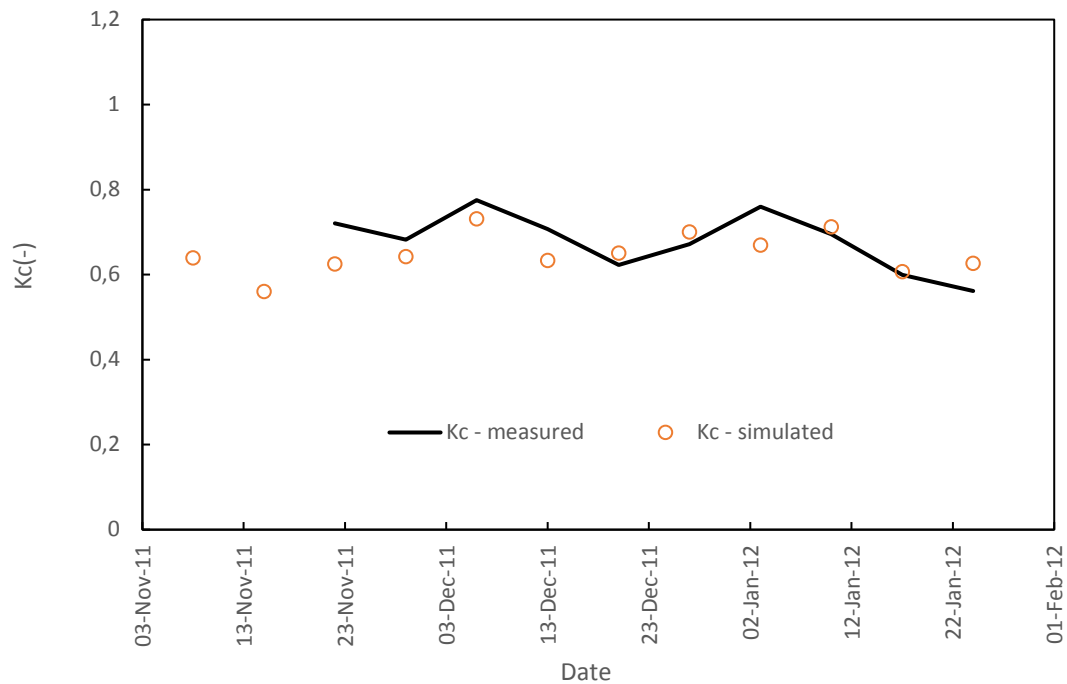


Figure 4.53: Comparison of the observed and calculated  $K_{cb}$  for a Midnight Valencia citrus orchard in Malelane, Mpumalanga.

Unlike the  $K_{cb}$  data, the simulated  $K_c$  values better matched the observed values as can be seen in Figure 4.54 suggesting that sap flow data quality may have contributed to the trend in Figure 4.53.



*Figure 4.54: Comparison of the observed and calculated weekly  $K_c$  for a Midnight Valencia citrus orchard in Malelane, Mpumalanga Province.*

Simulated changes in the crop coefficients from November 2011 to January 2012 for the Midnight Valencia orchard are shown in Figure 4.55. The data suggests that  $K_c$  values rarely exceeded 1.0 while  $K_{cb}$  fluctuated around 0.4 and  $K_e$  around 0.20.

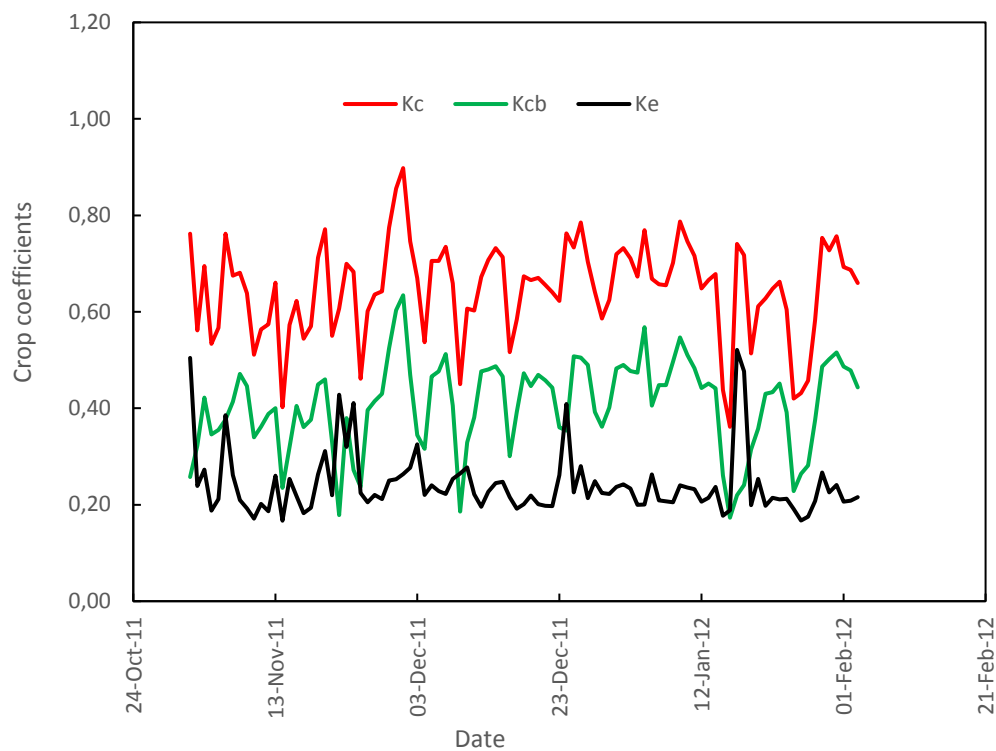


Figure 4.55: Simulated daily crop coefficients for a Midnight Valencia orchard at Malelane.

### ***Bahianinha navel citrus orchard***

#### ***a) Description of study site and data collection methods***

The Bahianinha navel citrus orchard in Groblersdal was approximately 7 years old planted on a Carizzo citrange rootstock (Figure 4.55). Height of the trees was approximately 2.5 m and tree density was 833 trees per hectare planted in a north-south row orientation. Irrigation was via drip irrigation with two drip lines per tree row delivering about  $1.8 \text{ L h}^{-1}$ . The drippers were spaced every 1.0 m along the drip line. Further information about the orchard is summarized in Table 4.33 and in Gush and Taylor (2014). Soil type was sandy loam.



Figure 4.56: Bahianinha navel citrus orchard at Groblersdal, Mpumalanga (after Gush and Taylor, 2014).

Table 4.33: Bahianinha navel citrus orchard at Groblersdal, Mpumalanga.

Age	6-7 years
Block size	2.7 ha
Planting density	833 trees per ha
Cultivar	Bahianinha Navel
Rootstock	Carizzo citrange
Height	2.5 m
Irrigation	Double line drip per row @ 1.8 L h <sup>-1</sup> every 1.0 m
Soils	Sandy loam
Yield	60 t ha <sup>-1</sup>

**b) Observed vs standardized crop coefficients for Bahianinha navel citrus orchards**

The observed and standardized basal and single crop coefficients for the Bahianinha navel orchard are shown in Tables 4.34 and 4.35, respectively. Despite the orchard being mature and full bearing, the crop coefficients remained low because of low transpiration and ET rates likely because of the strong stomatal control of transpiration. The observed  $K_{cb}$  values peaked in late winter and declined through the spring and summer seasons when the atmospheric evaporative demand was high.

*Table 4.34: Observed and standardized basal crop coefficients for Midnight Valencia citrus in Groblersdal, Mpumalanga*

Month	Kcb_obs	Kcb_std
Jul	0.42	0.35
Aug	0.44	0.37
Sep	0.17	0.17
Oct	0.17	0.18
Nov	0.23	0.24
Dec	0.19	0.19
Jan	0.14	0.17
Feb	0.43	0.43

*Table 4.35: Observed and standardized crop coefficients for Midnight Valencia citrus Groblersdal, Mpumalanga.*

Month	Kc_obs	Kc_std
Jul	0.67	0.60
Aug	0.57	0.48
Sep	-	-
Oct	-	-
Nov	-	-
Dec	-	-
Jan	0.77	0.86
Feb	0.79	0.63

A comparison of the observed and simulated  $K_{cb}$  values is shown in Figure 4.57 indicating an initial poor match at the start of the season in August 2008. After this period the simulated weekly values were of the same order of magnitude as the measured ones. It is probable that the quality of the measured sap flow data may have been problematic at the start of the season before the probes settled after installation. The simulations were performed using a mean leaf resistance of  $2\,000\text{ s m}^{-1}$  and  $\alpha$  was equal to  $50\text{ s m}^{-1}$ .

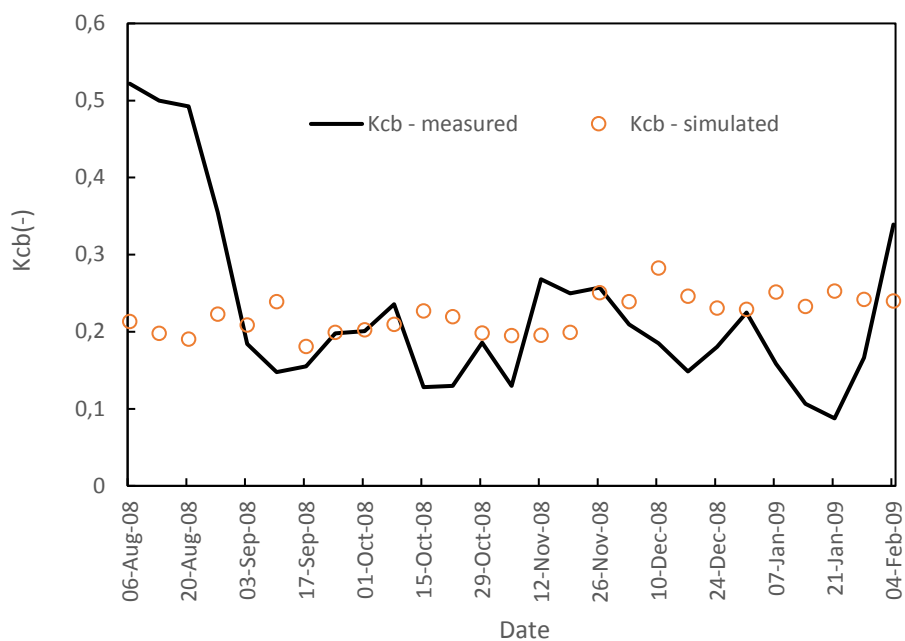


Figure 4.57: Comparison of the measured and simulated  $K_{cb}$  for a mature Midnight Valencia orchard in Groblersdal, Mpumalanga Province.

Two evapotranspiration measurement campaigns were done, the first in July 2008 to capture the water use rates during winter. The second campaign was in summer in January-February 2009 to capture the water use rates when the atmospheric evaporative demand was high. Figure 4.58 shows the performance of the simulated daily  $K_c$  values relative to the measured ones. There seems to be a reasonable agreement although the trend could have been better with a longer time series of

measured data. The simulated seasonal changes in the crop coefficients are shown in Figure 4.59. These tended to be low likely because of the strong stomatal control of transpiration. The small canopy size was likely the reason for  $K_e$  exceeding  $K_{cb}$  on most occasions.

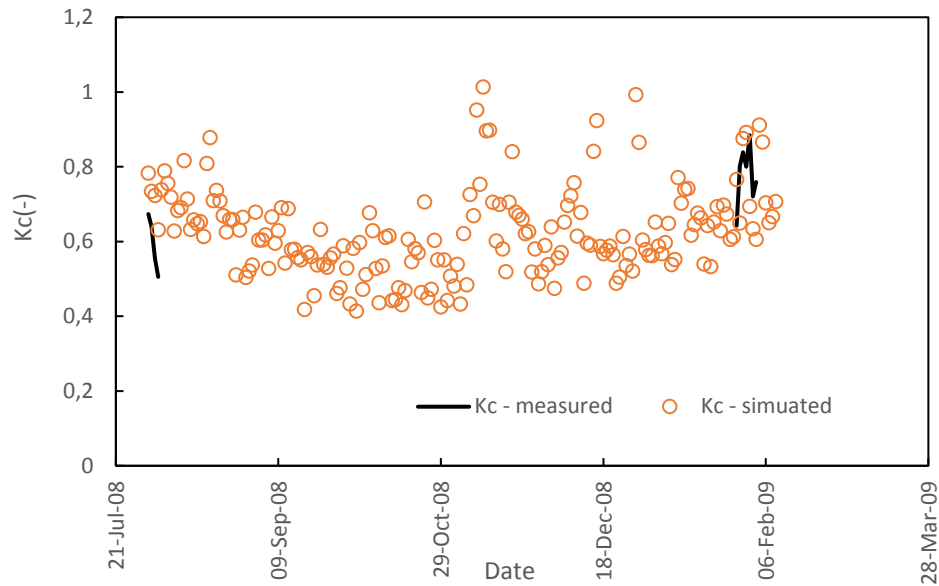


Figure 4.58: Comparison of the measured and simulated  $K_c$  for a mature Bahianinha navel citrus orchard in Groblersdal, Mpumalanga Province.

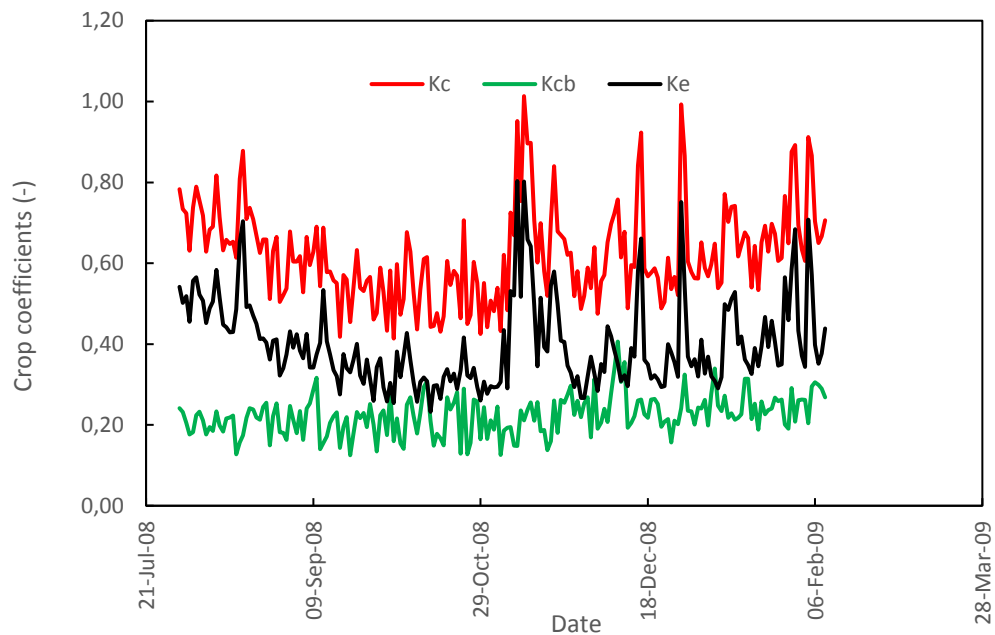
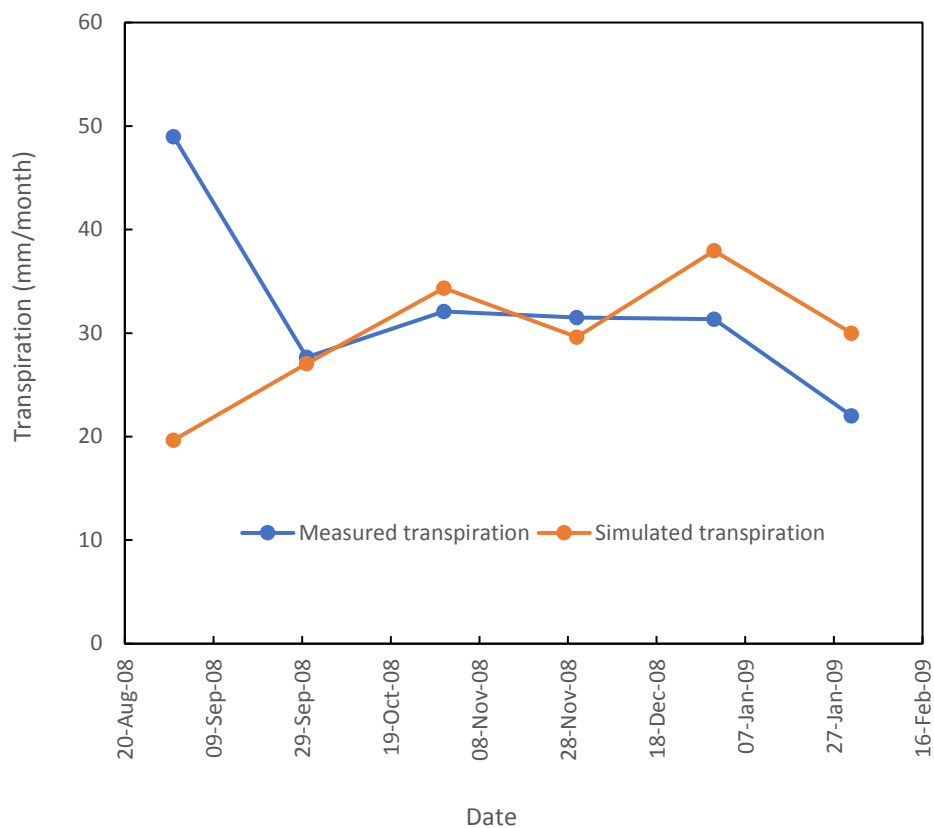


Figure 4.59: Seasonal changes in the crop coefficients for a mature Bahianinha navel citrus orchard in Groblersdal, Mpumalanga.

**c) Monthly transpiration rates for a Bahianinha navel orange orchard in Citrusdal**

If one were to use the  $K_{cb}$  values derived for this crop species to estimate the monthly transpiration rates, the comparison with the actual measured values is shown in Figure 4.60. There is a huge discrepancy between the estimated and measured values at the beginning of the campaign and this is consistent with the  $K_{cb}$  trend shown in Figure 4.57. If we exclude the first month, the  $R^2$  between the simulated and measured monthly transpiration was about 0.31, which is not high. The MAE was  $\pm 8.1$  mm/month and the RMSE  $\pm 5.7$  mm/month. These represent daily errors of about 0.26 and 0.18 mm  $d^{-1}$ , respectively. There is need to further fine-tune the performance of the A&P calculations for the citrus cultivars to come up with a more general expression that is cultivar independent.



*Figure 4.60: Comparison of the measured and simulated monthly total transpiration rates for a mature Midnight Valencia orchard at Groblersdal, Mpumalanga.*

### 4.3 CONCLUSIONS

In this chapter we have validated the calculations of the crop coefficients for various fruit types against actual observed values determined using sap flow and eddy covariance water use measurement techniques. There are two main observations from this assessment. The first is that the ratio of the leaf resistance to the standard resistance denoted by  $\alpha$  is critical to the accurate calculations of the crop coefficients using the A&P method. The second observation is that different standard resistances ( $\alpha$ ) exist for different fruit tree species; it is not possible to come up with a single value that works across all species. For example, the value of  $100 \text{ s m}^{-1}$  proposed by Allen and Pereira (2009) and in the FAO 56 paper has been shown to be inaccurate in many tree crops. In this report we suggest typical values that work for the various species. More work is still needed to fine-tune the calculations, as the performance on some species is not satisfactory. Similarly, there is need to further validate the simulations with newer data where this has been collected in recent studies.

The data presented in this chapter builds towards the development of the crop coefficients calculator APP in the following ways. The APP has two main functions. It can be used with Experimentally derived data. These are now presented as standardized crop coefficients for the ease of transferability to other locations and fields. The second functionality is the “Derived crop coefficients”. This allows the user to enter their field-specific information and to get reasonably accurate estimates of the crop coefficients. Validation of these calculations is what was done in the present chapter. In the next Chapter we summarize key features of the APP which is still being developed.

## **CHAPTER 5: DEVELOPMENT OF AN ONLINE CROP COEFFICIENTS DATABASE FOR IRRIGATED TREE CROPS**

### **5.1 DESCRIPTION OF THE CROP COEFFICIENTS SMARTPHONE APPLICATION**

This section seeks to consolidate the data collected in the various fruit orchards described in Chapter 4 into a Smartphone APP for estimating crop coefficients. Recognizing the value of the crop coefficients determined directly from experimental data from the various completed and ongoing projects, we package these into a format that can be readily used by the end user anywhere in the country. Potential end users include farm managers (for irrigation scheduling and water allocation planning), catchment managers, irrigation boards, engineers, consultants, and researchers, among others.

Generally, crop coefficients derived in one field cannot be applied directly to another field even when planted to the same crop. This is because crop coefficients vary as a result of crop phenological stage, planting density, microclimate, row orientation, canopy and crop load, understorey vegetation management, mulching, and other practices. So, each orchard is unique. The FAO 56 paper and Pereira et al. (2021b) described a procedure to transform the crop coefficients observed at a given location into standard values. Standard crop coefficients are defined as values that are derived in a temperate subhumid climate where the average windspeed is around  $2.0 \text{ m s}^{-1}$ , and the minimum relative humidity is around 45%.

To facilitate the transferability of crop coefficients from one location to another, they describe a method in which the observed values are related to the standard crop coefficients by adjusting for deviations in the microclimatic conditions from the standard conditions using equations 7 and 8 presented in Chapter 2. The APP

developed in this study has two main features. The first is the “Experimental Crop Coefficients” tab, and the second is the “Derived Crop Coefficients” tab (Figure 5.1). In the Experimental tab, we seek to use the crop coefficients as measured under local South African conditions. But we convert them to standard values which are stored in the database of the APP. However, tree crops are irrigated from planting throughout their life-time. There is a huge variability in orchard attributes, e.g. canopy cover, tree height, soil type, wetted soil fraction, etc. To account for these variations, we have created the “Derived Crop Coefficients” tab in which the user inputs information that is relevant to their specific field. Each of these functions are described in detail in the next section.

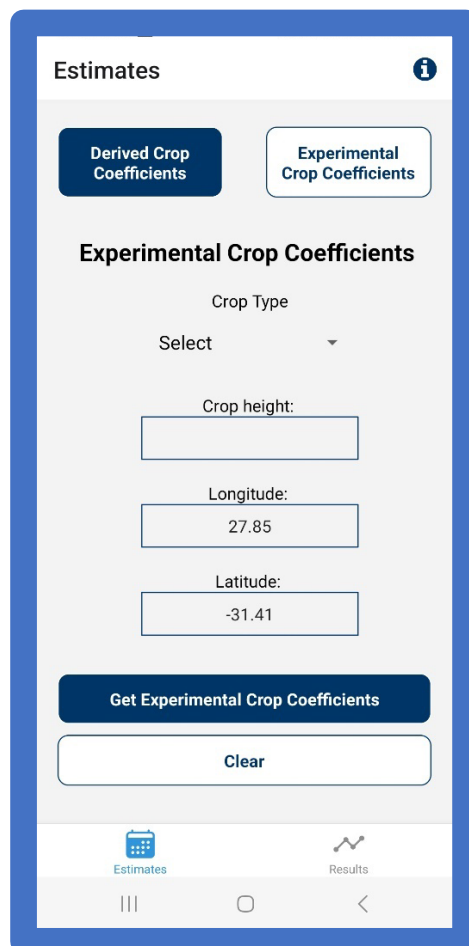


Figure 5.1. Landing page for the fruit orchards Crop Coefficients APP.

## 5.2. EXPERIMENTAL CROP COEFFICIENTS

Input data to the Experimental crop coefficients are site coordinates, crop type, and average crop height as shown in Figure 5.2. Once these are entered, their information is linked to a 50-year daily climate record (1950-1999) located at the centroid of the quaternary catchment (QC) nearest to the user. The long-term average climate data for that QC, namely the minimum relative humidity ( $RH_{min}$ ) and wind speed at two meters ( $u_2$ ) height for each month is retrieved and combined with the standard crop coefficients (in the database) to derive the crop coefficients for the specific location. Figure 5.2 illustrates the calculation procedure for a fruit tree species in QC U20A as an example.

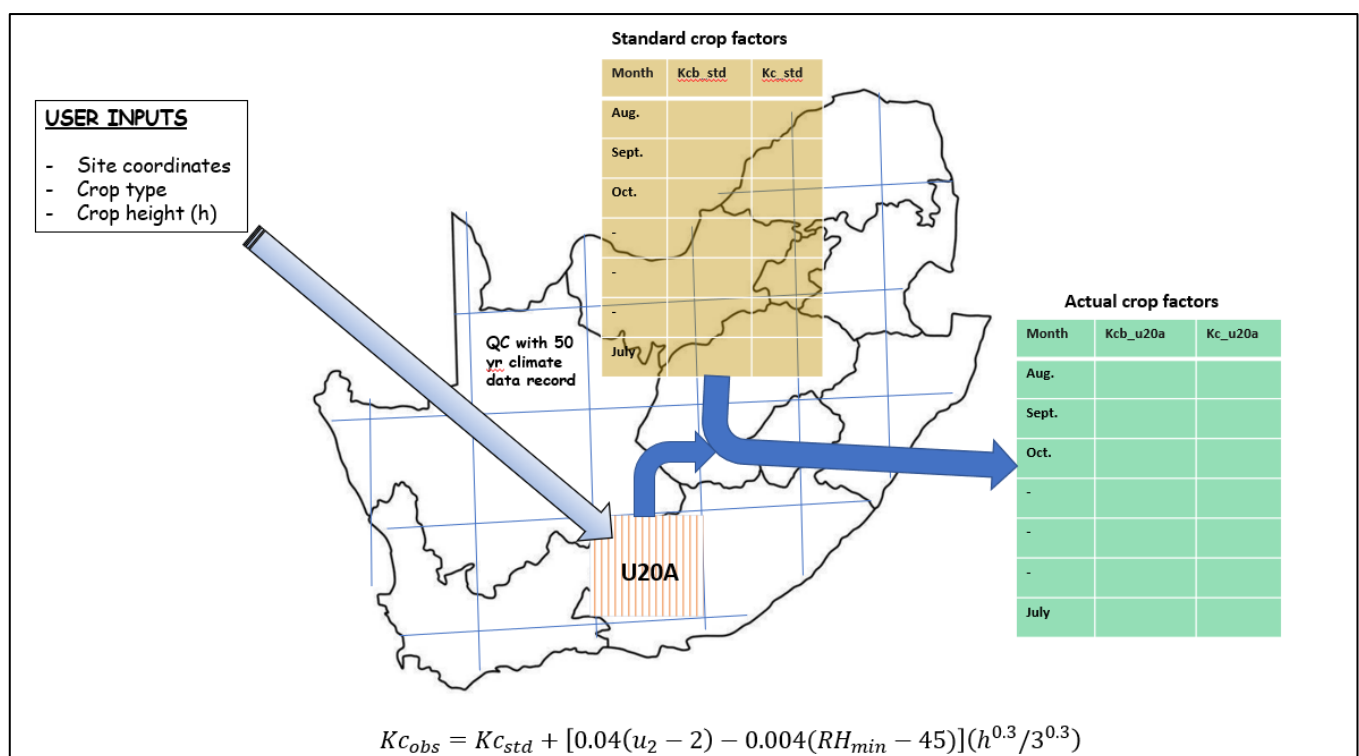


Figure 5.2. Schematic representation of the Experimental Crop Coefficients calculator APP.

The nationwide 50-year climate database which is about 9.0 GB in size is hosted at a remote server and it is only interrogated during simulations. In this way the huge volume of data does not affect the computational speed of the APP. With the approach implemented in the APP the crop coefficients can be estimated at any location in the country as the climate database covers the whole country. The outputs from the Experimental database are displayed as shown in Figure 5.3.



Figure 5.3. Typical outputs from the experimental database for a macadamia orchard.

### 5.3 DERIVED CROP COEFFICIENTS

In this tab we use the modified A&P method described in Chapter 3 and validated in Chapter 4 to estimate three crop coefficients, one at each of the initial, mid, and late stages of growth of the specific tree crop (see red dots in Figure 5.4). The crop coefficient curve is then constructed by interpolation using information about the length of the growth stage according to the FAO 56 procedure. The growth stage length data was obtained from the values published in SAPWAT shown in Appendix A.

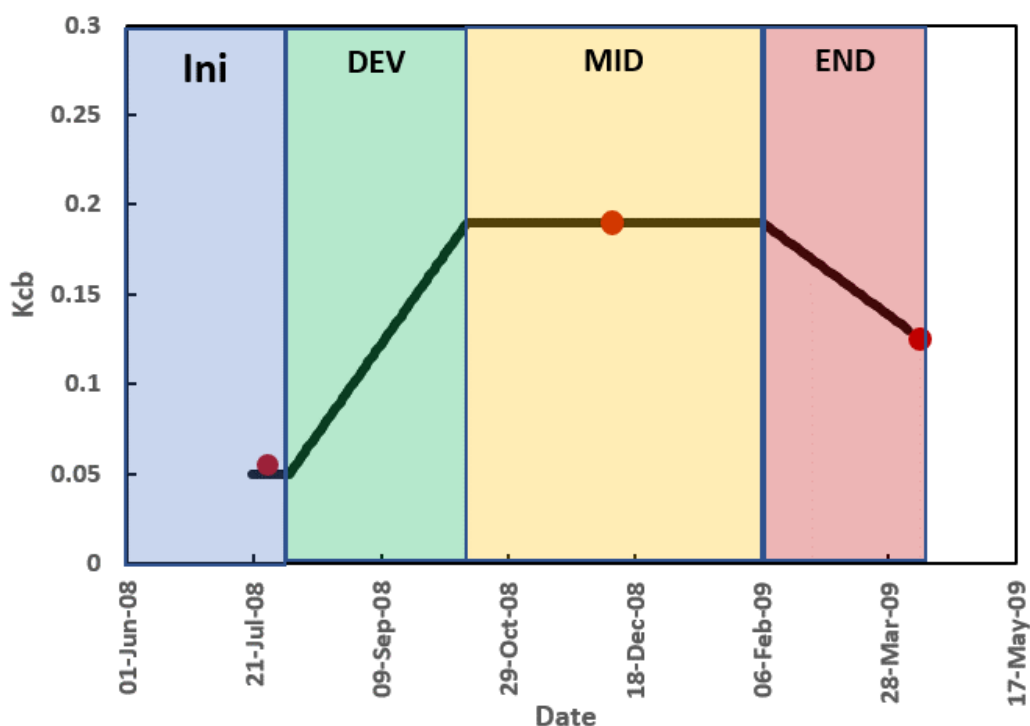


Figure 5.4. Derivation of the 4-stage crop coefficient curve using the modified A&P approach.

The information required to calculate the crop coefficients at each stage, i.e. the initial, mid and late stage include:

- 1) estimate of fractional vegetation cover ( $f_c$ ),

- 2) average tree height,
- 3) soil texture,
- 4) irrigation system (wetted soil fraction)
- 5) understory vegetation status, i.e. whether bare ground, intermediate or tall vegetation and;
- 6) Canopy size factor (ML = 2.0 for large canopies and 1.5 for small canopies).

The stomatal sensitivity information, i.e. the mean leaf resistance and the empirical function  $\alpha$  are stored in the crops database.

An example of the derived crop coefficients for a mature macadamia is presented in Figs 5.5 and 5.6, respectively.

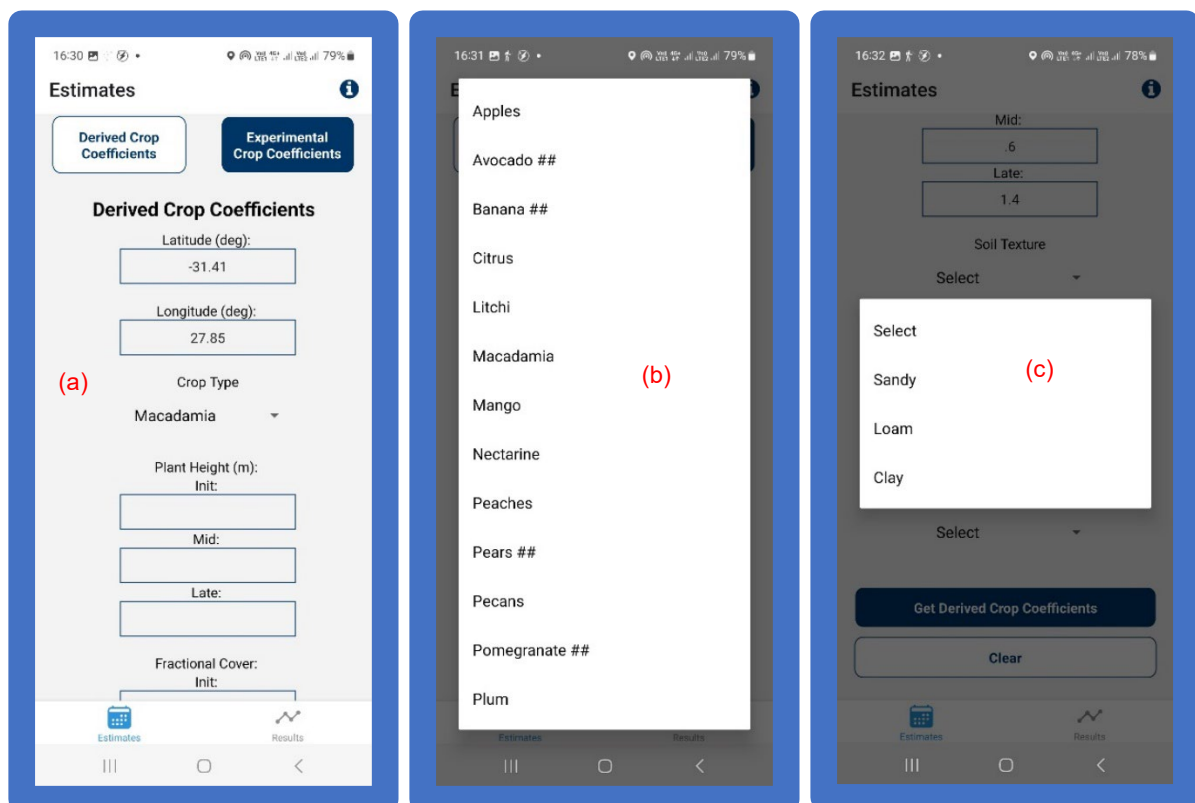


Figure 5.5. (a) Input page for the Derived crop coefficients tab; (b) range of tree crops included in the database (data not available for avocado and banana), and (c)

soils information required.

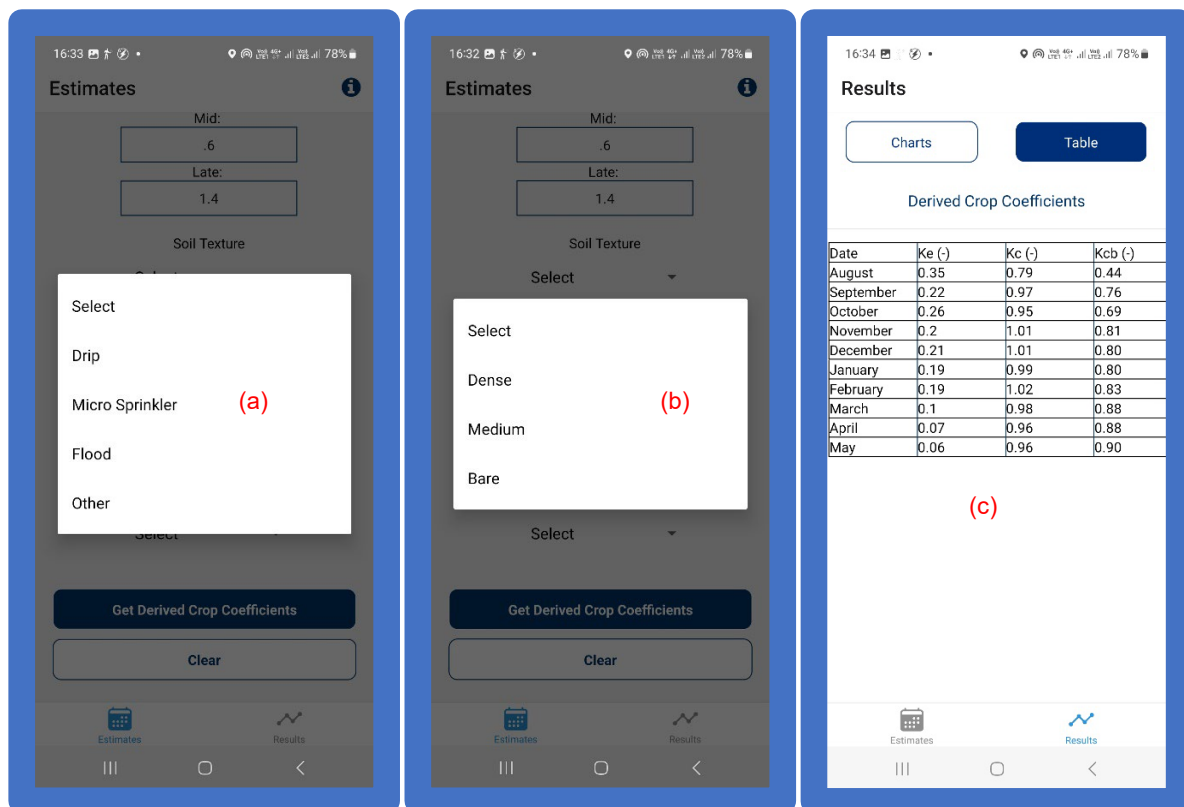


Figure 5.6. (a) Wetted soil fraction information represented by default values for drip, micro sprinkler and flood, (b) user inputs based on the amount of vegetation cover on the orchard floor, and (c) tabular outputs of the crop coefficients. These can also be plotted graphically.

A smartphone and good network connectivity is required to run the application. The APP requires about 50 MB of space on the smartphone and data bundles or wi-fi connectivity are essential to run the application. The APP has been built for both android and ios phones and the link to the google playstore can be accessed below:

<http://play.google.com/apps>

## **CHAPTER 6: CONCLUSIONS AND RECOMMENDATIONS**

Considerable investment by the WRC and other entities has gone into quantifying the water requirements of irrigated crops in the country. The goal of these studies is to provide information to improve irrigation scheduling, water allocation planning, and irrigation system designs, etc. in the agricultural sector. However, there is need to bring all these data into a single platform that can aid in irrigation decision making and this was the intention of this study, at least for irrigated fruit tree crops. This study has created tabulated crop coefficients for irrigated fruit tree crops using locally derived data. To achieve this, we follow the approach proposed by Pereira et al. (2021b) in which the coefficients are first converted into standard values. These standard crop coefficients can then be transferred to any other region provided data to characterize the differences in aerodynamic properties between the standard and local conditions is available. We built these data into a Smartphone APP that can be used anywhere in the country provided the tree crop is included in the database.

The second contribution of this study is that we, for the first time, assessed the utility of the A&P method on different fruit tree crops using actual measured data. This yielded valuable insights regarding the current parameterization of the A&P approach for tree crops. This study demonstrated that the improved A&P method can be used to fill in the gaps in crop coefficients which are prevalent in the existing data set. Lastly, we integrated these two aspects into a single platform which is in the form of a Smartphone APP that can be used by various water resources managers. While this study has used data from many fruit tree species, considerable research is still

required to fully validate the APP developed in this study. The following are recommendations for further research:

- 1) While the current APP has been validated for selected tree crops, there is need to further test the APP with independent data to ascertain its accuracy.
- 2) More crops should be added to the database to cover the wide range of irrigated crops in the country.
- 3) Point no 2 requires further support for primary research to collect data on water use and its environmental drivers.
- 4) Some of the methods proposed here can built into more sophisticated methods such as SAPWAT which has the option for the user to enter their own crop coefficients. Lack of accurate crop coefficients is often cited as a major cited as major source of uncertainty despite the science behind the model being sound.

## REFERENCES

- Abiodun, B. J., Makhanya, N., Petja, B., Abatan, A. A., & Oguntunde, P. G. (2019). Future projection of droughts over major river basins in Southern Africa at specific global warming levels. *Theoretical and Applied Climatology*, 137, 1785-1799.
- Allen, R.G., Pereira, L.S., Raes, D., & Smith, M. (1998). Crop evapotranspiration. FAO Irrigation and Drainage Paper 56. Food and Agriculture Organization (FAO), Rome, Italy.
- Allen, R.G. (2000). Using the FAO-56 dual crop coefficient method over an irrigated region as part of an evapotranspiration intercomparison study. *Journal of Hydrology*. 229, 27-41. [https://doi.org/10.1016/S0022-1694\(99\)00194-8](https://doi.org/10.1016/S0022-1694(99)00194-8)
- Allen, R.G., Asce, M., Pereira, L.S., Asce, M., Smith, M., Raes, D., Wright, J.L., & Asce, M., (2005). FAO-56 Dual Crop Coefficient Method for Estimating.pdf 2-13.
- Allen, R. G., & Pereira, L. S. (2009). Estimating crop coefficients from fraction of ground cover and height. *Irrigation Science*, 28(1), 17-34. <https://doi.org/10.1007/s00271-009-0182-z>
- Allen, R.G., Pereira, L.S., Howell, T.A., & Jensen, M.E., (2011a). Evapotranspiration information reporting: I. Factors governing measurement accuracy. *Agricultural Water Management*, 98, 899-920. <https://doi.org/10.1016/j.agwat.2010.12.015>.
- Allen, R. G., Pereira, L. S., Howell, T. A., & Jensen, M. E. (2011b). Evapotranspiration information reporting: II. Recommended documentation. *Agricultural Water Management*, 98(6), 921-929.
- Annandale, J.G., Benadé, N., Jovanovic, N.Z., Steyn, J.M., & Sautoy, D.U. (1999) Facilitating Irrigation Scheduling by Means of the Soil Water Balance Model. WRC Report No. 753/1/99, Water Research Commission, Pretoria, South Africa. 285 pp

Annandale, J. G., Stirzaker, R. J., Singels, A., Van der Laan, M., & Laker, M. C. (2011). Irrigation scheduling research: South African experiences and future prospects. *Water SA*, 37(5), 751-764. <https://doi.org/10.4314/wsa.v37i5.12>

Baker, J.M., & Van Bavel, C.H.M. (1987). Measurement of mass flow of water in stems of herbaceous plants. *Plant Cell Environ*, 10, 777-782.

Bastiaanssen, W.G., Menenti, M., Feddes, R., Holtslag, A. (1998). A remote sensing surface energy balance algorithm for land (SEBAL) Formulation. *Journal of Hydrology*, 212, 198-212.

Bastiaanssen, W. G. M., Simons, G. W. H., & Sheridan, P. F. (2012). The Potential of Satellite-based Information for Monitoring Water and Production Related Aspects of the Sustainability of Biofuels.

Burba, G., & Anderson, D. (2010). *A brief practical guide to eddy covariance flux measurements: principles and workflow examples for scientific and industrial applications*. Li-Cor Biosciences. [www.licor.com](http://www.licor.com).

Burgess, S.S.O., Adams, M.A., Turner, N.C., Beverly, C.R., Ong, C.K., Khan, A.A.H., & Bleby, T.M., (2001). An improved heat pulse method to measure low and reverse rates of sap flow in woody plants. *Tree Physiology*. 21, 589-598. <https://doi.org/10.1093/treephys/21.9.589>

Campbell, G. S., and Norman, J. M. 1998. *An Introduction to Environmental Biophysics* (2nd ed.). New York: Springer-Verlag. 286 pp.

Casa, R., Russell, G., & lo Cascio, B. (2000). Estimation of evapotranspiration from a field of linseed in central Italy. In *Agricultural and Forest Meteorology* (Vol. 104).

Dent, M. C. (1988). *Crop water requirements for irrigation planning in South Africa* (Doctoral dissertation).

Dye, P.J. (1996). Response of Eucalyptus grandis trees to soil water deficits. *Tree Physiology*, 16: 233-238.

Dzikiti, S., Ntuli, N. R., Nkosi, N. N., Ntshidi, Z., Ncapai, L., Gush, M. B., ... & Pienaar, H. H. (2022a). Contrasting water use patterns of two drought adapted native fruit tree species growing on nutrient poor sandy soils in northern KwaZulu-Natal. *South African Journal of Botany*, 147, 197-207.

Dzikiti, S., Steppe, K., Lemeur, R., & Milford, J. R. (2007). Whole-tree level water balance and its implications on stomatal oscillations in orange trees [*Citrus sinensis* (L.) Osbeck] under natural climatic conditions. *Journal of Experimental Botany*, 58(7), 1893-1901. <https://doi.org/10.1093/jxb/erm023>

Dzikiti, S., Verreyne, J. S., Stuckens, J., Strever, A., Verstraeten, W. W., Swennen, R., & Coppin, P. (2010). Determining the water status of Satsuma mandarin trees [*Citrus Unshiu* Marcovitch] using spectral indices and by combining hyperspectral and physiological data. *Agricultural and Forest Meteorology*, 150(3), 369-379. <https://doi.org/10.1016/j.agrformet.2009.12.005>

Dzikiti, S., Verreyne, S. J., Stuckens, J., Strever, A., Verstraeten, W. W., Swennen, R., Theron, K. I., & Coppin, P. (2011). Seasonal variation in canopy reflectance and its application to determine the water status and water use by citrus trees in the Western Cape, South Africa. *Agricultural and Forest Meteorology*, 151(8), 1035-1044. <https://doi.org/10.1016/j.agrformet.2011.03.007>

Dzikiti, S., Schachtschneider, K., Naiken, V., Gush, M.B., Le Maitre, D. (2013). Comparison of water-use by alien invasive pine trees growing in riparian and non-riparian zones in the Western Cape province, South Africa. *Forest Ecology and Management*, 293: 92-102.

Dzikiti, S. and Schachtschneider, K. (2015). Water stewardship for stone fruit farmers. WWF Technical Report. Available at [www.wwf.org.za/freshwater](http://www.wwf.org.za/freshwater).

Dzikiti, S., Gush, M. B., Taylor, N. J., Volschenk, T., Midgley, S., Lötze, E., Schmeisser, M., & Doko, Q. (2017). Measurement and modelling of water use by high yielding apple orchards and orchards of different age groups in the winter rainfall areas of South Africa. *Acta Horticulturae*, 1150, 31-38. <https://doi.org/10.17660/ActaHortic.2017.1150.5>.

Dzikiti, S., Volschenk, T., Midgley, S.J.E., Lötze, E., Taylor, N.J., Gush, M.B., Ntshidi, Z., Zirebwa, S.F., Doko, Q., Schmeisser, M., Jarman, C., Steyn, W.J., Pienaar, H.H. (2018a). Estimating the water requirements of high yielding and young crop orchards in the winter rainfall areas of South Africa using a dual source evapotranspiration model. *Agricultural Water Management*. 208, 152-162.

Dzikiti, S., Volschenk, T., Midgley, S., Gush, M.B., Taylor, N., Lötze, E., Zirebwa, S., Ntshidi, Z., Mobe, N.T., Schmeisser, M., Doko, Q. (2018b). Quantifying water use and water productivity of high performing crop orchards of different canopy sizes. WRC Report No. TT 751/18. Pretoria: Water Research Commission.

Fessehazion, M.K., Stirzaker, R.J., Annandale, J.G., & Everson, C.S. (2012) Improving nitrogen and irrigation water use efficiency through adaptive management: A case study using annual ryegrass. *Agric. Ecosyst. Environ.* 141 350-358.

García Petillo, M. and Castel, J. (2007) Water balance and crop coefficient estimation of a citrus orchard in Uruguay. *Spanish Journal of Agricultural Research*, 5, 232-243.

Gontia, N.K. and Tiwari, K.N. (2010). Estimation of crop coefficient and evapotranspiration of wheat (*Triticum aestivum*) in an irrigation command using remote sensing and GIS. *Water resources management*, 24(7), 1399-1414.

Granier, A. (1985). Une nouvelle méthode pour la mesure du flux de sève brute dans le tronc des arbres. *Annales des Sciences Forestières* 42, 193-200.

Granier, A. (1987). Evaluation of transpiration in a Douglas-fir stand by means of sap flow measurements. *Tree Physiology*. 3, 309-20.

Green, G.C. (1985) Estimated Irrigation Requirements of Crops in South Africa, Part 1. Memoirs on the Agricultural Resources of South Africa, No. 2. Department of Agriculture and Water Supply. Pretoria, South Africa.

Green, S.R., Vogeler, I., Clothier, B.E., Mills, T.M., & Van Den Dijssel, C. (2003). Modelling water uptake by a mature apple tree. *Aust. J. Soil Res.* 41, 365-380. <https://doi.org/10.1071/SR02129>

Gush, M.B. and Taylor, N.J. (2014). The water use of selected fruit tree orchards (Volume 2): Technical report on measurements and modelling. WRC report No. 1770/2/14. 1-285.

Gush, M., Dzikiti, S., Van der Laan, M., Steyn, M., Manamathela, S., & Pienaar, H. (2019). Field quantification of the water footprint of an apple orchard, and extrapolation to watershed scale within a winter rainfall Mediterranean climate zone. *Agricultural and Forest Meteorology*, 271, 135-147. <https://doi.org/10.1016/j.agrformet.2019.02.042>.

Gu, A., Teng, F., & Wang, Y. (2014). China energy-water nexus: Assessing the water-saving synergy effects of energy-saving policies during the eleventh Five-year Plan. *Energy conversion and management*, 85, 630-637.

Hortgro, 2020. Key Deciduous Fruit Statistics-2018, South Africa. [www.hortgro.co.za](http://www.hortgro.co.za).

Hu, Y., Buttar, N.A., Tanny, J., Snyder, R.L., Savage, M.J., & Lakhari, I.A. (2018). Surface Renewal Application for Estimating Evapotranspiration: A Review. *Advances in Meteorology*. <https://doi.org/10.1155/2018/1690714>.

Ibraimo, N. A., Taylor, N. J., Steyn, J. M., Gush, M. B., & Annandale, J. G. (2016). Estimating water use of mature pecan orchards: A six stage crop growth curve approach. *Agricultural Water Management*, 177, 359-368.

Jarmain, C., Singels, A., Obando, E., Paraskevopoulos, A., Olivier, F., Munch, Z., Van Der Merwe, B., Walker, S., Van Der Laan, M., Fessehazion, M. (2014). Water use

efficiency of irrigated agricultural crops determined with satellite imagery. WRC Project No. K5/2079//4, Deliverable 6: Water use efficiency report 2012/13. Water Research Commission, Pretoria

Jayanthi, H., Neale, C. M., & Wright, J. L. (2007). Development and validation of canopy reflectance-based crop coefficient for potato. *Agricultural water management*, 88(1-3), 235-246.

Jiang, X., Kang, S., Tong, L., Li, F., Li, D., Ding, R., & Qiu, R. (2014). Crop coefficient and evapotranspiration of grain maize modified by planting density in an arid region of northwest China. *Agricultural Water Management*, 142, 135-143. <https://doi.org/10.1016/j.agwat.2014.05.006>.

Jones, H. G. (2004). Irrigation scheduling: advantages and pitfalls of plant-based methods. *Journal of experimental botany*, 55(407), 2427-2436.

Kadam, S.A., Gorantiwar, S.D., & Mandre, N.P. (2021). Crop Coefficient for Potato Crop Evapotranspiration Estimation by Field Water Balance Method in Semi-Arid Region, Maharashtra, India. *Potato Res.* 64, 421-433 (2021). <https://doi.org/10.1007/s11540-020-09484-8>.

Lambers, H., Shane, M. W., Cramer, M. D., Pearse, S. J., & Veneklaas, E. J. (2006). Root structure and functioning for efficient acquisition of phosphorus: matching morphological and physiological traits. *Annals of botany*, 98(4), 693-713.

Lascano, R. J. (2000). A general system to measure and calculate daily crop water use. *Agronomy Journal*, 92(5), 821-832. <https://doi.org/10.2134/agronj2000.925821x>

Lategan, E. L., & Howell, C. L. (2016). *Deficit irrigation and canopy management practices to improve water use efficiency and profitability of wine grapes* (No. 2080/1, p. 16). WRC Report.

Le Maitre, D., Seyler, H., Holland, M., Smith Adao, L., Maherry, A., Nel, J., & Witthüser, K. (2019). Strategic water source areas: Vital for South Africa's water, food and energy security. *Water Research Commission. Pretoria: South Africa.*

Mengistu, M. G., Everson, C. S., Moyo, N. C., & Savage, M. J. (2014). The validation of the variables (evaporation and soil moisture) in hydrometeorological models. *Water Research Commission, Pretoria, South Africa.*

Mobe, N. T., Dzikiti, S., Zirebwa, S. F., Midgley, S. J. E., von Loeper, W., Mazvimavi, D., Ntshidi, Z., & Jovanovic, N. Z. (2020). Estimating crop coefficients for apple orchards with varying canopy cover using measured data from twelve orchards in the Western Cape Province, South Africa. *Agricultural Water Management*, 233. <https://doi.org/10.1016/j.agwat.2020.106103>.

Mobe, N. T., Dzikiti, S., Dube, T., Mazvimavi, D., & Ntshidi, Z. (2021). Modelling water utilization patterns in apple orchards with varying canopy sizes and different growth stages in semi-arid environments. *Scientia Horticulturae*, 283, 110051.

Monteith, J., Unsworth, M. (1990). Radiation environment. *Principles of environmental physics*, 2nd ed., Edward Arnold, London, 36-57.

Ngxaliwe, S. (2014). Water stress effects on growth, development, resource capture and resource use efficiency of two contrasting sugarcane genotypes. MSc thesis, University of KwaZulu-Natal.

Ntshidi, Z., Dzikiti, S., Mazvimavi, D., & Mobe, N. T. (2021a). Contribution of understorey vegetation to evapotranspiration partitioning in apple orchards under Mediterranean climatic conditions in South Africa. *Agricultural Water Management*, 245. <https://doi.org/10.1016/j.agwat.2020.106627>

Ntshidi, Z., Dzikiti, S., Mazvimavi, D., Mobe, N. T., & Mkunyana, Y. P. (2021b). Water use of selected cover crop species commonly grown in South African fruit orchards and their response to drought stress. *Physics and Chemistry of the Earth*, 124. <https://doi.org/10.1016/j.pce.2021.103070>

NWRS-2. (2013). National Water Resource Strategy. Department of Water and Sanitation. South Africa. Available from. [www.dwa.gov.za/nwrs2013](http://www.dwa.gov.za/nwrs2013).

Olivier, F., & Singels, A. (2001). A database of crop water use coefficients for irrigation scheduling of sugarcane. *Proc S Afr Sug Technol Ass*, 75: 81-83.

Olivier, F.C., Lecler, N.L., & Singels, A. (2009) Increasing Water Use Efficiency of Irrigated Sugarcane by Means of Specific Agronomic Practices. WRC Report No. 1577/1/09. Water Research Commission, Pretoria, South Africa. 127 pp.

Paco, T. A., Paredes, P., Pereira, L. S., Silvestre, J., & Santos, F. L. (2019). Crop coefficients and transpiration of a super intensive Arbequina olive orchard using the dual Kc approach and the Kcb computation with the fraction of ground cover and height. *Water (Switzerland)*, 11(2). <https://doi.org/10.3390/w11020383>

Pasqualotto G., Carraro V., Menardi R., & Anfodillo T. (2019). Calibration of Granier-Type (TDP) Sap Flow Probes by a High Precision Electronic Potometer. *Sensors*, 19, 2419; doi:10.3390/s19102419

Paudel, I., Naor, A., Gal, Y., & Cohen, S. (2015). Simulating nectarine tree transpiration and dynamic water storage from responses of leaf conductance to light and sap flow to stem water potential and vapor pressure deficit. *Tree Physiology*, 35(4), 425-438. <https://doi.org/10.1093/treephys/tpu113>

Paw U, K. T., J. Qiu, H.B. Su, T. Watanabe, and Y. Brunet. (1995). Surface renewal analysis: a new method to obtain scalar fluxes without velocity data. *Agric. For. Meteorol.*, 74,119-137

Pereira, L. S., Paredes, P., Melton, F., Johnson, L., Wang, T., López-Urrea, R., Cancela, J. J., & Allen, R. G. (2020). Prediction of crop coefficients from fraction of ground cover and height. Background and validation using ground and remote sensing data. In *Agricultural Water Management* (Vol. 241). Elsevier B.V. <https://doi.org/10.1016/j.agwat.2020.106197>

Pereira, L. S., Paredes, P., López-Urrea, R., Hunsaker, D. J., Mota, M., & Mohammadi Shad, Z. (2021a). Standard single and basal crop coefficients for vegetable crops, an update of FAO56 crop water requirements approach. In *Agricultural Water Management* (Vol. 243). Elsevier B.V. <https://doi.org/10.1016/j.agwat.2020.106196>

Pereira, L. S., Paredes, P., Hunsaker, D. J., López-Urrea, R., & Mohammadi Shad, Z. (2021b). Standard single and basal crop coefficients for field crops. Updates and advances to the FAO56 crop water requirements method. In *Agricultural Water Management* (Vol. 243). Elsevier B.V. <https://doi.org/10.1016/j.agwat.2020.106466>

Reinders, F. B. (2011). Irrigation methods for efficient water application: 40 years of South African research excellence. *Water SA*, 37(5), 765-770. <https://doi.org/10.4314/wsa.v37i5.13>

Reinders, F.B., Van der Stoep, E., & Backeberg, G.R. (2013). Improved efficiency of irrigation water use: a South African framework. *Irrigation and Drainage*. <https://doi.org/10.1002/ird.1742>

Sakuratani, T. (1981). A heat balance method for measuring water flux in the stem of intact plants. *Journal of Agricultural Meteorology*, 37(1), 9-17.

Savage, M. J., AND Graham, & Lightbody, K. E. (2000). *An investigation of the stem steady state heat energy balance technique in determining water use by trees*. Water Research Commission.

Schultze, R. E. (2012). *A 2011 perspective on climate change and the South African water sector*. Pretoria: Water Research Commission.

Smith, D. M., & Allen, S. J. (1996). Measurement of sap flow in plant stems. In *Journal of Experimental Botany* (Vol. 47, Issue 305).

Steppe, K., & Lemeur, R. (2004). An experimental system for analysis of the dynamic sap-flow characteristic in young trees: results of a beech tree. *Funct Plant Biol*, 31, 83-92.

Steppe, K., Dzikiti, S., Lemeur, R., & Milford, J.R. (2006). Stomatal oscillations in orange trees under natural climatic conditions. *Annals of Botany*, 92, 831-835.

Steppe, K., De Pauw, D.J.W., Doody, T.M., Teskey, R.O. (2010). A comparison of sap flux density using thermal dissipation, heat pulse velocity and heat field deformation methods. *Agricultural and Forest Meteorology*, 150: 1046-1056.

Stevens, J.B., Duvel, G.H., Steyn, G.J., & Marobane, W. (2005) *The Range, Distribution and Implementation of Irrigation Scheduling Models and Methods in South Africa*. WRC Report No.1137/1/05. Water Research Commission, Pretoria, South Africa. 208 pp.

Taylor, N. J., Smit, T., Smit, A., Midgley, S. J. E., Clulow, A., Annandale, J. G., ... & Roets, N. (2021). Water Use of Macadamia Orchards. WRC Report No. 2552/2/21 volume 2. <https://www.wrc.org.za/wp-content/uploads/mdocs/2552%20Vol%202.pdf>.

Taylor, N. J., Mahohoma, W., Vahrmeijer, J. T., Gush, M. B., Allen, R. G., & Annandale, J. G. (2015). Crop coefficient approaches based on fixed estimates of leaf resistance are not appropriate for estimating water use of citrus. *Irrigation Science*, 33, 153-166.

Tfwala, C. M., Van Rensburg, L. D., Bello, Z. A., & Green, S. R. (2018). Calibration of compensation heat pulse velocity technique for measuring transpiration of selected indigenous trees using weighing lysimeters. *Agricultural Water Management*, 200, 27-33.

Trout, T. J., & DeJonge, K. C. (2018). Crop Water Use and Crop Coefficients of Maize in the Great Plains. *Journal of Irrigation and Drainage Engineering*, 144(6). [https://doi.org/10.1061/\(asce\)ir.1943-4774.0001309](https://doi.org/10.1061/(asce)ir.1943-4774.0001309)

Van Bavel, M.G., & Van Bavel, C.H.M. (1990). Dynagage installation and operational manual. Dynamax Inc., Houston, TX, USA.

Van Heerden, P.S., & Walker, S. (2016). Upgrading of SAPWAT3 as a management tool to estimate the irrigation water use of crops, revised edition, SAPWAT4. Water Res. Comm. Rep. no. TT662/16, Water Res. Comm. South Africa.

Van Niekerk, A., Jarman, C., Goudriaan, R. (2018) An earth observation approach towards mapping irrigated area and quantifying water use by irrigated crops in South Africa. WRC Report TT 745/17. Water Research Commission, Pretoria

Volschenk, T., de Villiers, J., & Beukes, O., (2003). The Selection and Calibration of a model for Irrigation scheduling of Deciduous Fruit Orchards.

Volschenk, T. (2017). Evapotranspiration and crop coefficients of Golden Delicious/M793 apple trees in the Koue Bokkeveld. *Agricultural Water Management*, 194, 184-191. <https://doi.org/10.1016/j.agwat.2017.09.002>.

Webb, E. K., Pearman, G. I., & Leuning, R. (1980). Correction of flux measurements for density effects due to heat and water vapour transfer. *Quarterly Journal of the Royal Meteorological Society*, 106(447), 85-100.

Wullschleger, S.D., & King, A.W. (2000). Radial variation in sap velocity as a function of stem diameter and sapwood thickness in yellow-poplar trees. *Tree Physiology*, 20, 511-518. <https://doi.org/10.1093/treephys/20.8.511>.

Xiang, Z., Chen, X., & Lian, Y. (2016). Quantifying the vulnerability of surface water environment in humid areas base on DEA method. *Water Resources Management*, 30, 5101-5112.

Zhang, H., Simmonds, L. P., Morison, J. I., & Payne, D. (1997). Estimation of transpiration by single trees: comparison of sap flow measurements with a combination equation. *Agricultural and Forest Meteorology*, 87(2-3), 155-169.

## **CAPACITY BUILDING**

### **Staff development**

CSIR emerging researchers developing their capabilities through their contribution in this project.

### **Community development**

N/A

### **Institutional development**

N/A

### **Students on course for graduation**

One MSc student graduated on 09/09/2022.

## **KNOWLEDGE DISSEMINATION & TECHNOLOGY TRANSFER**

### **Scientific articles**

Mashabatu et al., (*article accepted subject to minor revisions*). Deriving crop coefficients for evergreen and deciduous fruit orchards in South Africa using the fraction of vegetation cover and tree height data. Journal of Agricultural Water Management.

### **Conference presentation**

Dzikiti et al. Deriving crop coefficients for fruit orchards in South Africa using readily available data. X International Symposium on the Irrigation of Horticultural Crops held from 29 January to 02 February 2023 in Stellenbosch.

### **Popular articles**

Ntshidi et al., 2021. Agricultural sector in South Africa. Opinion. Current investigations in agriculture and current research.

## APPENDIX A

### A1. LENGTH OF GROWTH STAGES (after Van Heerden et al., 2016).

Crop type	Stage name	Length (days)	Approximate budbreak date
Apples			
	Ini	20	
	Dev	70	15-Aug
	Mid	120	
	Late	60	
Avocado			
	Ini	30	
	Dev	60	
	Mid	215	15-Aug
	Late	60	
Banana			
	Ini	120	
	Dev	60	
	Mid	180	15-Aug
	Late	5	
Citrus			
	Ini	60	
	Dev	90	
	Mid	120	15-Aug
	Late	95	
Litchi			
	Ini	30	
	Dev	60	15-Aug
	Mid	120	
	Late	150	
Macadamia			
	Ini	45	
	Dev	30	15-Aug
	Mid	260	
	Late	30	
Mango			
	Ini	45	
	Dev	60	15-Aug
	Mid	90	
	Late	165	
Nectarine			
	Ini	20	
	Dev	70	
	Mid	120	
	Late	60	
	Ini	20	

Crop type	Stage name	Length (days)	Approximate budbreak date
Peaches			
	Dev	70	15-Jul
	Mid	120	
	Late	60	
Pears	Ini	30	
	Dev	70	15-Aug
	Mid	80	
	Late	30	
Pecans	Ini	20	
	Dev	30	15-Aug
	Mid	90	
	Late	120	
Pomegranate	Ini	20	
	Dev	60	15-Aug
	Mid	70	
	Late	30	
Plum	Ini	20	
	Dev	70	15-Jul
	Mid	120	
	Late	60	